The Prebiotic Synthesis of Soluble Organic Matter in Carbonaceous Chondrites and the Influence of Asteroidal Aqueous Alteration

by

Danielle Nicole Simkus

A thesis submitted in partial fulfillment of the requirements for the degree of

Doctor of Philosophy

Department of Earth and Atmospheric Sciences
University of Alberta

ABSTRACT

Carbonaceous chondrite meteorites are derived from primitive asteroids in the solar system and often contain prebiotic organic compounds including amino acids, carboxylic acids, nucleobases, and smaller precursor molecules. These soluble organic compounds, synthesized via non-biological chemical reactions in space, are key precursors to several biologically-relevant compounds including proteins, membrane lipids, DNA and RNA. Asteroidal aqueous alteration processes have been shown to play an important role in the synthesis and preservation of soluble organic compounds in carbonaceous chondrites, though the chemical processes associated with parent body aqueous alteration are not fully understood. This Ph.D. thesis incorporates method development with meteorite analyses to gain insight into the influence of aqueous alteration during prebiotic organic synthesis. The organic contents of two specific carbonaceous chondrites were investigated: (1) the Murchison meteorite, selected as a reference standard due to the large dataset of organic analyses available in the literature for comparison, and (2) the Tagish Lake meteorite, selected for its pristine nature and unique alteration-derived heterogeneity.

Method optimization was carried out for the extraction, derivatization and analysis of meteoritic aldehydes and ketones, and the procedure was applied to the analysis of both the Murchison and Tagish Lake meteorites. This thesis reports the first compound-specific $\delta^{13}C$ compositions for meteoritic aldehydes and ketones. The relatively ^{13}C-depleted compositions (particularly for the Tagish Lake samples) indicate that the aldehydes and ketones are not primordial unreacted Strecker synthesis precursors, but rather products of secondary alteration reactions on the parent body asteroid. Potential alteration-driven sources of aldehydes and ketones (e.g. degradation of amino acids or oxidation of insoluble organic matter) are discussed.

In addition to the aldehyde and ketone analyses, previously unstudied Tagish Lake specimens (TL1, TL4 and TL10a) were investigated for indigenous amino acids, carboxylic acids, and aliphatic and aromatic hydrocarbons. The analyses revealed distinct organic contents likely indicating distinct parent body aqueous alteration histories. Specimen TL1 exhibited relatively high abundances of organics and a soluble organic composition that was similar to those of previously analyzed specimens TL5b and TL11h. Specimen TL4 appeared to be minimally aqueously altered and exhibited an overall low soluble organic content, attributed to the absence of water during key synthesis reactions. Specimen TL10a contained a unique and unusual soluble

organic content, apparently devoid of carboxylic acids and weakly polar aliphatic and aromatic compounds, but exhibiting low abundances of amino acids and aldehydes and ketones. Overall, these analyses support a theory of a "sweet spot" of aqueous alteration that allows for optimal synthesis and preservation of soluble organic compounds. The data also suggest that the absence of key precursor compounds in certain Tagish Lake specimens (e.g. TL10a) may have precluded subsequent organic synthesis reactions.

Lastly, time-of-flight secondary ion mass spectrometry (TOF-SIMS) analysis was applied to the analysis of both the Murchison and the Tagish Lake meteorites to demonstrate the potential utility of the TOF-SIMS method for detecting amino acids in situ on meteorite fresh fracture surfaces, without the need for bulk solvent extractions. Although amino acids and characteristic amino acid fragments were positively identified in the Tagish Lake meteorite, the compounds were not confidently identified in the Murchison samples, possibly due to mass interferences between organic species. The amino acids detected in the Tagish Lake meteorite did not appear to be associated with specific minerals or textures in the meteorite, but rather appeared to be homogeneously distributed throughout the matrix.

PREFACE

This Ph.D. thesis includes scientific work produced by research collaborators Dr. Jamie Elsila, Dr. José Aponte and Dr. Hannah McLain at NASA Goddard Space Flight Center and with assistance from Dr. Robert Hilts (MacEwan University), Dr. Yulia Goreva (Smithsonian Institution) and Dr. Timothy McCoy (Smithsonian Institution). Danielle Simkus was the lead researcher and author for all chapters in this thesis. Dr. Christopher Herd was the supervisory author and was involved with concept formation for all chapters. No part of this thesis has been previously published.

In Chapter 2, all method development experiments, meteorite extractions, aldehyde and ketone analyses, and data interpretations were carried out by D. Simkus. Dr. Robert Hilts assisted with the organization and interpretation of the method development experiments. Data processing for $\delta^{13}C$ measurements was carried out by Drs. José Aponte and Jamie Elsila.

In Chapter 3, all meteorite extractions, aldehyde and ketone analyses, carboxylic acid analyses, DCM extractions, and data interpretations were carried out by D. Simkus. Dr. Robert Hilts assisted with the meteorite extractions. Drs. José Aponte, Jamie Elsila, and Hannah McLain carried out the amino acid analyses.

In Chapter 4, all laboratory analyses and data interpretations were carried out by D. Simkus. Drs. Yulia Goreva and Timothy McCoy assisted with TOF-SIMS data collection and concept formation.

ACKNOWLEDGEMENTS

First and foremost, I would like to express my heartfelt appreciation for my Ph.D. supervisor, Dr. Christopher Herd. It was one generous research opportunity that Chris offered to me during my undergraduate degree that sparked my interest for astrochemistry and steered my entire scientific career and I'm so grateful for all the opportunities, wisdom, and guidance that he has continued to provide since then. I could not have asked for a more supportive supervisor.

Thank you as well to my supervisory committee members, Dr. Daniel Alessi and Dr. Long Li, and internal and external examiners, Dr. Thomas Chacko and Dr. Monica Grady, for their thoughtful and constructive feedback for this dissertation.

There are several other people who were instrumental to the completion of this dissertation: I would like to thank Dr. Robert Hilts, not only for sharing his chemistry knowledge with me but also for sharing his enthusiasm for space science research. Our casual discussions about current space missions, the origin of life, and the possibility for life beyond Earth have been a continuous source of inspiration for me over the years. I would like to thank Dr. Jamie Elsila and Dr. José Aponte for their input and mentorship throughout my studies. Thank you to Dr. Yulia Goreva and Dr. Tim McCoy for their guidance and support during my Smithsonian fellowship. Thank you to Dr. Anqiang He and the University of Alberta nanoFAB facility for their assistance with our TOF-SIMS analyses. And thank you to Dr. Matthew Ross and Dr. Aaron Skelhorne at MacEwan University for their technical assistance during our GC-MS analyses.

I am very grateful for generous financial support from a Natural Sciences and Engineering Research Council (NSERC) CGS D3 scholarship, an Izaak Walton Killam Memorial scholarship, and a Graduate Student Fellowship from the Smithsonian Institution.

I am incredibly thankful for Noah Hahn, for his unwavering support, for being my cheerleader every step of the way and for somehow managing to make me feel confident even at the most stressful of times. Thank you as well to Carolyn Furlong, Janina Czas, Cosette Gilmour, Nicole Spring, Lauren Davies, the Grace Anne Stewart Series girls, Kate Carlson, Ashley Underhill, Maggie Hill and Justina Mak for great memories, inspiration, and support throughout these last four years.

Lastly, I would like to thank my parents, my sister, my aunts and uncles for their love and support throughout this entire journey, from encouraging me to pursue my passion for astrobiology, to designing and sporting Enceladus apparel, to patiently hosting me during thesis writing, to maintaining their confidence in my abilities through every step of my career. I am incredibly grateful to have such a supportive family and I cannot thank them enough. It is to them that I dedicate this dissertation.

TABLE OF CONTENTS

LIST OF TABLES

LIST OF FIGURES

LIST OF SCHEMES

CHAPTER 1:

INTRODUCTION TO FUNDAMENTAL CONCEPTS AND RESEARCH

1.1. INTRODUCTION TO METEORITES

1.1.1. The origin and classification of meteorites

While all meteorites must meet a single unifying classification requirement – that they impact the surface of a planetary body – meteorites can originate from various sources. For example, a meteorite can be derived from fragments of planets or moons that were ejected from their planetary surfaces during large impact events, while others, such as those discussed in this thesis, originate from asteroids. Meteorites are subdivided into two main categories: chondrite meteorites and non-chondritic meteorites (Krot et al., 2014). Chondrites are derived from undifferentiated asteroid parent bodies and are generally characterized by the presence of chondrules – small, round olivine- and pyroxene-rich grains that formed as molten or partially-molten droplets prior to solar system formation. The other four main components of chondrites are: (1) Fe-Ni metal, (2) refractory calcium-aluminum-rich inclusions (CAIs), (3) amoeboid olivine aggregates, and (4) fine-grained matrix (Krot et al., 2014). Non-chondritic meteorites lack chondritic textures and have experienced partial or complete melting and planetary differentiation. The non-chondritic meteorites include achondrites, stony-iron meteorites, and iron meteorites.

This thesis focuses on the composition of carbonaceous chondrites, a class of chondrites that includes some of the most carbon-rich meteorites (Figure 1.1). Carbonaceous chondrites are classified into eight groups (CI, CM, CO, CR, CB-CH, CV, CK; Figure 1.1), based on elemental and mineralogical compositions (Sears and Dodd, 1988). The degree of aqueous and/or thermal alteration of a meteorite, representing its history on the parent asteroid, is described by its petrologic type, a number ranging between 1 and 6 (Van Schmus and Wood, 1976). Petrologic types 1 to 3 have experienced aqueous alteration at low temperature, with type 1 chondrites being the most aqueously altered and type 3 chondrites being the least aqueously altered. Types 4 to 6 represent chondrites with increasing thermal alteration histories. The analyses carried out for this thesis project focus specifically on the organic contents of CI and CM chondrites which have experienced low-temperature aqueous alteration (petrologic types 1 and 2). Section 1.1.2 describes the compositions of these two groups of carbonaceous chondrites in more detail.

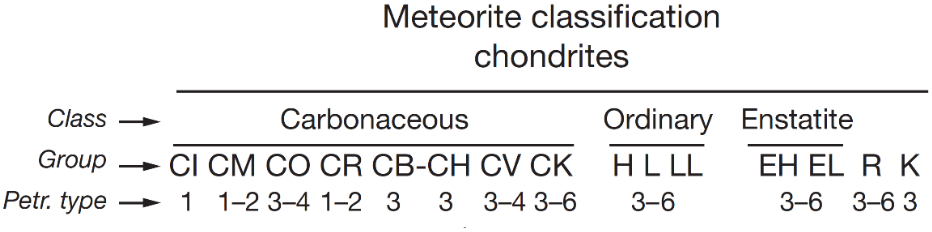

Meteorite classification
chondrites

Class →	Carbonaceous							Ordinary	Enstatite		
Group →	CI	CM	CO	CR	CB-CH	CV	CK	H L LL	EH EL	R	K
Petr. type →	1	1–2	3–4	1–2	3 3	3–4	3–6	3–6	3–6	3–6	3

Figure 1.1. Classification system for chondrite meteorites, including classes, groups and petrologic types (from Krot et al., 2014). The ordinary and enstatite chondrites are subdivided into three and two groups, respectively, based on differences in total- and metallic-iron contents.

1.1.2. The effects of aqueous alteration

The degree of asteroid parent body aqueous alteration is reflected in the mineralogy, petrology, stable isotope compositions and organic contents of carbonaceous chondrites. Mineralogical and petrological evidence for parent body aqueous alteration in carbonaceous chondrites includes the presence of secondary minerals (hydrous phyllosilicates, carbonates, sulfates, sulfides and oxides), replacement of chondrule glass by phyllosilicate minerals, and the presence of phyllosilicate-rich and sulfide veins (Brearley, 2006). Aqueous alteration processes influence the synthesis and preservation of prebiotic organic compounds, and the associated chemical reactions can result in stable isotopic fractionations (see Section 1.2.5 for details). The mineralogical and chemical compositions of CI and CM chondrites reflect their distinct alteration histories. CI chondrites are considered the most primitive carbonaceous chondrites as their chemical compositions closely match that of the solar photosphere (Palme et al., 2014). Despite their primitive nature, CI chondrites are also the most highly aqueously altered group (petrologic type 1). They are highly brecciated, composed primarily of hydrated lithic fragments, and are generally devoid of chondrules and CAIs (Brearley, 2014). CM chondrites are more diverse in terms of both their alteration and brecciation histories. Chondrules are abundant in CM chondrites and are generally only partially replaced by phyllosilicates (Brearley, 2014). CM chondrites commonly contain CAIs and AOAs and a high abundance of matrix material composed of secondary minerals (e.g. phyllosilicates, carbonates, sulfides, magnetite) (Rubin et al., 2007).

1.2. ORGANIC CHEMISTRY OF CARBONACEOUS CHONDRITES

1.2.1. Prebiotic organic content of carbonaceous chondrites

The organic matter in carbonaceous chondrites can be divided into two components: (1) a solvent-soluble fraction, including a wide range of prebiotic organic compounds which can be extracted from the meteorite using organic solvents of varying polarities; and (2) a largely uncharacterized macromolecular fraction that is insoluble in organic solvents. This thesis focuses on the composition of the solvent-soluble fraction and covers a range of analytical methods for analyzing prebiotic organic compounds contained within this fraction (Section 1.2.3). Prebiotic organic compounds (e.g. amino acids, carboxylic acids, aldehydes, ketones, amines, sugars, nucleobases) are molecules that can be synthesized via non-biological chemical reactions and are precursors to other known biological compounds. Thus, these molecules are chemical building blocks for life as we know it (Figure 1.2). Carbonaceous chondrites may have been a significant source of prebiotic organic compounds to the early Earth via meteorite impacts (particularly during the Late Heavy Bombardment ~ 3.8 Ga) (Chyba et al., 1990). For this reason, understanding the non-biological reactions and conditions involved in synthesizing prebiotic organic compounds in astromaterials provides us with insights into the origin of life on Earth and the potential for life to arise beyond our planet.

There are numerous potential formation relationships between the different prebiotic organic compound classes, and studies have aimed to understand which specific reactions played key roles during the evolution of prebiotic organic matter in the solar system. The most widely studied mechanism for amino acid synthesis is Strecker-cyanohydrin synthesis (Peltzer et al., 1984), whereby an aldehyde or ketone reacts with ammonia in the presence of hydrogen cyanide to form an α-amino acid. In the absence of ammonia, this reaction yields α-hydroxy acids. Other commonly discussed origins for meteoritic amino acids include the Michael-type addition of ammonia to unsaturated nitriles to yield β-amino acids (Cronin and Chang, 1993), reductive amination of keto acids (Huber and Wächtershäuser, 2003), and CO_2 addition to amines (Hudson et al., 2009). The aldehyde and ketone Strecker-cyanohydrin reactants are of particular interest for prebiotic chemistry, not only because of their structural relationship to α-amino acids, but also because they can be oxidized to form carboxylic acids, the chemical building blocks of biological lipids (Deamer et al., 2002). The simplest aldehyde, formaldehyde, is also potentially a key precursor to sugars, sugar-alcohols and insoluble organic matter via formose reactions (Cooper et al., 2001; Cody et al., 2011; Meinert et al., 2016). Nucleobases, though beyond the scope of this thesis, are also found in carbonaceous chondrites (Martins et al., 2008; Callahan et al., 2011) and are the chemical building blocks of DNA and RNA (Figure 1.2).

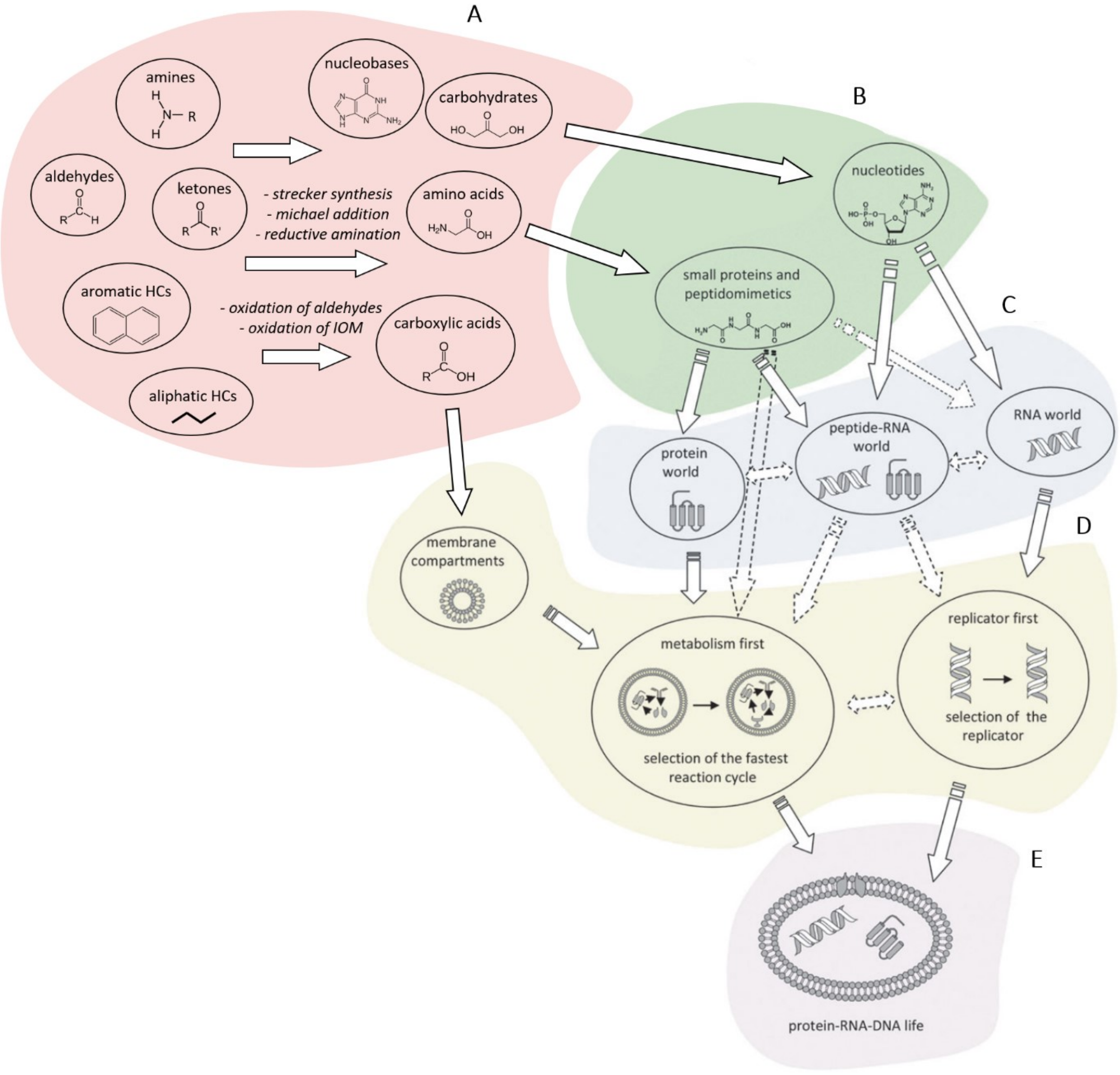

Figure 1.2. Schematic adapted from Domagal-Goldman and Wright et al. (2016) illustrating the evolution of prebiotic organic matter and origin of life. **A.** Prebiotic organic chemistry of the early solar system and astromaterials. **B.** Self-organization of small organic molecules into larger, more complex compounds. **C.** Protein world, peptide-RNA world, RNA world. **D.** Self-assembly of membrane compartments and development of compartmentalized reaction cycles. **E.** Protein-RNA-DNA life capable of shifting from chemical equilibrium, evolving, and maintaining homeostasis. This Ph.D. thesis focuses solely on the chemical processes involved in synthesizing prebiotic organic compounds contained in astromaterials (Category A).

1.2.2. Analytical techniques

1.2.2.1. Bulk solvent extractions and chemical derivatizations

Analytical techniques for determining the soluble organic contents of carbonaceous chondrites vary depending on the target class of compounds; however, the general procedure for meteorite sample extractions and analyses is carried out as follows: The meteorite sample, typically 0.1–10 grams, is homogenized by crushing the sample to a fine powder with a mortar and pestle. Soluble organic compounds are extracted from the powder using a solvent of appropriate polarity (e.g. water, dichloromethane, methanol) for 3-24 hours, often at elevated temperatures (100-110°C). The extract may be subjected to acid-vapor hydrolysis to hydrolyze and release any organic compounds that are minerally-bound within the sample. The target organic compounds are often reacted with a derivatizing reagent, modifying their chemical structures so that their chemical and physical properties are more suitable for analysis. The isolated derivatives are then separated chromatographically, identified, and quantified via gas chromatography-mass spectrometry (GC-MS), liquid chromatography-mass spectrometry (LC-MS), or high performance liquid chromatography (HPLC).

1.2.2.2. Solid-phase microextraction technique (SPME)

A chemical derivatization reaction is often necessary for improving chromatographic results if the target compounds are unstable or non-volatile and difficult to separate on a GC-MS column. However, the derivatization reaction time can be time-consuming and full recoveries of the analytes may be difficult if there are several transfer steps involved in the method. For some compound classes, a solid-phase microextraction technique (SPME) can be used to side-step the derivatization process. SPME analysis involves the use of a solid fiber coated with an extracting phase which can be used to extract specific analytes from a solution. The fiber is then transferred into the injection port of the GC-MS instrument where the analytes are desorbed and analyzed. The procedure is relatively quick and simple and the SPME fiber is highly sensitive, allowing for the detection of trace abundances of organic compounds (Dias and Freeman, 1997). This thesis applies the SPME technique (following the optimized method of Huang et al., 2005) to the analysis of monocarboxylic acids contained within Tagish Lake meteorite hot-water extracts (Chapter 3).

1.2.2.3. In-situ analysis of soluble organic compounds

While the bulk solvent extraction procedure outlined in Section 1.2.2.1 provides information about the identities, quantities, and isotopic compositions of soluble organic compounds, the process of homogenizing bulk meteorite samples means losing information about the distribution of soluble organic compounds across mineral grains and textures. Understanding the distribution of organics on a micrometer scale may be particularly valuable for meteorite samples that are known to exhibit heterogeneous compositions (e.g. the Tagish Lake carbonaceous chondrite; Section 1.3). As such, in addition to utilizing several solvent extraction techniques for meteorite analyses, this thesis investigates the applicability of a specific in-situ method – time-of-flight secondary ion mass spectrometry (TOF-SIMS) – for detecting soluble organic compounds across fresh fracture meteorite sample surfaces (Chapter 4).

1.2.3. Compound-specific stable carbon isotope ($\delta^{13}C$) analysis

Compound-specific stable carbon isotope ($\delta^{13}C$) compositions of organic compounds can act as signatures for chemical pathways and can be used to trace structural relationships between different compound classes (Sephton and Gilmour, 2001). A carbon isotope composition (reported as a $\delta^{13}C$ value) is a measurement of the ratio of the two stable isotopes of carbon (^{13}C and ^{12}C) compared to a terrestrial reference standard, the Vienna Pee Dee Belemnite (VPDB) carbonate ($^{13}C/^{12}C$ ratio of 0.0112372) (Sephton, 2002). The relative $\delta^{13}C$ value of a given sample is reported in parts per million (‰) and calculated using equation 1.

$$\delta^{13}C_{sample} = [(^{13}C/^{12}C_{sample} - {}^{13}C/^{12}C_{standard})/ (^{13}C/^{12}C_{standard})] \text{ x } 1000 \text{ ‰} \quad (1)$$

Kinetic isotope effects associated with chemical reactions result in the preferential utilization of ^{12}C over ^{13}C atoms. As a result, primitive extraterrestrial organic compounds are generally enriched in the heavier isotope (^{13}C) (Penzias, 1980) while products of both non-biological and biological chemical reactions exhibit relatively ^{13}C-depleted values (Sephton and Gilmour, 2001). The magnitude of this isotope fractionation effect depends on several factors, including the number of carbon atoms and the number of steps involved in a chemical pathway, as well as the reaction temperature, with the largest isotope fractionations occurring at low temperature (Sephton and Gilmour, 2000; 2001).

1.2.4. Amino acid enantiomeric compositions

Enantiomers are two non-superimposable mirror-image isomers of a molecule. Most enantiomers contain a chiral center (i.e., a single carbon attached to four different moieties; Figure 1.3). In extraterrestrial organic compounds, the two enantiomers (designated D and L) are generally found in equal abundances (referred to as "racemic" mixtures), as abiotic synthetic reactions yield 1:1 mixtures of D- and L-enantiomers in the absence of a chiral driving force. In some cases, however, amino acids exhibit excesses of the L-enantiomer (e.g. Pizzarello and Cronin, 2000; Glavin and Dworkin, 2009). These observations are of particular astrobiological interest as biological amino acids are composed entirely of the L-enantiomer, with a rare few exceptions, raising the possibility that the origin of biological homochirality on Earth may have stemmed from the enantiomeric compositions of meteoritic amino acids. The mechanisms by which enantiomeric excesses are produced and amplified are still debated, but asteroidal aqueous alteration processes may be a driving factor (Glavin et al., 2012).

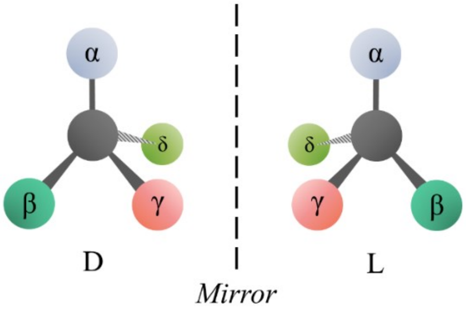

Figure 1.3. Illustration of the non-superimposable mirror images (D and L configurations) of a chiral molecule. The α, β, γ, and δ groups represent four different moieties attached to the chiral carbon center.

1.2.5. Factors influencing the organic chemistry of carbonaceous chondrites

The structure, distribution and abundances of soluble organic compounds in carbonaceous chondrites are dependent on a range of factors (both extraterrestrial and terrestrial) and understanding the effects of these outside influences allows us to use the soluble organic compositions to gain insight into the history of the meteorite samples. The source of the meteoritic organic compounds (primary species from the interstellar medium/protoplanetary disk vs. secondary species from asteroid parent body alteration reactions) will influence the types of organic compounds present and their stable isotopic compositions, as each source involves distinct formation mechanisms (Grady and Wright, 2003). The effects of parent body aqueous alteration on the soluble organic chemistry of carbonaceous chondrites are not fully understood, though the presence of liquid water is a key requirement for many reactions and exceptionally high degrees of aqueous alteration (i.e. high water/rock ratios, long-duration alteration, and/or high temperatures) appear to result in the degradation of soluble organic compounds. The stable isotopic compositions of the secondary species are often relatively ^{13}C-depleted compared to the precursor primary species, though the effect of kinetic and equilibrium isotope effects depends on whether the reactions take place in an open or closed system (Figure 1.4). The length of time between the meteorite fall and the collection of the meteorite samples can also have a major effect on the chemical composition of the samples, as terrestrial organic contaminants in the environment can be quickly introduced. Meteorite samples that have landed in wet or warm environments also risk losing indigenous soluble organic compounds due to leaching and volatilization, respectively. Storing the meteorite samples in cold, clean conditions can help retain volatile organic compounds that would otherwise be lost and can help slow or prevent potential activity of microorganisms introduced from the landing environment (Herd et al., 2016). Careful sample handling with clean tools and laboratory gloves should also be employed to prevent contamination (Herd et al., 2016).

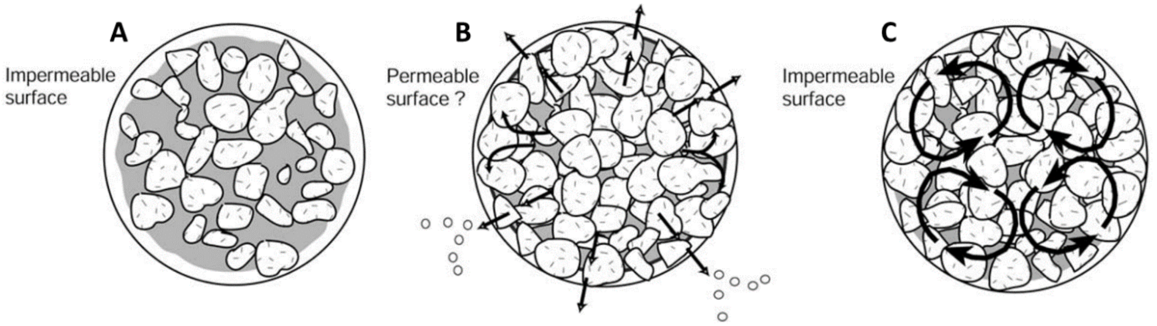

Figure 1.4. Three models for the process of aqueous alteration on the asteroid body (diagrams from Young et al., 2003): (A) Closed-system, two-reservoir model where water-rock interactions are static and the asteroid surface is impermeable to water loss (Clayton and Mayeda, 1984). (B) The exhalative fluid model, in which water can be lost at the asteroid's permeable outer surface (Young et al., 1999). (C) Convecting, closed-system, hydrothermal model (Grimm and McSween, 1989; Palguta et al., 2010).

1.3. THE TAGISH LAKE METEORITE

1.3.1. Fall, collection and storage

The fall of the Tagish Lake carbonaceous chondrite was observed as a bright fireball illuminating the sky above southern Yukon, northern British Columbia and parts of Alaska, in the early morning of January 18th, 2000 (8:43 a.m. local time). It is estimated that the Tagish Lake meteoroid weighed approximately 200,000 kg and measured 4 to 6 meters in diameter before it entered the Earth's atmosphere; however, the bulk of the meteoroid was vaporized or ablated away during its entry through the upper atmosphere (Brown et al., 2000). The atmospheric trajectory of the meteoroid was reconstructed by consolidating information from photos and videos of the resulting dust cloud, as well as from over 70 eyewitness reports (Brown et al., 2000). Based on the calculated orbit and the meteorite's reflectance spectrum, the Tagish Lake meteorite is believed to have originated from a D- or P-type asteroid, located in the outer asteroid belt (Brown et al., 2000; Hiroi et al., 2001). On January 25th, a local resident collected the first Tagish Lake fragments – nearly 1 kg of material – from the frozen surface of Tagish Lake (Hildebrand et al., 2006). Care was taken during collection to minimize the meteorite's exposure to terrestrial contaminants and retain any indigenous volatile compounds; the specimens were collected without direct hand contact, stored in plastic bags, and have been kept below 0°C ever since (Brown et al., 2000; Herd et al., 2016). An additional 410 specimens were recovered from Tagish Lake later that spring. The specimens from this second collection are referred to as "degraded" samples as they were found embedded in the lake ice and have, therefore, been immersed in lake meltwater during freeze-thaw cycles (Hildebrand et al., 2006).

The Tagish Lake meteorite is classified as a type 2 carbonaceous chondrite; it has experienced some aqueous alteration, but still contains recognizable chondrules and relatively unaltered isolated olivine and pyroxene grains and has not been thermally metamorphosed. The meteorite does not belong to any known group, but it shares affinities with both CI and CM carbonaceous chondrites (Brown et al., 2000). The meteorite is exceptionally carbon-rich (5.8 wt%; Grady et al., 2002), extremely friable and porous (~ 40% porosity; Bland et al., 2004), and has a very low bulk density (1.6 g/cm^3; Zolensky et al., 2002). Sparse chondrules and calcium aluminum inclusions (CAIs), as well as compact lithic fragments and isolated olivine and pyroxene grains, are set in a fine-grained matrix of phyllosilicates, magnetite, sulphides and carbonates, which were formed through low-temperature parent-body aqueous alteration reactions (Blinova et al., 2014a).

1.3.2. Heterogeneity of the Tagish Lake meteorite

Four Tagish Lake meteorite specimens (TL5b, TL11h, TL11i and TL11v; Figure 1.5) have been previously thoroughly investigated for their mineralogical and chemical compositions (Blinova et al., 2014a,b; Glavin et al., 2012; Herd et al., 2011). Mineralogical indicators for aqueous alteration in these samples (i.e. increasing replacement of chondrule glass by phyllosilicates, in combination with relatively low porosity and a lower proportion of amorphous silicate material) suggest that the degree of aqueous alteration of the subsamples is in the increasing order of TL5b < TL11h << TL11i. The observed differences in compositions may have resulted from varying durations of alteration, differing water/rock ratios, and/or a temperature gradient across the parent body asteroid. The abundances of soluble organic compounds appear to vary concurrently with the degree of alteration with the highly altered lithologies containing relatively low concentrations of amino acids, carboxylic acids and weakly polar aliphatic and aromatic compounds (Herd et al., 2011; Hilts et al., 2014).

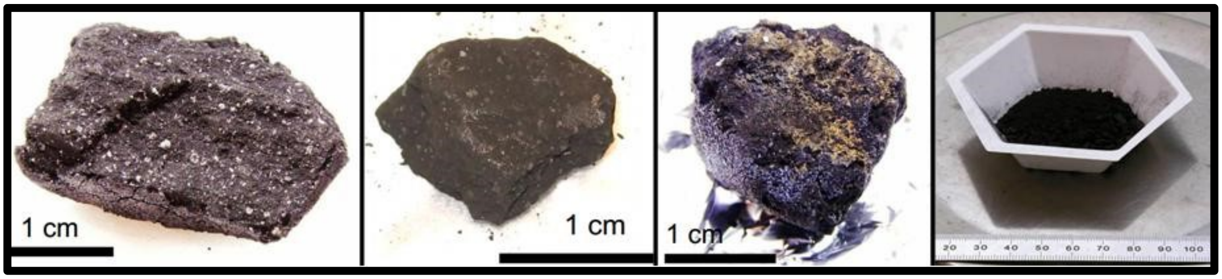

Figure 1.5. Four sample subsets of the Tagish Lake meteorite previously analyzed for their mineralogy, petrology, bulk chemistry and organic contents (from left to right): TL5b, TL11h, TL11i, TL11v. The TL11v specimen is a disaggregated sample that shares compositional similarities with the three other specimens.

1.4. THE MURCHISON METEORITE

The Murchison meteorite fell near Murchison, Victoria, Australia on September 28th, 1969. Several specimens were collected within a few days of the fall and over > 100 kg of meteorite material was collected over the following few months. Murchison is classified as a type 2 CM chondrite and has experienced a relatively low degree of aqueous alteration compared to other CM chondrites, based on relative abundances of phyllosilicates (Mg-serpentine clay) and relative volume percentages of matrix silicates and chondrule alteration (Browning et al., 1996). Murchison is one of the most widely studied carbonaceous chondrites for organic analyses due to the large mass of material available, as well as its high abundance and diversity of organic compounds and its relatively pristine nature (Botta and Bada, 2002). As a result, the Murchison meteorite is often used as a reference standard in the field of organic astrochemistry. Organic compounds identified in the Murchison meteorite to date include amino acids (e.g. Kvenvolden, 1970), carboxylic acids (e.g. Yuen et al., 1984; Lawless and Yuen, 1979), PAHs (e.g. Sephton et al., 1998; Sephton and Gilmour, 2000; Huang et al., 2015), aliphatic and aromatic hydrocarbons (e.g. Kvenvolden, 1970), carbonyl compounds (Jungclaus et al., 1976a; Pizzarello and Holmes, 2009), alcohols (Jungclaus et al., 1976b), amines (e.g. Jungclaus et al., 1976a; Aponte et al., 2014), and nucleobases (e.g. Martins et al., 2008; Callahan et al., 2011).

1.5. RESEARCH OBJECTIVES

This Ph.D. thesis comprises three overarching research objectives aiming to gain insight into the prebiotic synthesis of soluble organic compounds in carbonaceous chondrites.

The first objective was to expand upon our understanding of the soluble organic content of carbonaceous chondrites by determining the first compound-specific $\delta^{13}C$ measurements for meteoritic aldehydes and ketones. Chapter 2 addresses this first objective by outlining the modification and optimization of an O-(2,3,4,5,6-pentafluorobenzyl)hydroxylamine (PFBHA) derivatization method for the identification, quantification and compound-specific $\delta^{13}C$ analysis of meteoritic aldehydes and ketones. This study includes the first compound-specific $\delta^{13}C$ measurements for aldehydes and ketones in the Murchison meteorite.

The second research objective was to gain further insight into the influence of aqueous alteration during prebiotic organic synthesis in the Tagish Lake meteorite. Chapter 3 addresses this objective by investigating the distribution and abundances of amino acids, carboxylic acids, aldehydes/ketones and weakly polar aliphatic and aromatic hydrocarbons in three previously unstudied Tagish Lake specimens, TL1, TL4 and TL10a. This paper includes compound-specific $\delta^{13}C$ measurements of amino acids, aldehydes, and ketones, as well as measurements of amino acid enantiomeric ratios.

The third research objective was to demonstrate the utility of an in-situ approach (TOF-SIMS) for detecting amino acids across fresh fracture surfaces of meteorite samples. Chapter 4 addresses the third objective by investigating the amino acid content of both the Murchison meteorite and the Tagish Lake meteorite (specimen TL1) using TOF-SIMS technique.

1.6. REFERENCES

Bland, P. A., G. Cressey, and O. N. Menzies (2004) Modal mineralogy of carbonaceous chondrites by X-ray diffraction and Mossbauer spectroscopy. *Meteoritics & Planetary Science* **39** (1), 3-16.

Blinova, A. I., C. D. K. Herd, and M. J. M. Duke (2014a) Testing variations within the Tagish Lake meteorite - II: Whole-rock geochemistry of pristine samples. *Meteoritics & Planetary Science* **49** (6), 1100-1118.

Blinova, A. I., T. J. Zega, C. D. K. Herd and R. M. Stroud (2014b) Testing variations within the Tagish Lake meteorite - I: Mineralogy and petrology of pristine samples. *Meteoritics & Planetary Science* **49** (4), 473-502.

Botta, O. and J. L. Bada (2002) Extraterrestrial organic compounds in meteorites. *Surveys in Geophysics* **23**, 411−467.

Brearley, A. J. (2014) Nebular versus parent body processing. *Treatise on Geochemistry 2nd Edition*, H. D. Holland and K. K. Turekian, Eds. (Elsevier, 2014), vol. 1, p. 309-334.

Brown, P. G., A. R. Hildebrand, M. E. Zolensky, M. Grady, R. N. Clayton, T. K. Mayeda, E. Tagliaferri, R. Spalding, N. D. MacRae, E. L. Hoffman, D. W. Mittlefehldt, J. F. Wacker, J. A. Bird, M. D. Campbell, R. Carpenter, H. Gingerich, M. Glatiotis, E. Greiner, M. J. Mazur, P. J. A. McCausland, H. Plotkin, T. R. Mazur (2000) The fall, recovery, orbit, and composition of the Tagish Lake meteorite: A new type of carbonaceous chondrite. *Science* **290**, 320-325.

Browning, L. B., H. Y. McSween Jr., and M. Zolensky (1996) Correlated alteration effects in CM carbonaceous chondrites. *Geochimica et Cosmochimica Acta* **60** (14), 2621-2633.

Callahan, M. P., K. E. Smith, J. Cleaves II, J. Ruzicka, J. C. Stern, D. P. Glavin, C. H. House, and J. P. Dworkin (2011) Carbonaceous meteorites contain a wide range of extraterrestrial nucleobases. *PNAS* **108** (34), 13995-13998.

Chyba, C. F., P. J. Thomas, L. Brookshaw, and C. Sagan (1990) Cometary delivery of organic molecules to the early Earth. *Science* **249**, 366-373.

Cody, G. D., E. Heying, C. M. O'D. Alexander, L. R. Nittler, A. L. D. Kilcoyne, S. A. Sandford, and R. M. Stroud (2011) Establishing a molecular relationship between chondritic and cometary organic solids. *PNAS* **108**, 19171-19176.

Cooper, G., N., N. Kimmich, W. Belisle, J. Sarinana, K. Brabham, and L. Garrel (2001) Carbonaceous meteorites as a source of sugar-related organic compounds for the early Earth. *Nature* **414**, 879-883.

Cronin, J. R. and S. Chang (1993) Organic matter in meteorites: Molecular and isotopic analyses of the Murchison meteorite. *The Chemistry of Life's Origin.* J. M. Greenberg, C. X. Mendoza-Gomez, and V. Pironello, Eds. (Kluwer Academic Publishers, 1993), p. 209-255.

Deamer, D., J. P. Dworkin, S. A Sandford, M. P. Bernstein, and L. J. Allamandola (2002) The first cell membranes. *Astrobiology* **2** (4), 371-381.

Domagal-Goldman, S. and K. E. Wright (2016) The Astrobiology Primer V2.0. *Astrobiology* 16 (8), 561-653.

Glavin, D. P. and J. P. Dworkin (2009) Enrichment of the amino acid L-isovaline by aqueous alteration on CI and CM meteorite parent bodies. *PNAS* **106** (14), 5487-5492.

Glavin, D. P., J. E. Elsila, A. S. Burton, M. P. Callahan, J. P. Dworkin, R. W. Hilts, and C. D. K. Herd (2012) Unusual nonterrestrial L-proteinogenic amino acid excesses in the Tagish Lake meteorite. *Meteoritics & Planetary Science* **47**, 1347-1364.

Grady, M. M., A. B. Verchovsky, I. A. Franchi, I. P. Wright, and C. T. Pillinger (2002) Light element geochemistry of the Tagish Lake CI1 chondrite: Comparison with CI1 and CM2 meteorites. *Meteoritics & Planetary Science* **37**, 713-735.

Grady, M. M., and I. P. Wright (2003) Elemental and isotopic abundances of carbon and nitrogen in meteorites. *Space Science Reviews* **106**, 231-248.

Herd, C. D. K, A. Blinova, D. N. Simkus, Y. Huang, R. Tarozo, C. M. O'D. Alexander, F. Gyngard, L. R. Nittler, G. D. Cody, M. L. Fogel, Y. Kebukawa, A. L. D. Kilcoyne, R. W. Hilts, G. F. Slater, D. P. Glavin, J. P. Dworkin, M. P. Callahan, J. E. Elsila, B. T. De Gregorio, and R. M. Stroud (2011) Origin and evolution of prebiotic organic matter as inferred from the Tagish Lake meteorite. *Science* **332**, 1304-1307.

Herd, C. D. K., R. W. Hilts, A. W. Skelhorne, and D. N. Simkus (2016) Cold curation of pristine astromaterials: Insights from the Tagish Lake meteorite. *Meteoritics & Planetary Science* **51**, 499-519.

Hildebrand, A. R., P. J. A. McCausland, P. G. Brown, F. J. Longstaff, S. D. J. Russell, E. Tagliaferri, J. F. Wacker, and M. J. Mazur (2006) The fall and recovery of the Tagish Lake meteorite. *Meteoritics & Planetary Science* **41** (3), 407-431.

Hilts, R. W, C. D. K. Herd, D. N. Simkus, and G. F. Slater (2014) Soluble organic compounds in the Tagish Lake meteorite. *Meteoritics & Planetary Science* **49** (4), 526-549.

Hiroi, T., M. E. Zolensky, and C. M. Pieters (2001) The Tagish Lake meteorite: A possible sample from a D-type asteroid. *Science* **293**, 2234-2236.

Huang, Y., Y. Wang, M. R. Alexandre, T. Lee, C. Rose-Petruck, M. Fuller, and S. Pizzarello (2005) Molecular and compound-specific isotopic characterization of monocarboxylic acids in carbonaceous meteorites. *Geochimica et Cosmochimica Acta* **69** (4), 1073-1084.

Huang, Y., J. C. Aponte, J. Zhao, R. Tarozo, and C. Hallmann (2015) Hydrogen and carbon isotopic ratios of polycyclic aromatic compounds in two CM2 carbonaceous chondrites and implications for prebiotic organic synthesis. *Earth and Planetary Science Letters* **426**, 101-108.

Huber, C., and G. Wächtershäuser (2003) Primordial reductive amination revisited. *Tetrahedron Letters* **44**, 1695-1697.

Hudson, R. L., Lewis, A. S., Moore, M. H., Dworkin, J. P., and M. P. Martin (2009) Enigmatic isovaline: investigating the stability, racemization and formation of a non-biological meteoritic amino acid. *ASP Conference Series* **420**, 157-162.

Jungclaus, G. A., G. U. Yuen, C. B. Moore (1976a) Evidence for the presence of low molecular weight alcohols and carbonyl compounds in the Murchison meteorite. *Meteoritics* **11**, 231-237.

Jungclaus, G., J. R. Cronin, C. B. Moore, and G. U. Yuen (1976b) Aliphatic amines in the Murchison meteorite. *Nature* **261**, 126-128.

Krot, A. N., K. Keil, E. R. D. Scott, C. A. Goodrich, and M. K. Weisberg (2014) Classification of meteorites and their genetic relationships. *Treatise on Geochemistry 2nd Edition*, H. D. Holland and K. K. Turekian, Eds. (Elsevier, 2014) vol. 1, p. 1-63.

Kvenvolden, K., J. Lawless, K. Pering, E. Peterson, J. Flores, C. Ponnamperuma, I. R. Kaplan, C. Moore (1970) Evidence for extraterrestrial amino acids and hydrocarbons in the Murchison meteorite. *Nature* **228**, 923-926.

Lawless, J. G., and E. Peterson (1975) Amino acids in carbonaceous chondrites. *Origins of Life* **6**, 3-8.

Martins, Z., O. Botta, M. L. Fogel, M. A. Sephton, D. P. Glavin, J. S. Watson, J. P. Dworkin, A. W. Schwartz, P. Ehrenfreund (2008) Extraterrestrial nucleobases in the Murchison meteorite. *Earth and Planetary Science Letters* **270**, 130-136.

Meinert, C., I. Myrgorodska, P. de Marcellus, T. Buhse, L. Nahon, S. V. Hoffmann, L. Le Sergeant d'Hendecourt, U. J. Meierhenrich (2016) Ribose and related sugars from ultraviolet irradiation of interstellar ice analogs. *Science* **352**, 208-212.

Palme, H., K. Lodders, and A. Jones (2014) Solar system abundances of the elements. *Treatise on Geochemistry 2nd Edition*, H. D. Holland and K. K. Turekian, Eds. (Elsevier, 2014), vol. 2, p. 15-36

Peltzer E. T., J. L Bada, G. Schlesinger, and S. L. Miller (1984) The chemical conditions on the parent body of the Murchison meteorite: Some conclusions based on amino, hydroxy and dicarboxylic acids. *Advances in Space Research* **4**, 69-74.

Penzias, A. A. (1980) Nuclear processing and isotopes in the galaxy. *Science* **208**, 663-669.

Pizzarello, S. and J. R. Cronin (2000) Non-racemic amino acids in the Murray and Murchison meteorites. *Geochimica et Cosmochimica Acta* **64** (2), 329-338.

Rubin, A. E., J. M. Trigo-Rodriguez, H. Huber, and J. T. Wasson (2007) Progressive aqueous alteration of CM carbonaceous chondrites. *Geochimica et Cosmochimica Acta* **71**, 2361-2382.

Sears, D. W. G. and R. T. Dodd (1988) Overview and classification of meteorites. *Meteorites and the Earth Solar System*. J. F. Kerridge and M. S. Matthews, Eds. (University of Arizona Press) p. 3-31.

Sephton, M. A. (2014) Organic geochemistry of meteorites. *Treatise on Geochemistry 2nd Edition*, H. D. Holland and K. K. Turekian, Eds. (Elsevier, 2014) vo1. 12, p. 1-31

Sephton, M. A., C. T. Pillinger, and I. Gilmour (1998) δ^{13}C of free and macromolecular aromatic structures in the Murchison meteorite. *Geochimica et Cosmochimica Acta* **62** (10), 1821-1828.

Sephton, M. A., and I. Gilmour (2000) Aromatic moieties in meteorites: Relics of interstellar grain processes. *The Astrophysical Journal* **540**, 588-591.

Sephton, M. A., and I. Gilmour (2001) Compound-specific isotope analysis of the organic constituents in carbonaceous chondrites. *Mass Spectrometry Reviews* **20**, 111-120.

Van Schmus, W. R. and J. A. Wood (1967) A chemical-petrologic classification for the chondritic meteorites. *Geochimica et Cosmochimica Acta* **31**, 747-765.

Yuen, G., N. Blair, D. J. Des Marais, and S. Chang (1984) Carbon isotope composition of low molecular weight hydrocarbons and monocarboxylic acids from Murchison meteorite. *Nature* **307**, 252-254.

Zolensky, M. E., K. Nakamura, M. Gounelle, T. Mikouchi, T. Kasama, O. Tachikawa, and E. Tonui (2002) Mineralogy of Tagish Lake: An ungrouped type 2 carbonaceous chondrite. *Meteoritics & Planetary Science* **37**, 737-761.

CHAPTER 2:

COMPOUND-SPECIFIC CARBON ISOTOPE COMPOSITIONS OF ALDEHYDES AND KETONES IN THE MURCHISON METEORITE

2.1. INTRODUCTION

Carbonaceous chondrite meteorites are some of the most primitive materials in our solar system, and their organic content contains a wealth of information about the chemistry of the presolar cloud, the protoplanetary disk, and the subsequent chemical processes that took place on and within parent body asteroids. Investigating the origins of prebiotic organic compounds in meteorites may provide insights into the chemical processes that led to the origin of life on Earth, as well as the potential for life to exist elsewhere in our solar system. The Murchison meteorite, a CM type 2 that fell in southeastern Australia in 1969, is one of the most widely studied carbonaceous chondrites due to the large mass of sample material available, the relatively pristine nature of the meteorite and the structural diversity of its organic content. The findings from ~50 years of research on the organic geochemistry of the Murchison meteorite have built a valuable reference dataset for all other carbonaceous chondrites. The organic inventory of the Murchison meteorite includes amino acids, carboxylic acids, polycyclic aromatic hydrocarbons (PAHs), amines, polyols, aldehydes, ketones, and many more compounds (see reviews and references therein: Botta and Bada, 2002; Pizzarello et al. 2006; Sephton, 2002, 2014).

Aldehydes and ketones (collectively referred to as "carbonyl compounds") may play an important role as precursors to many biologically relevant organic compounds in the solar system. One of the most widely studied chemical reactions involving aldehyde and ketone precursors is Strecker-cyanohydrin synthesis, a proposed source of α-amino acids and α-hydroxy acids in meteorites (Scheme 2.1; Peltzer and Bada, 1978). The α-amino acid products of Strecker synthesis are of particular astrobiological interest as they are monomers of proteins and enzymes in living systems and may hold clues to the origins of prebiotic organic compounds on the early Earth (Kvenvolden et al., 1970). For this reason, the distribution and stable isotopic compositions of amino acids in meteorites have been extensively analyzed to elucidate their synthetic pathways (e.g., Strecker synthesis (Peltzer et al., 1984), Michael addition (Miller et al., 1957), CO_2 addition to amines (Hudson et al., 2009), and reductive amination of keto acids (Huber and Wächtershäuser, 2003)). Despite the potential significance of Strecker synthesis and the relevance of aldehydes and ketones in prebiotic organic chemistry, the stable carbon isotopic compositions ($\delta^{13}C$) of aldehydes and ketones in meteorites have not yet been measured. Thus, the synthetic relationships between meteoritic aldehydes, ketones and amino acids have not been fully investigated, representing a significant gap in the literature.

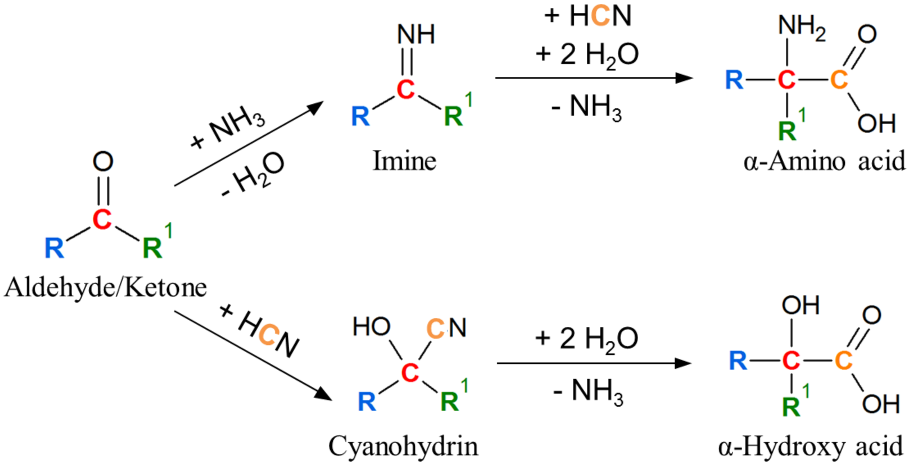

Scheme 2.1. The Strecker-cyanohydrin synthesis reaction (illustration adapted from Elsila et al., 2016), yielding α-amino acids in the presence of NH_3 and α-hydroxy acids in the absence of NH_3 (Peltzer et al., 1984). Colors are used to trace the path of different carbon atoms from precursor to products.

In addition to the Strecker reaction, aldehydes and ketones are potentially structurally related to several other prebiotic organic compounds (Figure 2.1), though some of these reactions have yet to be evaluated under astrochemically-relevant conditions. Carbonyl compounds and alcohols may be interconverted via oxidation/hydrogenation reactions (Bisschop et al., 2007). Aldehydes can be further oxidized to produce carboxylic acids (Corey et al., 1968), the chemical building blocks of biological membranes (Deamer et al., 2002). Aldehydes and ketones may also be converted to amines via reductive amination (Burk et al., 1994; Abdel-Magid et al., 1996), and these amines may be subsequently converted to amino acids via CO_2 addition from photochemical and/or ion-irradiation reactions (Holtom et al., 2005; Hudson et al., 2009; Bossa et al., 2009; Lee et al., 2009). The simplest aldehyde, formaldehyde, is thought to play a particularly important role in the synthesis of prebiotic organic compounds (Cleaves, 2008). In addition to the reactions summarized above, formaldehyde has been proposed as a precursor to meteoritic sugars, sugar-alcohols and insoluble organic matter (IOM) via formose reactions (Cooper et al., 2001; Cody et al., 2011; Meinert et al., 2016).

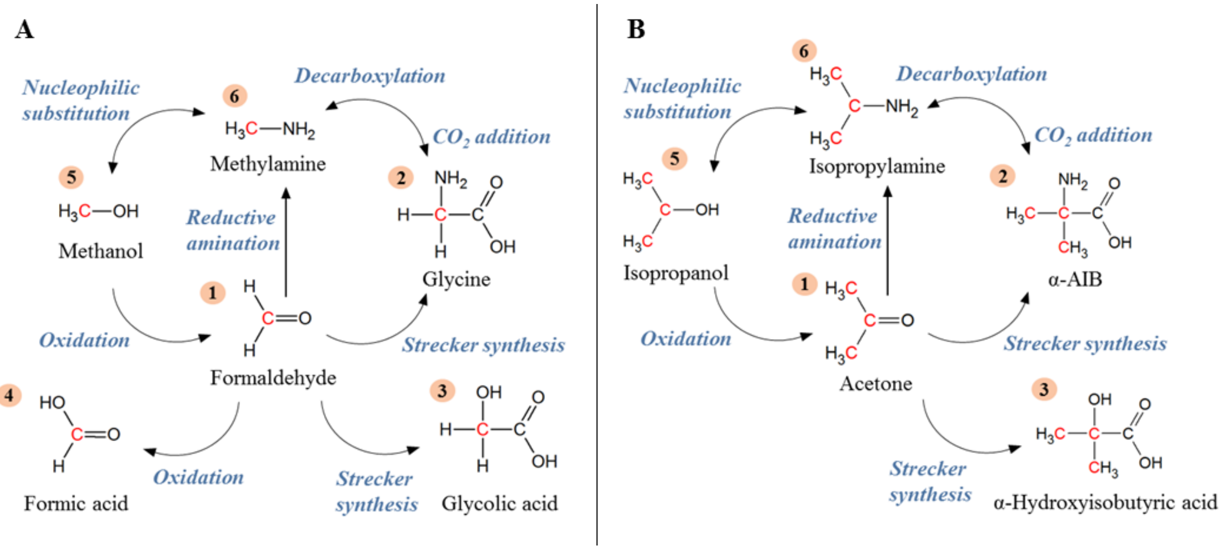

Figure 2.1. Schematic of potential synthetic relationships between carbonyl compounds(1) and other structurally-related organic compounds. Illustrated are the amino acid(2) and hydroxy acid(3) products of Strecker synthesis, carboxylic acids(4) produced via oxidation of aldehydes, alcohol(5) precursors to aldehydes/ketones, and amines(6) formed through reductive amination of aldehydes/ketones, decarboxylation of amino acids, and nucleophilic substitution of alcohols. **A.** The simplest aldehyde (formaldehyde) and structurally-related organics. **B**. The simplest ketone (acetone) and structurally-related organics.

Formaldehyde is ubiquitous in the interstellar medium (ISM) and comets (Irvine, 1999; Cleaves, 2008; Mumma and Charnley, 2011). Proposed mechanisms for the formation of interstellar formaldehyde include successive hydrogenation of CO on ice surfaces (Tielens and Whittet, 1997; Watanabe and Kouchi, 2002; Awad et al., 2005), gas-phase reactions (Shalabiea and Greenberg, 1994), and UV photolysis of H_2O-CO ices (Allamandola et al., 1988; Schutte et al., 1996). Higher molecular weight carbonyl compounds in the interstellar medium can be synthesized by further addition of carbon from CO (Charnley et al., 2004), and subsequently incorporated into comets and asteroids during early solar system formation (Botta and Bada, 2002).

Aldehydes and ketones have been previously investigated in Murchison meteorite samples via colorimetric analysis, gas chromatography (GC), and gas chromatography-mass spectrometry (GC-MS) analysis of water extracts and headspace gas (Jungclaus et al., 1976) and by applying the 1998 Environmental Protection Agency (EPA) O-(2,3,4,5,6-pentafluorobenzyl) hydroxylamine (PFBHA) derivatization method (EPA Method #556 (1998); Pizzarello and

Holmes (2009); Monroe and Pizzarello (2011)). This PFBHA-derivatization method (Scheme 2.2) is commonly used for the analysis of carbonyl compounds in environmental and biological samples and it has been modified in the literature for various suites of terrestrial compounds (see Table A1.1); however, the procedure has not yet been optimized specifically for the analysis of carbonyl compounds extracted from carbonaceous chondrites. Method optimization is particularly important for maximizing yields for isotopic analyses when working with limited quantities of extraterrestrial samples of low organic content. The previous reports of aldehydes and ketones in Murchison identified similar suites of compounds, dominated by low molecular weight acetaldehyde, formaldehyde and acetone; however, the explanation of their origin was limited by the absence of stable isotopic measurements. Compound-specific $\delta^{13}C$ analysis of meteoritic aldehydes and ketones is a key next step for understanding the origins of these carbonyl compounds in the solar system.

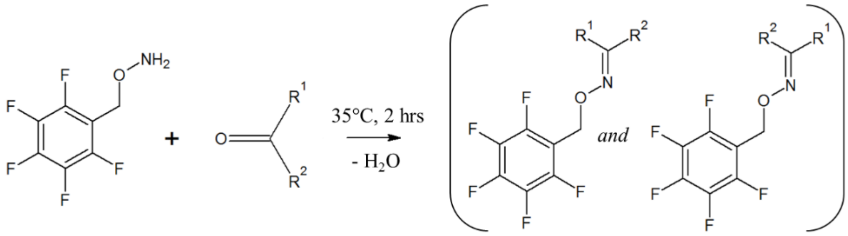

Scheme 2.2. PFBHA derivatization reaction. PFBHA reacts with an aldehyde or ketone to produce the (*E*)- and (*Z*)-*N*-[(pentafluoro-benzyl)oxy] imine derivative.

The objectives of the present study were: (a) to optimize the EPA PFBHA derivatization method specifically for the analysis of aldehydes and ketones in astromaterials in order to maximize both yields and reproducibility for the detection of low molecular weight aldehydes and ketones in samples with organic contents in the parts per billion range; (b) to identify, quantify, and, for the first time, measure the compound-specific $\delta^{13}C$ values of aldehydes and ketones in the Murchison meteorite; and (c) to compare the measured $\delta^{13}C$ values of indigenous aldehydes and ketones with previously measured $\delta^{13}C$ values of other meteoritic organics including amino acids, hydroxy acids, HCN, amines, carboxylic acids, and IOM in Murchison, in order to investigate potential synthetic relationships between these compound classes.

2.2. MATERIALS AND METHODS

2.2.1. Chemicals and reagents

Standards and reagents were purchased from Sigma Aldrich and Fisher Scientific. Five aldehydes and five ketones previously identified in carbonaceous chondrites (Jungclaus et al., 1976; Pizzarello and Holmes, 2009; Monroe and Pizzarello, 2011) were used for the method development experiments and as the standards: formaldehyde, acetaldehyde, propionaldehyde, butyraldehyde, benzaldehyde, acetone, 2-butanone, 2-pentanone, 2-hexanone, and acetophenone. Ultrapure water (Millipore Direct Q3 UV, 18.2 MΩ, 3 ppb total organic carbon; hereafter referred to as "water"), HPLC grade dichloromethane (DCM), double-distilled 6 M HCl, and O-(2,3,4,5,6-pentafluorobenzyl) hydroxylamine hydrochloride of ≥ 99.0% purity were used. All glassware and tools were wrapped in aluminum foil and heated at 450°C for a minimum of 6 hours before use. All vials were capped with PTFE-lined lids.

2.2.2. Murchison sample extraction

An interior chip of the Murchison carbonaceous chondrite (CM2, USNM 5454; extracted mass: 0.5255 g) was provided by the Smithsonian National Museum of Natural History, Washington, D.C. The sample was powdered using an alumina mortar and pestle and extracted with 1 mL of water in a flame-sealed glass ampule at 100°C for 24 hours. After extraction, the sample was centrifuged and the supernatant was transferred to a glass vial. The residual meteorite solid was rinsed three more times using 0.5 mL of water for each rinse. The aqueous supernatant and rinses were combined into one fraction and filtered through quartz wool to remove any remaining solid material from the solution. The quartz wool filter was rinsed two more times using 0.5 mL of water for each rinse. The entire extraction procedure was carried out in parallel with a procedural solvent blank and a serpentine mineral analogue blank (0.420 g; powdered and combusted at 450°C for > 6 hours before extraction).

2.2.3. Derivatization of aldehydes and ketones

Carbonyl compounds were derivatized using an optimized EPA Method #556 for PFBHA derivatization (see Section 2.4.1), as follows: 1 mL of 0.2 mg/mL PFBHA solution was added to the 3.5 mL of combined water extract and rinses. The solution was agitated for 5 minutes and then left to react for 24 hours to allow the derivatization reaction to go to completion. The reaction was quenched by adding 100 μL of 0.4 M HCl solution. 2 mL of dichloromethane were then added to the solution to extract the derivatized carbonyl compounds. The resulting mixture was agitated for 5 minutes and then left undisturbed for 30 minutes to allow the dichloromethane and water layers to settle. The dichloromethane layer was separated from the aqueous layer and brought through an acid-wash step (3 mL of 0.4 M HCl). The extraction of the aqueous layer was repeated with another 2 mL of dichloromethane and the isolated dichloromethane layer was washed with 3 mL of 0.4 M HCl. The 2 x 2 mL dichloromethane extracts containing the oxime derivatives were combined, the volume was reduced to 200 μL under a stream of nitrogen, and the resulting concentrated solution was analyzed by gas chromatography with mass spectrometry and isotope ratio mass spectrometry (GC-MS/IRMS; section 2.2.4).

2.2.4. Identification, quantification and compound-specific $\delta^{13}C$ analysis of aldehydes and ketones

The analysis of derivatized carbonyl compounds was performed using GC-MS/IRMS, which provides compound-specific identification and stable carbon isotopic ratios in parallel (Elsila et al., 2012; Aponte et al. 2014). The GC separation was accomplished using a Thermo Trace GC equipped with a 5 m base-deactivated fused silica guard column (Restek, 0.25 mm ID) and three 30 m length × 0.25 mm I.D. × 0.5 μm film thickness Rxi-5ms capillary columns (Restek) connected using Press-Tight connectors (Restek). The oven program was set as follows: initial temperature was 40 °C, ramped at 10 °C/min to 160 °C, ramped at 5 °C/min to 190 °C, ramped at 10 °C/min to 290 °C and held for 7 min. The carrier gas used was UHP helium (5.0 grade) at 2.6 mL/min flow rate. Triplicate injections of PFBHA-derivatives were made in splitless mode in aliquots of 1 μL. The mass spectrum was used to identify and quantify the meteoritic carbonyl compounds by comparison to reference standards and applying a calibration curve. Targeted ion mass-to-charge ratio (*m/z* = 181.0) was used to identify and quantify compounds (see Table 2.1 for compound identifications). Approximately 10% of the sample eluting from the GC column was directed into a Thermo DSQII electron-impact quadrupole mass spectrometer (ion source set at 200 °C and 70 eV). The remaining 90% of each eluting compound was directed through a Thermo GC-C III interface for oxidation of the compounds to carbon dioxide; the carbon stable isotopic measurement was then made on a Thermo MAT 253 IRMS. The $\delta^{13}C$ values of the eluting compounds were obtained after injection of three pulses of precalibrated CO_2 ($\delta^{13}C = -24.23$‰

VPDB) into the IRMS and computation using Thermo Isodat 2.5 software. In order to correct for the amount of carbon added by the derivatization reagent, underivatized standards were analyzed on a Costech ECS 4010 combustion elemental analyzer (EA) connected to the IRMS. The final $\delta^{13}C$ values of the meteoritic aldehydes and ketones (carbonyls) were calculated using equation 1.

$$\delta^{13}C_{\text{sample carbonyl}} = [((n_{\text{carbonyl}} + n_{\text{d}})/n_{\text{carbonyl}}) \times (\delta^{13}C_{\text{derivatized sample carbonyl}} - \delta^{13}C_{\text{derivatized std carbonyl}})] + \delta^{13}C_{\text{underivatized std carbonyl}} \tag{1}$$

where n_{carbonyl} = number of carbon atoms in underivatized carbonyl and n_{d} = number of carbons added by derivatizing reagent. The precision (standard deviation) of the $\delta^{13}C$ values was obtained using equation 2 (Docherty et al., 2001).

$$\sigma^2_{\text{sample carbonyl}} = \sigma^2_{\text{underivatized std}} + [\sigma^2_{\text{derivatized std}} \times ((n_{\text{carbonyl}} + n_{\text{d}})/n_{\text{carbonyl}})^2] + [\sigma^2_{\text{derivatized sample}} \times ((n_{\text{carbonyl}} + n_{\text{d}})/n_{\text{carbonyl}})^2] \tag{2}$$

2.3. RESULTS

2.3.1. Identification, quantification and compound-specific $\delta^{13}C$ analysis of aldehydes and ketones in the Murchison meteorite

A suite of aldehydes and ketones were identified and quantified in the Murchison meteorite and the $\delta^{13}C$ values were measured for those compounds present in sufficient abundance (formaldehyde, acetaldehyde and acetone). Table 2.1 lists the concentrations and $\delta^{13}C$ values for the measurable aldehydes and ketones in the Murchison sample. Figure 2.2 illustrates the selected ion (*m/z* = 181.0) GC-MS chromatogram of representative injections from the derivatized Murchison meteorite extract, the procedural blanks, and a mixture of derivatized aldehydes and ketone standards. Two chromatographic peaks are observed for most compounds, as (*E*)- and (*Z*)-isomers (two molecules with the same molecular formula but different stereometric configurations) are produced for those carbonyl compounds with asymmetrical chemical structures. Abundances are reported as sums of the (*E*)- and (*Z*)-isomers, whereas the $\delta^{13}C$ values for the two isomers are reported individually. The elution order of the acetaldehyde (*E*)- and (*Z*)-isomer peaks reported here is based on peak identities from previous studies that have used similar GC-MS columns (EPA Method #556, 1998; Cancho et al., 2001). The Murchison sample was dominated by the low molecular weight aldehyde acetaldehyde (89.1 nmol/g), followed by formaldehyde (23.4 nmol/g), acetone (25.8 nmol/g), propionaldehyde (21.4 nmol/g) and higher molecular weight carbonyl compounds at lower abundances. $\delta^{13}C$ values for the three carbonyl compounds measured ranged from +5.3 to +29.1‰, with formaldehyde being the most ^{13}C-depleted and acetaldehyde as the most highly ^{13}C-enriched. The δ^{13}C values for the acetaldehyde (*E*)- and (*Z*)-isomers fell within one standard deviation of one another. A trace amount of formaldehyde was observed in the procedural blank (1.7 nmol) and combusted serpentine blank (1.4 nmol), with δ^{13}C values of −28.1‰ and −27.2‰, respectively. The Murchison formaldehyde abundance and δ^{13}C value were corrected using the procedural blank measurements (Table 2.1). The formaldehyde peak in the Murchison sample is partially co-eluting with an unidentified compound (Table 2.1). The mass spectrum of the compound does not contain the characteristic 181.0 m/z ion targeted for quantification; therefore, the co-elution has not affected the abundance estimate for formaldehyde in the sample. The co-eluting peak may have had a minor influence on the formaldehyde δ^{13}C measurement, shifting the value towards a slightly more ^{13}C-depleted composition.

Table 2.1. Concentrations (nmol/g) and δ^{13}C values of aldehydes and ketones identified in the Murchison meteorite.

Peak label	Compound	Abundance (nmol/g)		δ^{13}C (‰)
		This study[a] (± S.D.[b])	Pizzarello and Holmes (2009)	
	Aldehydes			
1	Formaldehyde[c]	23.4 ± 1.6	10.0	+5.3 ± 4.6
2	(E)-Acetaldehyde	89.1 ± 9.8	24.0	+29.1 ± 3.3
3	(Z)-Acetaldehyde			+16.9 ± 3.6
5,6	Propionaldehyde	21.4 ± 1.1	23.5	n.d.
9,10	Butyraldehyde	13.3 ± 0.9	32.2	n.d.
16.17	Benzaldehyde	10.9 ± 1.6	7.6	n.d.
	Ketones			
4	Acetone	25.8 ± 3.8	47.3	+8.4 ± 6.0
7,8	2-Butanone	10.2 ± 1.4	6.9	n.d.
11,12	2-Pentanone	5.6 ± 0.4	1.5	n.d.
13,14	2-Hexanone	6.0 ± 0.3	25.0	n.d.
15,18	Acetophenone	1.7 ± 0.3	n.d.	n.d.
	Total abundance	*207.3 ± 20.8*	*200*	

[a] Abundances represent the sum of the two (*E*) and (*Z*) isomers, where applicable.

[b] S.D. − Standard deviation of three sequential injections.

[c] Partially co-eluting with an unidentified compound

n.d. − not determined.

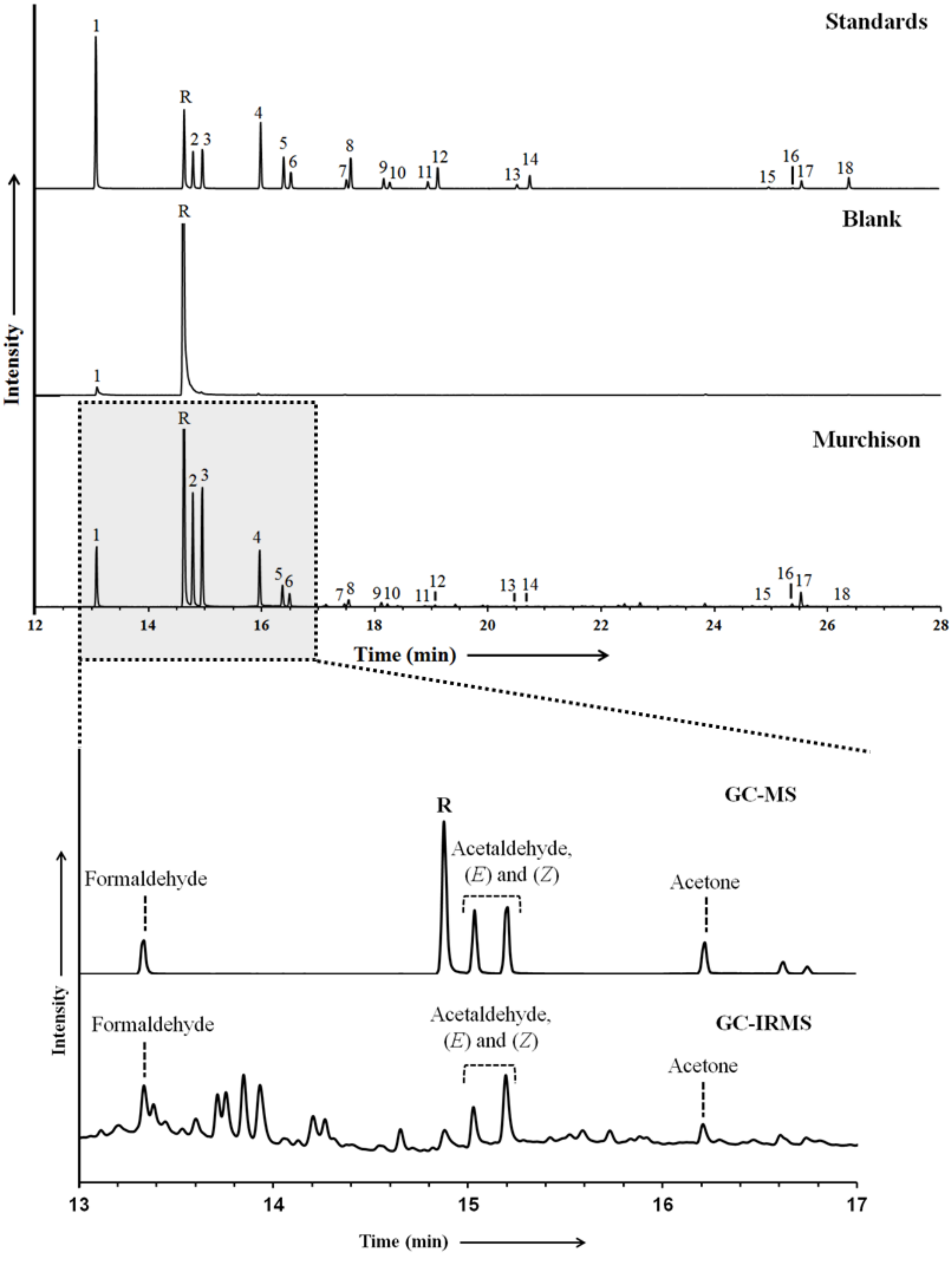

Figure 2.2. GC-MS chromatograms of derivatized aldehyde and ketone standards, the procedural blank, and the Murchison meteorite extract, and a GC-IRMS chromatogram of carbonyl compounds in the Murchison sample measured for $\delta^{13}C$. GC-MS peaks represent PFBHA derivatives, containing the characteristic ion of *m/z* = 181.0. Peak *R* represents unreacted PFBHA derivatization reagent. The identities of the peaks are presented in Table 2.1.

For all three replicate injections of the Murchison sample, the PFBHA reagent peak and the (*E*)-acetaldehyde isomer peak in the GC-IRMS chromatogram appeared relatively small compared to the corresponding peaks in the GC-MS chromatograms (Figure 2.2). This difference in peak height was not observed for any compounds in the standard samples. The relative decrease in peak heights observed for the PFBHA reagent and (*E*)-acetaldehyde peaks in the Murchison GC-IRMS data suggests that these two compounds experienced incomplete combustion in the GC-IRMS combustion reactor after eluting off of the GC-MS column. Incomplete combustion would be expected to induce some stable isotopic fractionation, which would have affected the (*E*)-acetaldehyde $\delta^{13}C$ value. As such, the (*Z*)-acetaldehyde $\delta^{13}C$ value reported here is considered to be a more representative composition for acetaldehyde in Murchison.

2.4. DISCUSSION

2.4.1. Method optimization for PFBHA derivatization and analysis of aldehydes and ketones in astromaterials

2.4.1.1. EPA Method #556 previously used for the quantification of meteoritic carbonyl compounds

The EPA Method #556 (Scheme 2.2), used previously for the analysis of the Murchison meteorite (Pizzarello and Holmes, 2009), is carried out as follows: carbonyl compounds are derivatized in water (pH = 4) by adding 1 mL of a 15 mg/mL *O*-(2,3,4,5,6-Pentafluorobenzyl) hydroxylamine hydrochloride (PFBHA) solution and heating the solution at 35°C for 2 hours. Following the derivatization step, 2-4 drops of concentrated H_2SO_4 are added to the sample to prevent extraction of excess PFBHA reagent. The oxime derivatives are extracted from solution with hexane and transferred to a vial containing 0.2 N H_2SO_4, as an acid-wash step. The hexane layer, containing the oxime derivatives, is then isolated, concentrated to a small volume via evaporation, and analyzed via GC-MS.

2.4.1.2. Modifications to the EPA Method #556

In the present study, we have optimized the EPA PFBHA derivatization method using a set of ten aldehyde and ketone standards previously identified in carbonaceous chondrites (see Section 2.2.1), with an aim to maximize yields and reproducibility between sample sets. Derivatization times reported in the literature vary widely, from 10 minutes to 96 hours at room temperature (see Table A1.1). While most aldehydes are expected to derivatize completely within a few hours, ketones are known to require much longer derivatization times and are generally given 24 hours for the reaction to reach completion (Kobayashi et al., 1980; Glaze et al., 1989; Yamada and Somiya, 1989). In the present study, we tested four derivatization times (2, 8, 16 and 24 hours) to confirm the influence of reaction time on our suite of standards (Figure 2.3a). While the total yields of the lower molecular weight aldehydes appear to plateau within 2 hours, the ketones required 16−24 hours in order to reach their highest relative yields. As such, we have chosen a 24-hour derivatization time to maximize our yields and reproducibility. The EPA Method #556 recommends using hexane to extract the carbonyl derivatives from aqueous solution; however, dichloromethane is also commonly used in the literature for this method (see Table A1.1). Thus, we compared the extraction efficiencies of dichloromethane and hexane for our suite of derivatized standards (Figure 2.3b). The use of dichloromethane resulted in relatively higher yields and greater reproducibility for all of our compounds of interest and was, therefore, selected as the extraction solvent for this study.

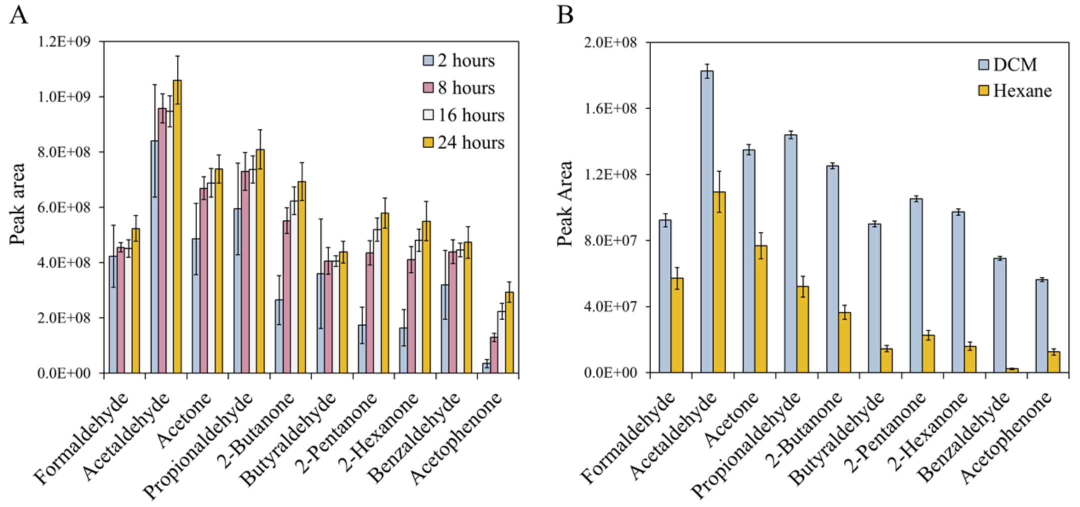

Figure 2.3. **A.** Total yields (GC-MS peak areas) of aldehyde and ketone oxime derivatives from 2-, 8-, 16- and 24-hour derivatization reactions (standard abundances: 1 mL of 50 µg/mL solution). Each individual bar represents 3 replicate samples and error bars represent one standard deviation from the mean. All oxime derivatives were isolated using dichloromethane (DCM) as the extraction solvent. **B.** Extraction efficiency of DCM vs. hexane for aldehyde and ketone oxime derivatives. Each bar represents the average of 12 replicate samples and the error bars represent one standard deviation from the mean. All derivatization reactions were carried out for 24 hours.

Other changes to the method included: (1) using a lower concentration of PFBHA solution (0.2 mg/mL), as the expected yields of aldehydes and ketones in astromaterials are much lower than terrestrial environmental samples and excess PFBHA reagent in solution can result in less effective extraction of the derivatives into the organic phase (Rodigast et al., 2015); (2) replacing H_2SO_4 with HCl, as HCl can be double-distilled for higher purity; (3) carrying out a 30 minute extraction time, to allow for a complete extraction of the target analytes, as recommended by Rodigast et al. (2015); and (4) storing samples in solution, at low temperature (4°C), to avoid decomposition of the oxime derivatives (see Section 2.4.1.3).

2.4.1.3. Stability of the PFBHA oxime derivatives

The stability of the aldehyde and ketone derivatives during sample work-up and long-term storage is particularly important when working with astromaterials, as sample abundances are generally small and limited, and degradation of the compounds may induce stable isotopic and enantiomeric fractionations. Our experiments revealed a notable drawback of the PFBHA derivatization method; the oxime derivatives appear to degrade when the sample solutions are evaporated to dryness, and the decomposition reaction appears to be accelerated when the samples are stored dry at room temperature, as opposed to in low temperature conditions (4°C) (see Figure A1.1). A decomposition product, identified by the NIST Mass Spectral Library as PFBHA, was observed in the GC-MS chromatograms of dried samples (see Figure A1.2), suggesting that the aldehyde and ketone derivatives decomposed back to their original constituents (i.e., PFBHA and volatile aldehydes and ketones) during or after the solvent evaporation step. This decomposition reaction, involving hydrolysis of the C-N bond (Kalia and Raines, 2008), could be taking place as a result of a small amount of residual acid in the vials, which becomes difficult to remove as the sample is concentrated. As a preventative measure, we stored the PFBHA oxime derivatives in solution, at low temperatures (<4ºC). Several studies report using amber vials and bottles for derivatizing and storing aldehyde and ketone samples, implying that the oxime derivatives may be light-sensitive (Glaze et al., 1989; Spaulding and Charles, 2002; Hudson et al., 2007; Serrano et al., 2013). We have ruled out photolysis as the cause of the decomposition reaction observed here by limiting sample exposure to light. The decomposition of the derivatives in dried samples persisted despite carrying out all derivatization reactions, clean-up steps, and storage in amber vials.

2.4.2. Distribution and abundances of aldehydes and ketones in Murchison

The total yield of aldehydes and ketones in Murchison reported here is similar to the total yield attained by Pizzarello and Holmes (2009), but the lower molecular weight aldehydes, formaldehyde and acetaldehyde, were detected at relatively higher abundances in the present study (Table 2.1). Differences in the relative abundances between the two studies may be partially attributable to sample heterogeneity, as has been reported for other compound classes (Cronin and Pizzarello, 1983; Krishnamurthy et al., 1992; Pizzarello et al., 2003; Aponte et al., 2014). Furthermore, Pizzarello and Holmes (2009) combined repeat water extractions of their Murchison sample material, which may have resulted in higher overall yields for the higher molecular weight aldehydes and ketones, as the higher molecular weight compounds are relatively less soluble in water and may require longer extraction times.

Considering the ubiquitous presence of formaldehyde in the ISM, the abundance of formaldehyde in the Murchison meteorite is lower than was expected. A relatively low abundance of formaldehyde in Murchison was similarly observed by Pizzarello and Holmes (2009) and Jungclaus et al. (1976) and may be partially attributable to its low boiling point (-19°C), as the Murchison meteorite samples have been stored long-term in room temperature conditions. Its low abundance relative to other carbonyl species in Murchison may also be a result of its high reactivity and involvement in prebiotic synthetic reactions inside the parent body, including for example the formose reaction; it is possible that formaldehyde may be present inside Murchison as an insoluble polymer (Cooper et al., 2001; Cody et al., 2011; Meinert et al., 2016).

2.4.3. Isotopic predictions for interpreting aldehyde and ketone δ^{13}C compositions

In order to make direct comparisons between δ^{13}C values of different meteoritic compound classes, some assumptions need to be made regarding the original isotopic compositions of the compounds, the alteration history of the asteroid parent body and the associated chemical reactions (Aponte et al., 2017). The carbon isotope compositions of early solar system aldehydes and ketones prior to their incorporation into the asteroid parent body are assumed to have been highly ^{13}C-enriched (δ^{13}C > +117‰), based on recent ^{12}C/^{13}C measurements for interstellar formaldehyde (^{12}C/^{13}C = 15-80, Wirström et al., 2012) and the average ^{12}C/^{13}C measurement for nearby molecular clouds (^{12}C/^{13}C = 80, Henkel et al., 1982). If the aldehydes and ketones detected in the

Murchison meteorite were relict, unreacted Strecker synthesis precursors, we would expect them to be relatively enriched in ^{13}C compared to their corresponding α-amino acid products. This prediction assumes that the Strecker synthesis reaction involves significant kinetic isotope fractionations and that the amino acid products have not been fractionated via subsequent chemical reactions during thermal/aqueous alteration (i.e. that the amino acid pool has not been shifted towards a relatively ^{13}C-enriched composition due to the preferential reaction of isotopically lighter amino acids). The isotopic composition of the unreacted carbonyl pool, and therefore the isotopic separation between carbonyl reactants and amino acid products, also depends on what proportion of the aldehydes and ketones have been converted into amino acids, which remains unknown. Lastly, it is assumed that any variation observed between studies primarily reflects differences in methodologies and that the Murchison meteorite does not exhibit large heterogeneity between subsamples.

2.4.4. Possible origins for the aldehydes and ketones in Murchison

2.4.4.1. Lack of a primordial isotopic signature

The $\delta^{13}C$ measurements for the aldehydes and ketones in Murchison are much less ^{13}C-enriched than would be expected for a primordial pool of unreacted Strecker synthesis precursors, assuming that early solar system aldehydes and ketones incorporated into the Murchison parent body asteroid exhibited highly ^{13}C-enriched isotopic signatures and that this signature would be amplified as Strecker synthesis shifts the reactant pool towards a more ^{13}C-enriched composition. The lack of a primordial ^{13}C-enriched isotopic signature for these compounds in Murchison may indicate that all of the early solar system aldehydes and ketones in the asteroid parent body were consumed early on, either via Strecker amino acid synthesis or through alternate chemical reactions. This is a reasonable possibility as aldehydes and ketones are highly reactive species and are likely to polymerize and react with other chemical species fairly readily in asteroidal conditions (Cleaves, 2008; Kebukawa and Cody, 2015). Our observations suggest that the aldehydes and ketones identified in this study were synthesized at a later stage, potentially during aqueous alteration reactions after accretion of the parent body asteroid. A secondary generation of aldehydes and ketones on asteroid parent bodies may imply that these compounds are more readily available in the solar system than previously thought.

2.4.4.2. Chemical oxidation of insoluble organic matter as a potential source of carbonyl compounds in Murchison

Low-temperature aqueous alteration of IOM has been proposed as a potential source of water-soluble organic compounds in carbonaceous chondrites (Cody and Alexander, 2005). The oxidation of IOM in aqueous solution has been shown to convert aliphatic carbon to CO moieties, in addition to organic acids and CO_2 (Cody and Alexander, 2005) and this mechanism may help to explain the lack of a primordial signature for the carbonyl compounds in Murchison. The more labile, aliphatic moieties of the IOM are expected to be relatively ^{13}C-enriched compared to the aromatic portions (Kerridge et al., 1987), as the aromatic components of the IOM are considered to reflect a longer history of chemical processing in the cold ISM and/or during early solar system formation, resulting in progressive ^{13}C-depletion over time. Consistent with this theory, the aldehyde and ketone $\delta^{13}C$ compositions reported here (+5.3 to +29.1‰) are relatively ^{13}C-enriched in comparison to measurements of IOM-derived aromatics in Murchison (-25‰ to -1‰; Sephton et al., 1998; Sephton and Gilmour, 2001).

2.4.4.3. Alteration-driven dissolution or decomposition of soluble organics

Another possible origin for the aldehydes and ketones detected in Murchison may be alteration-driven degradation of other soluble organic compound classes (e.g. amino acids, keto acids) in the parent body asteroid, as discussed in detail below.

2.4.5. Investigating synthetic relationships between aldehydes and ketones and other soluble organics in Murchison

Similarities or trends observed between the compound-specific carbon isotope compositions of the carbonyl compounds in Murchison and other indigenous organics may act as isotopic signatures for precursor-product formation relationships. While these values and data comparisons are not definitive indicators for specific chemical reactions, they provide a basis for elucidating the reaction history of aldehydes and ketones in the asteroid parent body.

2.4.5.1. Strecker-cyanohydrin synthesis precursors and products

The $\delta^{13}C$ values of Strecker α-amino acid and α-hydroxy acid products depend on a combination of: (1) the carbon isotope composition of the precursor carbonyl compound, (2) the carbon isotope composition of the reactant HCN, and (3) the kinetic isotope fractionation effects associated with each step of the reaction (Scheme 2.1). The α-carbon and the alkyl (R) groups of the amino acid and hydroxy acid products are derived from the precursor aldehyde or ketone, while the carboxyl carbon is derived from HCN (Scheme 2.1). The relative influence of the aldehyde or ketone $\delta^{13}C$ value on the amino acid/hydroxy acid $\delta^{13}C$ value depends on the number of carbon atoms contained in, and thus contributed from, the R groups. Comparing the $\delta^{13}C$ values of carbonyl compounds, amino acids, hydroxy acids and HCN can be used to evaluate a potential Strecker precursor-product relationship between these compounds. In this study, we focus primarily on isotopic comparisons between aldehydes, ketones and their structurally analogous α-amino acids, due to the large data set of stable isotopic measurements previously attained for amino acids in Murchison (Engel et al., 1990; Pizzarello et al., 2004; Elsila et al., 2012).

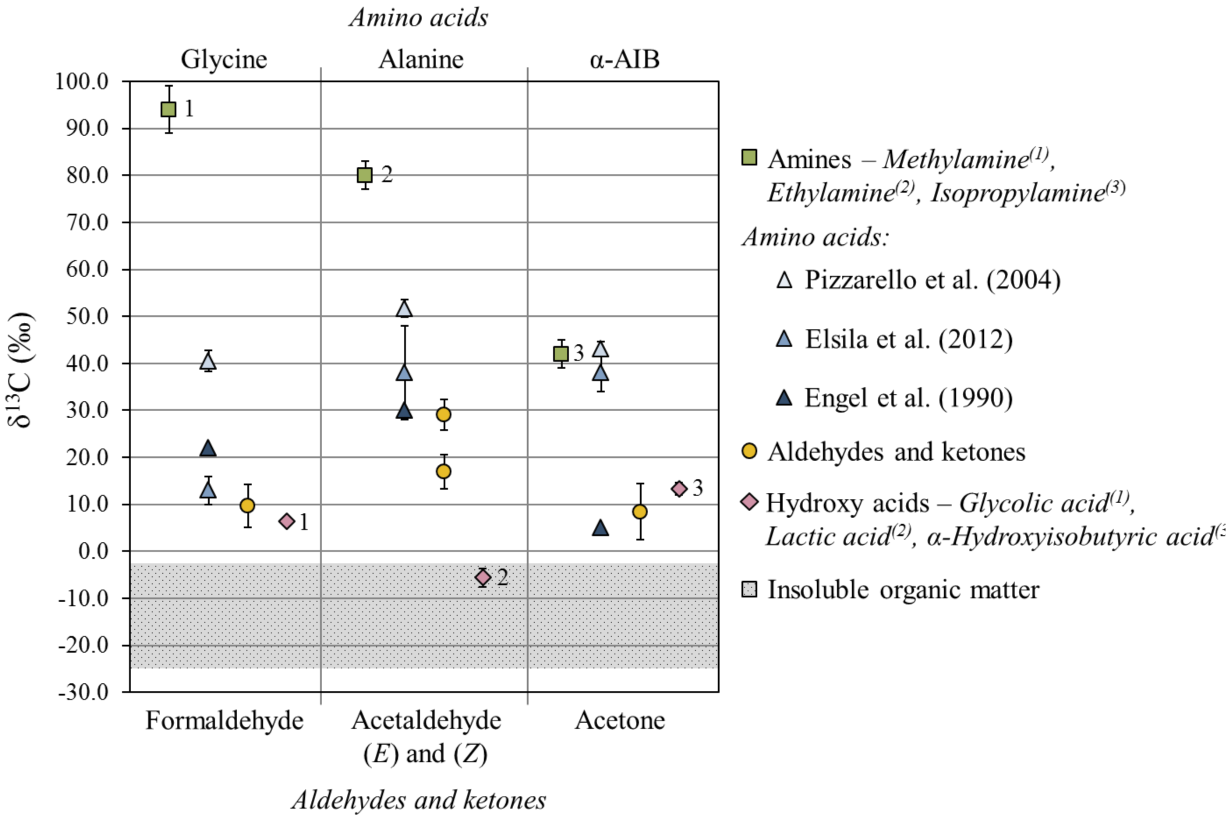

Figure 2.4. Carbon stable isotope compositions of aldehydes and ketones (this study), their corresponding amines (Aponte et al., 2014), amino acids (Engel et al., 1990; Pizzarello et al., 2004; Elsila et al., 2012), hydroxy acids (Pizzarello et al., 2010) and aromatics derived from macromolecular insoluble organic material (Sephton et al., 1998; Sephton and Gilmour, 2001) in the Murchison meteorite. The two acetaldehyde data points represent the (*E*) and (*Z*) isomers.

The carbon isotope compositions of formaldehyde, acetaldehyde and acetone in Murchison share some similarities with the $\delta^{13}C$ values of their structurally-analogous Strecker amino acids, falling within error of alanine and α-AIB $\delta^{13}C$ values from Engel et al. (1990) and glycine and alanine $\delta^{13}C$ values from Elsila et al. (2012) (Figure 2.4). Acetaldehyde and its structurally analogous amino acid, alanine, are the most highly ^{13}C-enriched compounds for both compound classes. It is entirely possible that these similar ranges of $\delta^{13}C$ values observed for the two compound classes resulted from separate formation reactions and alteration histories. However, if these similarities in compositions do represent a synthetic relationship between the carbonyl compounds and amino acids in Murchison, there are three possibilities to consider: (1) that the aldehydes and ketones in Murchison are the Strecker precursors to the indigenous amino acids; (2) that the aldehydes and ketones identified are derived from alteration-driven decomposition of the amino acids; or (3) that the aldehydes and ketones and amino acids are all derived from a common ^{13}C-enriched source.

Strecker amino acid products are expected to be relatively depleted in ^{13}C compared to their aldehyde and ketone precursors, unless the chemical reactions do not involve significant carbon isotope fractionations, in which case the $\delta^{13}C$ values for the reactants and products would be approximately equal. Amino acids with $\delta^{13}C$ values that are relatively enriched in ^{13}C compared to their structurally analogous aldehydes and ketones can be interpreted as having been isotopically fractionated to some extent via subsequent chemical reactions following Strecker synthesis, or as having been derived, at least partially, from another carbon source. In this study, the similar $\delta^{13}C$ ratios of the aldehydes, ketones and amino acids suggests that a precursor-product Strecker relationship may relate these compound classes. However, aldehydes and ketones are ^{13}C-depleted relative to some of the amino acids, implying that other factors may have also affected the measured isotopic values. $\delta^{13}C$ values measured for the Strecker reactant HCN (ranging from +1.4 to +7.3‰; Pizzarello et al., 2004) are similarly ^{13}C-depleted and offset from the amino acid $\delta^{13}C$ values, with the exception of the Engel et al. (1990) α-AIB value. The hydroxy acid $\delta^{13}C$ values reported by Pizzarello et al. (2010) share some similarities with the aldehyde and ketone $\delta^{13}C$ values reported here (Figure 2.4); the glycolic acid and α-hydroxyisobutyric acid values overlap within the error limits of the structurally analogous formaldehyde and acetone values, respectively. The lactic acid $\delta^{13}C$ value is an exception, as it is highly ^{13}C-depleted compared to its structural analogue, acetaldehyde; however, the authors discussed a low recovery for the extraction and work-up procedure, which may have resulted in some isotopic fractionation in the analysis of this particular compound (Pizzarello et al., 2010). With the exception of the lactic acid−acetaldehyde comparison, the aldehydes and ketones are more ^{13}C-depleted than would be expected for a pool of unreacted Strecker precursors to α-hydroxy acids. The fact that both pools of Strecker reactants contained in Murchison (i.e. carbonyls and HCN) exhibit more ^{13}C-depleted compositions than the corresponding amino acid and hydroxy acid products suggests that some other chemical processes have been recorded in these values. For example, the α-amino acids and α-hydroxy acids detected in Murchison may have been partially generated from an earlier pool of Strecker reactants or via another synthetic mechanism, or they may have been further fractionated to more ^{13}C-enriched compositions via alteration-driven chemical reactions.

We consider the possibility that the aldehydes, ketones and amino acids may be intimately connected, not solely by Strecker synthesis, but also by decomposition of the amino acids during aqueous alteration on the parent body asteroid. An episodic decomposition or dissolution of α-amino acids in between intermittent Strecker synthesis could explain the similar δ^{13}C values amongst the aldehydes, ketones and amino acids, although this is currently only speculative, as the temperatures experienced during aqueous alteration on the Murchison asteroid are arguably insufficient for amino acid degradation. Aqueous solutions of α-amino acids can undergo decomposition at elevated temperatures, yielding aldehyde and ketone products (Schonberg and Moubacher, 1951); however, these reactions generally take place at temperatures > 220°C (Lien and Nawar, 1974) and temperature estimates for aqueous alteration on the Murchison parent body asteroid are much lower, ranging from 0-80°C (Clayton and Mayeda, 1999; Baker et al., 2002; Guo and Eiler, 2007). Whether or not long-duration (several million years; Krot et al., 2015) aqueous alteration, catalyzed by mineral interactions, would be sufficient to induce amino acid degradation at these low temperatures has not been evaluated experimentally; however, laboratory simulations of aqueous alteration in the presence of mineral surfaces at high temperatures (>156°C) have shown that amino acid degradation via decarboxylation and deamination is greatly accelerated under these conditions (McCollom, 2013).

2.4.5.2. δ^{13}C comparisons with keto acids, amines, and carboxylic acids

The similar δ^{13}C compositions of aldehydes, ketones and amino acids in Murchison could also indicate that they are all partially derived from a common source of soluble organic carbon.

For example, some of the aldehydes, ketones and amino acids could be linked by reactions involving keto acids; aldehydes and ketones could be derived from degradation of keto acids during aqueous alteration, while the amino acids may be synthesized from the α-keto acids via reductive amination (Huber and Wächtershäuser, 2003). For instance, thermal decomposition of pyruvic acid yields acetaldehyde (Taylor, 1987), while reductive amination of pyruvic acid yields its structurally analogous amino acid, alanine (Yanagawa et al., 1982). Keto acids, including pyruvic acid, acetoacetic acid, oxaloacetic acid, and citric acid, have been detected in carbonaceous chondrites (Cooper et al., 2005; Cooper et al., 2011); however, their stable isotopic compositions have not yet been measured, limiting our ability to investigate this theory. Furthermore, these types of chemical reactions have only been described for terrestrial samples and have not yet been evaluated for cosmochemical conditions.

Amines and carboxylic acids are also potential structural relatives of carbonyl compounds as they can be synthesized via reductive amination of aldehydes and ketones and oxidation of aldehydes, respectively (Figure 2.1). The amine $\delta^{13}C$ values reported by Aponte et al. (2014) were generally much more ^{13}C-enriched than the aldehydes and ketones reported here, suggesting that the amines in Murchison were not produced via reductive amination of the aldehydes and ketones identified. As for carboxylic acids, there are currently no reported $\delta^{13}C$ values for formic acid in Murchison, though Yuen et al. (1984) reported a +22.7‰ $\delta^{13}C$ ratio for acetic acid in Murchison, which falls within the error limits of the acetaldehyde $\delta^{13}C$ compositions reported here. Huang et al. (2005) reported a relatively lower $\delta^{13}C$ value for acetic acid (-7.7‰); however, the authors attributed this depletion to some terrestrial contribution during sample storage. The potential relationship between carboxylic acids and aldehydes in Murchison is difficult to fully assess with very few data points to consider.

2.5. CONCLUSIONS

The aldehyde and ketone content of the Murchison meteorite and their carbon isotope compositions provide a snapshot of the post-alteration prebiotic organic chemistry of the parent body asteroid, as well as some important information about the history of the asteroid and the synthetic reactions involved. Our carbon isotope analyses of aldehydes and ketones in Murchison revealed a distinct composition, dominated by acetaldehyde, formaldehyde and acetone, with relatively ^{13}C-depleted compositions that appear to share isotopic similarities with other prebiotic organic compound classes. This is in contrast to the formaldehyde-dominated, highly ^{13}C-enriched, carbonyl content of the interstellar medium. This large disparity in composition between the two environments suggests that the prebiotic chemistry and alteration history of the parent body asteroid plays a major role in generating a secondary source of carbonyl compounds in the solar system. Given the long history of the Murchison parent body asteroid and the complexity of its organic content, this compilation of data indicates that the aldehydes, ketones, and other compound classes are interconnected by a dynamic series of chemical reactions, and suggests that aldehydes and ketones are potentially more common in the Universe than previously thought.

2.6. REFERENCES

Abdel-Magid A. F., K. G. Carson, B. D. Harris, C. A. Maryanoff, and R. D. Shah (1996) Reductive amination of aldehydes and ketones with sodium triacetoxyborohydride. Studies on direct and indirect reductive amination procedures. *Journal of Organic Chemistry* **61**, 3849-3862.

Allamandola, L. J., S. A. Sandford, and G. J. Valero (1988) Photochemical and thermal evolution of interstellar/precometary ice analogs. *Icarus* **76**, 225-252.

Aponte, J. C., J. P. Dworkin, and J. E. Elsila (2014) Assessing the origins of aliphatic amines in the Murchison meteorite from their compound-specific carbon isotopic ratios and enantiomeric composition. *Geochimica et Cosmochimica Acta* **141**, 331-345.

Aponte, J. C., J. E. Elsila, D. P. Glavin, S. N. Milam, S. B. Charnley, and J. P. Dworkin (2017) Pathways to meteoritic glycine and methylamine. *ACS Earth and Space Chemistry*, DOI: 10.1021/acsearthspacechem.6b00014

Awad, Z., T. Chigai, Y. Kimura, O. M. Shalabiea, and T. Yamamoto (2005) New rate constants of hydrogenation of CO on H_2O-CO ice surfaces. *The Astrophysical Journal* **626**, 262-271.

Baker, L., I. A. Franchi, I. P. Wright, and C. T. Pillinger (2002) The oxygen isotopic composition of water from Tagish Lake: Its relationship to low-temperature phases and to other carbonaceous chondrites. *Meteoritics & Planetary Science* **37**, 977-985.

Bisschop, S. E., G. W. Fuchs, E. F. van Dishoeck, and H. Linnartz (2007) H-atom bombardment of CO_2, HCOOH, and CH_3CHO containing ices. *Astronomy & Astrophysics* **474**, 1061-1071.

Bossa, J.-B. F. Duvernay, P. Theulé, F. Borget, L. d'Hendecourt, T. Chiavassa (2009) Methylammonium methylcarbamate thermal formation in interstellar ice analogs: a glycine salt precursor in protostellar environments. *Astronomy & Astrophysics* **506**, 601-608.

Botta, O. and J. L. Bada (2002) Extraterrestrial organic compounds in meteorites. *Surveys in Geophysics* **23**, 411–467.

Burk M. J., J. P. Martinez, J. E. Feaster, and N. Cosford (1994) Catalytic asymmetric reductive amination of ketones via highly enantioselective hydrogenation of the C=N double bond. *Tetrahedron* **50**, 4399-4428.

Cancho, B., F. Ventura and M. T. Galceran (2001) Determination of aldehydes in drinking water using pentafluorobenzylhydroxylamine derivatization and solid-phase microextraction. *Journal of Chromatography* **943**, 1-13.

Charnley, S. B., P. Ehrenfreund, T. J. Millar, A. C. A. Boogert, A. J. Markwick, H. M. Butner, R. Ruiterkamp, and S. D. Rodgers (2004) Observational tests for grain chemistry: Posterior Isotopic labelling. *Monthly Notices of the Royal Astronomical Society* **347**, 157-162.

Clayton, R. N., and T. K. Mayeda (1999) Oxygen isotope studies in carbonaceous chondrites. *Geochimica et Cosmochimica Acta* **63**, 2089-2104.

Cleaves, H. J. (2008) The prebiotic geochemistry of formaldehyde. *Precambrian Research*, **164**, 111-118.

Cody, G. D., and C. M. O'D. Alexander (2005) NMR studies of chemical structural variation of insoluble organic matter from different carbonaceous chondrite groups. *Geochimica et Cosmochimica Acta* **69**, 1085-1097.

Cody, G. D., E. Heying, C. M. O'D. Alexander, L. R. Nittler, A. L. D. Kilcoyne, S. A. Sandford, and R. M. Stroud (2011) Establishing a molecular relationship between chondritic and cometary organic solids. *PNAS* **108**, 19171-19176.

Cooper, G., N., N. Kimmich, W. Belisle, J. Sarinana, K. Brabham, and L. Garrel (2001) Carbonaceous meteorites as a source of sugar-related organic compounds for the early Earth. *Nature* **414**, 879-883.

Cooper, G., A. Dugas, A. Byrd, P. M. Chang and N. Washington (2005) Keto-acids in carbonaceous meteorites. *36th Lunar and Planetary Science Conference*, #2381.

Cooper, G., C. Reed, D. Nguyen, M. Carter, and Y. Wang (2011) Detection and formation scenario of citric acid, pyruvic acid, and other possible metabolism precursors in carbonaceous meteorites. *PNAS* **108**, 14015-14020.

Corey, E. J., N. W. Gilman, and B. E. Ganem (1968) New methods for the oxidation of aldehydes to carboxylic acids and esters. *Journal of the American Chemical Society* **90**, 5616-5617.

Cronin, J. R. and S. Pizzarello (1983) Amino acids in meteorites. *Advances in Space Research* **3**, 5-18.

Deamer, D., J. P. Dworkin, S. A. Sandford, M. P. Bernstein, and L. J. Allamandola (2002) The first cell membranes. *Astrobiology* **2**, 371-381.

de Marcellus, P., C. Meinert, I. Myrgorodska, L. Nahon, T. Buhse, L. Le Sergeant D'Hendecourt, and U. J. Meierhenrich (2015) Aldehydes and sugars from evolved precometary ice analogs: Importance of ices in astrochemical and prebiotic evolution. *PNAS* **112**, 965-970.

Elsila, J. E., S. B. Charnley, A. S. Burton, D. P. Glavin, and J. P. Dworkin (2012) Compound-specific carbon, nitrogen, and hydrogen isotopic ratios for amino acids in CM and CR chondrites and their use in evaluating potential formation pathways. *Meteoritics & Planetary Science* **47**, 1517-1536.

Engel, M. H., S. A. Macko, and J. A. Silfer (1990) Carbon isotope composition of individual amino acids in the Murchison meteorite. *Nature* **348**, 47-49.

EPA Method 556: Determination of carbonyl compounds in drinking water by pentafluorobenzylhydroxylamine derivatization and capillary gas chromatography with electron capture detection (1998) National exposure research laboratory office of research and development. US Environmental Protection Agency, Cincinnati, Ohio, 45268.

Glaze, W. H., M. Koga and D. Cancilla (1989) Ozonation byproducts. 2. Improvement of an aqueous-phase derivatization method for the detection of formaldehyde and other carbonyl compounds formed by the ozonation of drinking water. *Environmental Science & Technology* **23**, 838-847.

Guo, W., and J. M. Eiler (2007) Temperatures of aqueous alteration and evidence for methane generation on the parent bodies of the CM chondrites. *Geochimica et Cosmochimica Acta* **71**, 5565-5575.

Henkel, C., T. L. Wilson, and J. Bieging (1982) Further ($^{12}C/^{13}C$) ratios from formaldehyde: A variation with distance from the galactic center. *Astronomy & Astrophysics* **109**, 344–351.

Holtom, P. D., C. J. Bennett, Y. Osamura, N. J. Mason, and R. I. Kaiser (2005). A combined experimental and theoretical study on the formation of the amino acid glycine (NH_2CH_2COOH) and its isomer ($CH_3NHCOOH$) in extraterrestrial ices. *The Astrophysical Journal* **626**, 940.

Huang, Y., Y. Wang, M. R. Alexandre, T. Lee, C. Rose-Petruck, M. Fuller, and S. Pizzarello (2005) Molecular and compound-specific isotopic characterization of monocarboxylic acids in carbonaceous chondrites. *Geochimica et Cosmochimica Acta* **69**, 1073-1084.

Huang, Y., J. C. Aponte, J. Zhao, R. Tarozo, and C. Hallmann (2015) Hydrogen and carbon isotopic ratios of polycyclic aromatic compounds in two CM2 carbonaceous chondrites and implications for prebiotic synthesis. *Earth and Planetary Science Letters* **426**, 101-108.

Huber, C., and G. Wächtershäuser (2003) Primordial reductive amination revisited. *Tetrahedron Letters* **44**, 1695-1697.

Hudson, E. D., K. Okuda, and P. A. Ariya (2007) Determination of acetone in seawater using derivatization solid-phase microextraction. *Analytical and Bioanalytical Chemistry* **388**, 1275-1282.

Hudson, R. L., Lewis, A. S., Moore, M. H., Dworkin, J. P., and M. P. Martin (2009) Enigmatic isovaline: investigating the stability, racemization and formation of a non-biological meteoritic amino acid. *ASP Conference Series* **420**, 157-162.

Irvine (1999) The composition of interstellar molecular clouds. *Space Science Reviews* **90**, 203-218.

Jungclaus, G. A., G. U. Yuen, C. B. Moore, J. G. Lawless (1976) Evidence for the presence of low molecular weight alcohols and carbonyl compounds in the Murchison meteorite. *Meteoritics* **11**, 231-237.

Kalia, J. and R. T. Raines (2008) Hydrolytic stability of hydrazones and oximes. *Angewandte Chemie* **47**, 7523-7526.

Kebukawa, Y., and G. D. Cody (2015) A kinetic study of the formation of organic solids from formaldehyde: Implications for the origin of extraterrestrial organic solids in primitive Solar System objects. *Icarus* **248**, 412-423.

Kobayashi, K., M. Tanaka, and S. Kawai (1980) Gas chromatographic determination of low-molecular-weight carbonyl compounds in aqueous solution as their O-(2,3,4,5,6-pentafluorobenzyl) oximes. *Journal of Chromatography* **187**, 413-417.

Krishnamurthy, R. V., S. Epstein, J. R. Cronin, S. Pizzarello, and G. U. Yuen (1992) Isotopic and molecular analyses of hydrocarbons and monocarboxylic acids of the Murchison meteorite. *Geochimica et Cosmochimica Acta* **56**, 4045-4058.

Krot, A. N., K. Nagashima, C. M. O'D Alexander, F. J. Ciesla, W. Fujiya, and L. Bonal (2015) Sources of water and aqueous activity on the chondrite parent asteroids. In *Asteroids IV*, P. Michel et al., Eds. University of Arizona Press, Tuscon, 635-660.

Kvenvolden, K., J. Lawless, K. Pering, E. Peterson, J. Flores, C. Ponnamperuma, I. R. Kaplan, C. Moore (1970) Evidence for extraterrestrial amino-acids and hydrocarbons in the Murchison meteorite. *Nature* **228**, 923-926.

Lee C.-W., J.-K. Kim, E.-S. Moon, Y. C. Minh, and H. Kang (2009) Formation of glycine on ultraviolet-irradiated interstellar ice-analog films and implications for interstellar amino acids. *The Astrophysical Journal* **697**, 428-435.

Lien, Y. C. and W. W. Nawar (1974) Thermal degradation of some amino acids. *Journal of Food Science* **39**, 911-913.

McCollom, T. M. (2013) The influence of minerals on decomposition of the n-alkyl-α-amino acid norvaline under hydrothermal conditions. *Geochimica et Cosmochimica Acta* **104**, 330-357.

Meinert, C., I. Myrgorodska, P. de Marcellus, T. Buhse, L. Nahon, S. V. Hoffmann, L. Le Sergeant d'Hendecourt, U. J. Meierhenrich (2016) Ribose and related sugars from ultraviolet irradiation of interstellar ice analogs. *Science* **352**, 208-212.

Miller, S. (1957) The mechanism of synthesis of amino acids by electric discharges. *Biochimica et Biophysica Acta* **23**, 480-489.

Monroe, A. A. and S. Pizzarello (2011) The soluble organic compounds of the Bells meteorite: Not a unique or unusual composition. *Geochimica et Cosmochimica Acta* **75**, 7585-7595.

Mumma, M. J., and S. B. Charnley (2011) The chemical composition of comets. *Annual Review of Astronomy and Astrophysics* **49**, 471-524.

Peltzer, E. T. and J. L. Bada (1978) A-Hydroxycarboxylic acids in the Murchison meteorite. *Nature* **272**, 443-444.

Peltzer, E. T., J. L. Bada, G. Schlesinger, and S. L. Miller (1984) The chemical conditions on the parent body of the Murchison meteorite: Some conclusions based on amino, hydroxy and dicarboxylic acids. *Advances in Space Research* **4**, 69–74.

Pizzarello, S., M. Zolensky, and K. A. Turk (2003) Non racemic isovaline in the Murchison meteorite: chiral distribution and mineral association. *Geochimica et Cosmochimica Acta* **67**, 1589-1595.

Pizzarello, S., Y. S. Huang, and M. Fuller (2004) The carbon isotopic distribution of Murchison amino acids. *Geochimica et Cosmochimica Acta* **68**, 4963-4969.

Pizzarello, S., G. W. Cooper, G. J. Flynn (2006) The nature and distribution of the organic material in carbonaceous chondrites and interplanetary dust particles. *Meteorites and the Early Solar System II*, D. S. Lauretta and H. Y. McSween, Eds. (University of Arizona Press, 2006), p. 625-650.

Pizzarello, S. and W. Holmes (2009) Nitrogen-containing compounds in two CR2 meteorites: ^{15}N composition, molecular distribution and precursor molecules. *Geochimica et Cosmochimica Acta* **73**, 2150-2162.

Pizzarello, S., Y. Wang, and G. M. Chaban (2010) A comparative study of the hydroxy acids from the Murchison, GRA 95229 and LAP 02342 meteorites. *Geochimica et Cosmochimica Acta* **74**, 6206-6217.

Rodigast, M., A. Mutzel, Y. Iinuma, S. Haferkorn, and H. Herrmann (2015) Characterisation and optimization of a sample preparation method for the detection and quantification of atmospherically relevant carbonyl compounds in aqueous medium. *Atmospheric Measurement Technique* **8**, 2409-2416.

Schonberg, A. and R. Moubacher (1951) The Strecker degradation of α-amino acids. *Chemical Reviews* **50**, 261-277.

Schutte, W. A., P. A. Gerakines, T. R. Geballe, E. F. vanDishoeck, and J. M. Greenberg (1996) Discovery of solid formaldehyde toward the protostar GL 2136: Observations and laboratory simulation. *Astronomy & Astrophysics* **309**, 633-647.

Seaman, V. Y., M. J. Charles, and T. M. Cahill (2006) A sensitive method for the quantification of acrolein and other volatile carbonyls in ambient air. *Analytical Chemistry* **78**, 2405-2412.

Sephton, M. A. (2002) Organic compounds in carbonaceous meteorites. *Natural Product Reports* **19**, 292-311.

Sephton, M. A. (2014) Organic geochemistry of meteorites. *Treatise on Geochemistry 2nd Edition*, H.D. Holland and K. K. Turekian, Eds. (Elsevier, 2014) vo1. 12, p. 1-31

Serrano, M., M. Silva, and M. Gallego (2013) Development of an environment-friendly microextraction method for the determination of aliphatic and aromatic aldehydes in water. *Analytica Chimica Acta* **784**, 77-84.

Shalabiea, O. M., and J. M. Greenberg (1994) Two key processes in dust/gas chemical modeling – photoprocessing of grain mantles and explosive desorption. *Astronomy & Astrophysics* **290**, 266-278.

Spaulding, R. S., and M. J. Charles (2002) Comparison of methods for extraction, storage, and silylation of pentafluorobenzyl derivatives of carbonyl compounds and multi-functional carbonyl compounds. *Analytical and Bioanalytical Chemistry* **372**, 808-816.

Taylor, R. (1987) The mechanism of thermal eliminations Part XXIII: [1] The thermal decomposition of pyruvic acid. *International Journal of Chemical Kinetics* **19**, 709-713.

Tielens, A. G. G. M. and D. C. B. Whittet (1997) Ice in star forming regions. *Molecules in Astrophysics: Probe and Processes*, E. F. van Dishoeck, Ed. (Springer Science & Business Media), 45-60.

Watanabe, N. and A. Kouchi (2002) Efficient formation of formaldehyde and methanol by the addition of hydrogen atoms to CO in H_2O-CO ice at 10 K. *The Astrophysical Journal* **571**, 173-176.

Wirström, E. S., S. B. Charnley, W. D. Geppert, and C. M. Persson (2012) Observations of carbon isotopic fractionation in interstellar formaldehyde. *43rd Lunar and Planetary Science Conference,* #1611.

Yamada, H., and I. Somiya (1989) The determination of carbonyl compounds in ozonated water by the PFBOA method. *Ozone Science & Engineering* **11**, 127-141.

Yanagawa, H., Y. Makino, K. Sato, M. Nishizawa, and F. Egami (1982) Novel formation of α-amino acids and their derivatives from oxo acids and ammonia in an aqueous medium. *The Journal of Biochemistry* **91**, 2087-2090.

Yuen, G., N. Blair, D. J. Des Marais, and S. Chang (1984) Carbon isotope composition of low molecular weight hydrocarbons and monocarboxylic acids from Murchison meteorite. *Nature* **307**, 252-254.

CHAPTER 3:

ASSESSING THE ROLE OF PARENT BODY AQUEOUS ALTERATION DURING PREBIOTIC ORGANIC SYNTHESIS IN THE TAGISH LAKE METEORITE

3.1. INTRODUCTION

The Tagish Lake meteorite is an ungrouped type 2 carbonaceous chondrite with compositional similarities to both CI and CM chondrites (Brown et al., 2000). The meteorite fell onto the surface of a frozen lake in British Columbia on January 18, 2000. The first Tagish Lake specimens were collected from the ice surface without direct hand contact within only a few days of the meteorite fall and have been stored < 0°C ever since (Brown et al., 2000; Herd et al. 2016). These specimens, currently housed in the Subzero Facility for Curation of Astromaterials at the University of Alberta, are considered the most pristine carbonaceous chondrite samples available for study (Hilts et al., 2014; Herd et al., 2016). Low-temperature storage of these meteorite specimens aims to lower reaction rates, inhibit potential microbial growth, and retain indigenous volatile organic species within the samples (Herd et al., 2016). In addition to the meteorite's pristine nature, the Tagish Lake meteorite has a unique mineralogical, petrological and geochemical heterogeneity that has been attributed to varying degrees of aqueous alteration across the parent body asteroid (Herd et al., 2011; Blinova et al., 2014a,b; Hilts et al., 2014). Such variation has not been observed before and affords the potential for an entirely new window into the processes occurring on asteroidal parent bodies in the early Solar System.

The Tagish Lake meteorite has an exceptionally low bulk density (1.6 g/cm^3) and high porosity and is highly friable compared to other carbonaceous chondrite samples (Zolensky et al., 2002; Bland et al., 2004; Ralchenko et al., 2014). The bulk mineralogy of the meteorite consists of olivine- and pyroxene-bearing chondrules, isolated olivine and pyroxene grains and lithic fragments, set within a fine-grained matrix of phyllosilicates (saponite and serpentine clays), sulphides, magnetite and carbonates (Brown et al., 2000; Blinova et al., 2014a). Three Tagish Lake specimens, TL5b, TL11h, and TL11i, have been previously analyzed in detail for their mineralogical and chemical compositions (Herd et al., 2011; Blinova et al., 2014a,b). Mineralogical indicators for aqueous alteration (e.g. increasing replacement of chondrule glass by phyllosilicates in combination with relatively low porosity and a lower proportion of amorphous silicate material) suggest that the degree of aqueous alteration is in the increasing order of TL5b < TL11h << TL11i.

The organic compositions of carbonaceous chondrites such as the Tagish Lake meteorite provide insight into the abiotic synthesis and preservation of prebiotic organic compounds during early solar system formation and asteroid parent body aqueous alteration. Prebiotic organic compounds such as amino acids, carboxylic acids, aldehydes, and ketones are particularly relevant for understanding the origin of life on Earth and the potential for life elsewhere as these compounds are the building blocks of biological molecules, including protein and lipids in living systems (Botta and Bada, 2002; Sephton, 2002). Amino acids, carboxylic acids and other aliphatic and aromatic organic species have been previously detected in other pristine Tagish Lake samples, and their total abundances, distributions and isotopic compositions have been shown to vary widely across the range of lithologies (Herd et al., 2011; Glavin et al., 2012; Hilts et al., 2014). In general, the samples more strongly affected by aqueous alteration (e.g. TL11i) have been shown to contain lower abundances of soluble organics, while the minimally/moderately altered samples (TL5b, TL11h) are relatively organic-rich. The amino acid compositions suggest that there is a “sweet spot” of moderate aqueous alteration that allows for optimal synthesis and/or preservation of amino acid molecules. The compound-specific stable isotope ratios and enantiomeric compositions also seem to be influenced by the degree of aqueous alteration. These cause and effect relationships, however, are difficult to assess without a larger dataset to evaluate.

In the present study, we have built upon the initial investigations of the Tagish Lake meteorite by exploring the soluble organic content of three previously unstudied meteorite specimens (TL1, TL4 and TL10a), including compound-specific carbon isotope analysis of amino acids, solid-phase microextraction (SPME) analysis of carboxylic acids, and dichloromethane (DCM) solvent extractions for determining the aliphatic and aromatic content of the samples. This study also includes the very first analysis of aldehydes and ketones in the Tagish Lake meteorite and their measured compound-specific carbon isotope compositions. The $\delta^{13}C$ values reported here are discussed in comparison to the $\delta^{13}C$ values of other compound classes in the meteorite to evaluate their origins and investigate potential formation relationships. By comparing our soluble organic data with previous analyses, we aim to place TL1, TL10a and TL4 into the previously described sequence of aqueous alteration, taking into consideration that the variability observed may not only reflect distinct alteration histories, but also a heterogenous distribution of key chemical precursor compounds across the parent body asteroid.

3.2. MATERIALS AND METHODS

3.2.1. Chemicals and reagents

All glassware and tools were wrapped in aluminum foil and heated at 450°C for a minimum of 6 hours before use in order to remove organic contamination. All vials were capped with PTFE-lined lids. Standards and reagents were purchased from Sigma Aldrich and Fisher Scientific. Ultrapure water (Millipore Direct Q3 UV, 18.2 MΩ, 3 ppb total organic carbon; hereafter referred to as “water”), HPLC grade dichloromethane (DCM), double-distilled 6 M HCl, and O-(2,3,4,5,6-Pentafluorobenzyl) hydroxylamine hydrochloride of ≥ 99.0% purity were used. Stock aldehyde/ketone, carboxylic acid, and amino acid solutions were prepared by mixing individual standards (97– 99% purity) in Millipore (18.2 MΩ) or double-distilled water. The OPA/NAC reagent used for amino acid derivatization was prepared by mixing 300 µl 0.1 M OPA in methanol, and then adding 670 µl 0.1 M sodium borate buffer (pH 9) and 30 µl 1 M NAC. A 0.1 M hydrazine (NH_2NH_2) solution was prepared by double vacuum distillation of anhydrous hydrazine (98% purity) and subsequent dilution in water. The ammonium formate buffer used for the liquid chromatography time-of-flight mass spectrometry (LC-TOF-MS) analyses was prepared by NH_4OH titration of a 50 mM formic acid solution to pH 8. A 0.09 µM Leucine Enkephalin solution in 50/50 acetonitrile/water with 0.1% formic acid was used for internal mass calibration of the TOF-MS. Details on the sources of specific five-carbon (C5) amino acids used as standards are available in Glavin and Dworkin (2009). To prepare standard solutions for liquid chromatography with fluorescence detection and time-of-flight mass spectrometry (LC-FD/TOF-MS) analysis, individual compounds were dissolved in water and then combined to enable their measurement in a single chromatographic separation. Solutions of sodium borate were prepared from solid sodium tetraborate (99.5–100% purity) that was pyrolyzed in air at 500°C for 3 hours to remove any organic contaminants prior to dissolution in water. All other solutions were prepared as described by Glavin et al. (2006).

3.2.2. Tagish Lake samples and procedural blanks

Three pristine samples of the Tagish Lake meteorite (TL1, TL4 and TL10a) were selected for this study based on macroscopic differences observed in hand-sample (i.e. presence or absence of chondrules, grain size, etc.), with the aim to cover the full range of lithological and chemical compositions contained within the Tagish Lake meteorite. In terms of macroscopic appearances, samples TL1 and TL10a appeared similar to TL5b and were, therefore, priority samples for targeting relatively high abundances of organic compounds. In comparison to the TL1 and TL10a lithologies, the TL4 specimen was relatively difficult to subsample and powder, consistent with the observation of a relatively low abundance of soft phyllosilicate minerals (saponite and serpentine clays) (Gilmour, 2017). TL4 also has a unique high porosity (36% vs. 30% for the rest of the sample suite; Ralchenko et al., 2014), suggesting that the primary pore spaces have remained devoid of secondary sheet silicates (Blinova et al., 2014a). The relatively low abundance of secondary minerals suggests that TL4 has experienced a relatively low degree of aqueous alteration compared to the other specimens. Concurrent hot water extractions of TL1, TL4 and TL10a revealed another notable difference in their compositions, as evidenced by varying amounts of a dark, water-insoluble film in the extracts (Figure 3.1); larger amounts of the oily film in the TL1 extract suggests that the specimen has a relatively higher water-insoluble organic content.

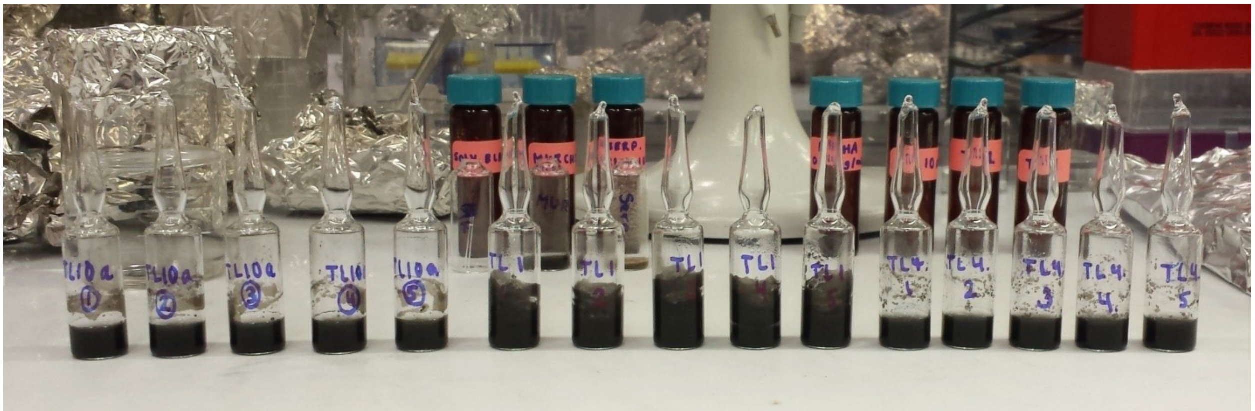

Figure 3.1. Flame-sealed glass ampules containing aldehyde and ketone water extracts of samples (from left; 5 ampules each) TL10a, TL1, and TL4. All three Tagish Lake samples contained a dark oily film that was insoluble in water and that naturally separated from the solution as a film on the ampules' inner glass surfaces. The TL1 extract was exceptionally oily compared to those of TL10a and TL4.

All meteorite subsampling was carried out in the Subzero Facility for Curation of Astromaterials at the University of Alberta. The facility consists of a purified Ar glove box located within a walk-in freezer (< -10°C), providing an inert, low-temperature atmosphere for meteorite subsampling (Herd et al., 2016). For each type of soluble organic analysis, two procedural blanks were carried through the meteorite extraction procedure and sample work-up, unless noted otherwise. The procedural blanks included one solvent blank, containing no mineral component, and one mineral analogue blank, typically consisting of ~ 500 mg of Allende meteorite powder or serpentine mineral powder (heated at 450°C for > 6 hours prior to the extraction step to drive off organics).

3.2.3. Aldehydes and ketones: Identification, quantification and $\delta^{13}C$ analysis

Subsamples of TL1, TL4 and TL10a (approximately 2.5 g per specimen) were subsampled and powdered using an alumina mortar pestle in the subzero purified Ar glovebox at the University of Alberta. The subsamples were stored and sealed in individual glass vials and kept cold (< 10°C) during shipment to the NASA Goddard Astrobiology Analytical Laboratory. Each sample was transferred to five 5 mL glass ampules in ~ 0.5 g aliquots. The total masses of the subsamples after powdering and transferring were: 2.492 g of TL1, 2.457 g of TL4 and 2.386 g of TL10a. 1 mL of water was added to each ampule, the ampules were flame-sealed and the solutions were heated at 100°C for 24 hours. The water extracts were centrifuged and the supernatants were combined into one vial for each Tagish Lake specimen. The residual solids were rinsed three times each with ~ 0.5 mL of water for each rinse. The supernatants were filtered through quartz wool to remove any solid remaining in suspension and the quartz wool filters were rinsed two times with ~ 0.5 mL of water for each rinse. The combined water extracts and rinses resulted in final volumes of ~ 13.5 mL for each specimen. The aldehydes and ketones in the water extracts were derivatized using an optimized EPA Method #556 for PFBHA derivatization, as follows: 1 mL of 0.2 mg/mL O-(2,3,4,5,6-Pentafluorobenzyl)hydroxylamine hydrochloride (PFBHA) solution was added to each water extract. The solutions were agitated for 5 minutes and left to react for 24 hours. 100 µL of 0.4 M HCl solution was added to each solution to quench the reaction and 2 mL of dichloromethane were added to each solution to extract the derivatized carbonyl compounds. The solutions were shaken for 5 minutes and then left undisturbed for 30 minutes to allow the dichloromethane and water layers to separate and settle. The dichloromethane layers were extracted and brought through an acid-wash step (3 mL of 0.4 M HCl). The dichloromethane extraction of derivatized carbonyl compounds and subsequent acid-wash step was repeated for each specimen with another 2 mL of dichloromethane. The 2 x 2 mL dichloromethane extracts containing the carbonyl derivatives were concentrated down to 200 µL volumes under a stream of nitrogen and analyzed by GC-MS/IRMS.

The GC-MS analysis was carried out using a Thermo Trace GC equipped with a 5 m base-deactivated fused silica guard column (Restek, 0.25 mm ID) and three 30 m length × 0.25 mm I.D. × 0.5 µm film thickness Rxi-5ms capillary columns (Restek) connected using Press-Tight connectors (Restek). The GC oven program was set as follows: initial temperature was 40 °C, ramped at 10 °C/min to 160 °C, ramped at 5 °C/min to 190 °C, ramped at 10 °C/min to 290 °C and held for 7 min. The carrier gas used was UHP helium (5.0 grade) at 2.6 mL/min flow rate. Triplicate injections (1 µL aliquots) of the oxime derivative solutions were made in splitless mode. The mass spectrum was used to identify and quantify the meteoritic carbonyl compounds by comparison to reference standards and applying a calibration curve. A targeted ion mass-to-charge ratio (*m/z* = 181.0) was used to identify and quantify compounds. Approximately 10% of the sample eluting from the GC column was directed into a Thermo DSQII electron-impact quadrupole mass spectrometer (ion source set at 200 °C and 70 eV). The remaining 90% of each eluting compound was directed through a Thermo GC-C III interface for oxidation of the compounds to carbon dioxide. The carbon isotope analyses were then carried out on a Thermo MAT 253 IRMS. The $\delta^{13}C$ values of the eluting compounds were obtained after injection of three pulses of precalibrated CO_2 ($\delta^{13}C = -24.23$‰ VPDB) into the IRMS and computation using Thermo Isodat 2.5 software. To correct for the amount of carbon added by the derivatization reagent, underivatized standards were analyzed on a Costech ECS 4010 combustion elemental analyzer (EA) connected to the IRMS. The final $\delta^{13}C$ values of the meteoritic aldehydes and ketones (carbonyls) were calculated using equation 1.

$$\delta^{13}C_{\text{sample carbonyl}} = [((n_{\text{carbonyl}} + n_{\text{d}})/n_{\text{carbonyl}}) \times (\delta^{13}C_{\text{derivatized sample carbonyl}} - \delta^{13}C_{\text{derivatized std carbonyl}})] + \delta^{13}C_{\text{underivatized std carbonyl}} \tag{1}$$

where n_{carbonyl} = number of carbon atoms in underivatized carbonyl and n_{d} = number of carbons added by derivatizing reagent. The precision (standard deviation) of the $\delta^{13}C$ values was obtained using equation 2 (Docherty et al., 2001).

$$\sigma^2_{\text{sample carbonyl}} = \sigma^2_{\text{underivatized std}} + [\sigma^2_{\text{derivatized std}} \times ((n_{\text{carbonyl}} + n_{\text{d}})/n_{\text{carbonyl}})^2] + [\sigma^2_{\text{derivatized sample}} \times ((n_{\text{carbonyl}} + n_{\text{d}})/n_{\text{carbonyl}})^2] \tag{2}$$

3.2.4. Amino acids: Identification, quantification and $\delta^{13}C$ analysis

Three Tagish Lake meteorite chips (interior chips that did not contain any visual evidence of fusion crust) – 3.615 g of TL1, 2.589 g of TL4 and 2.027 g of TL10a – were subsampled in the subzero purified Ar glovebox at the University of Alberta. The TL10a specimen was extracted at the University of Alberta, as follows: The sample was powdered with an alumina mortar and pestle within the subzero purified Ar glovebox and subdivided into four ~ 0.5 g aliquots in glass vials. The sealed vials containing the powders were removed from the glovebox and kept cold until the powders were transferred to four 5 mL glass ampules. 2 mL of water were added to each ampule, the ampules were flame-sealed and the solutions were heated at 100°C for 24 hours. The water extracts were centrifuged and the supernatants were combined. The residual solids were rinsed three more times using 0.5 mL of water per rinse. The combined supernatants and rinses were evaporated to dryness using a rotary evaporator. The dried extract was then shipped to the NASA Goddard Astrobiology Analytical Laboratory for analysis, along with a dried procedural blank that was carried through the same procedure.

The TL1 and TL4 meteorite chips were shipped directly to the NASA Goddard Astrobiology Analytical Laboratory for the water extraction and sample work-up, carried out as follows: TL1 and TL4 were powdered and homogenized using a mortar and pestle in a positive pressure ISO 5 HEPA-filtered laminar flow hood, and separated into ~ 300 mg portions. The total masses of the samples after powdering were: 3.525 g for TL1 and 2.537 g for TL4. Each portion was extracted at 100 °C for 24 hours inside flame-sealed glass ampules each containing 1 mL of water. Extracts were separated from the residues by centrifugation, the residues were rinsed with water (3 × 0.5 mL), and the rinses were combined with the aqueous portion. The TL1 and TL4 extracts were divided into two equal portions; one portion was used for the analysis of free amino acids, while the other was subjected to acid-vapor hydrolysis using 6 M HCl (150 °C for 3 h; Glavin et. al., 2006) to determine the total (free plus hydrolyzable) amino acid content. Only the total amino acid content (no "free" amino acid data) was determined for sample TL10a. All of the unhydrolyzed and acid-hydrolyzed extracts were re-dissolved in water and passed through equilibrated cation-exchange resin (AG50W-X8, 100–200 mesh, hydrogen form; BIO-RAD) columns to remove salts, and the amino acids recovered by elution with 2 M NH_4OH. After desalting, the NH_4OH eluates were dried in 0.1 M sodium borate buffer (pH 9) under vacuum to remove excess NH_3, resuspended in 20 μL of water and derivatized with 5 μL *o*-phthaldialdehyde/N-acetyl-L-cysteine (OPA/NAC) (Glavin et. al., 2006; 2010).

The amino acid content of the Tagish Lake samples and procedural blank were then determined via UPLC-FD/ToF-MS using a Waters ACQUITY H Class UPLC with fluorescence detector and Waters Xevo G2 XS. The instrument parameters and analytical conditions used were similar to those described elsewhere (Glavin et al., 2006; 2010). For the Xevo mass calibrations, an automatically applied lock mass of a fragment of Leucine Enkephalin (278.1141 Da) with a scan time of 1 second every 120 seconds is used. The capillary voltage was set to 1.2 kV. The amino acids and their enantiomeric ratios were quantified from the peak areas generated from both fluorescence detection and from the mass chromatogram of their OPA/NAC derivatives as described previously (Glavin et al., 2006). The reported amino acid abundances in the Tagish Lake meteorite sample are the average value of three separate UPLC-FD/ToF-MS measurements. The errors given are based on the standard deviation of the average value of three separate measurements. The TL1 and TL4 values are blank-corrected to account for trace levels of contamination present in the blanks. The TL10a abundances were not blank-corrected as the procedural blank contained unusually high levels of terrestrial amino acids that did not appear to similarly affect the TL10a sample.

Because of sufficient compound abundances, carbon isotopic compositions could be determined for glycine, β-alanine, and D- and L-alanine in both the unhydrolyzed and hydrolyzed TL1 extracts, and for ɣ-aminobutyric acid in the hydrolyzed extract. Non-hydrolyzed and hydrolyzed TL1 samples were dried down separately, as were procedural blanks. Each aliquot was dried under vacuum using a LabConco CentriVap centrifugal concentrator. Samples were esterified with isopropanol and the isopropyl esters reacted with trifluoroacetic anhydride (TFAA) using established methods (e.g., Elsila et al., 2009). The TFAA-isopropanol derivatives were dissolved in 5 μL of ethyl acetate (Fisher Chemical, Optima Grade). The $\delta^{13}C$ values of the TFAA-isopropanol derivatized samples were analyzed by gas chromatography coupled with mass spectrometry and isotope ratio mass spectrometry (GC-MS/IRMS), which provides compound-specific structural and stable isotopic information from a single sample injection. The GC-MS/IRMS instrument consists of a Thermo Trace GC whose output is split, with approximately 10% directed into a Thermo DSQII electron-impact quadrupole mass spectrometer that provides mass and structural information for each eluting peak. The remaining ~90% passes through either a Thermo GC-C III interface, where eluting amino acids are oxidized to carbon dioxide and passed into a Thermo MAT 253 IRMS for carbon isotope analysis. Derivatized extracts were injected in 1 µL aliquots into the GC in triplicate. The GC was outfitted with a 5-m base-deactivated fused silica guard column (Restek, 0.25 mm ID) and four 25-m Chirasil L-Val columns (Varian, 0.25 mm ID) connected using Press-Tight connectors (Restek). The following oven program was used: initial temperature was 50 °C, ramped at 10 °C/min to 85 °C, ramped at 2 °C/min to 120 °C, ramped at 4 °C/min to 200 °C, and held at 200 °C for 10 min. Six pulses of CO_2 ($\delta^{13}C$ = -24.23‰ VPDB) that had been pre-calibrated against commercial reference gases (Oztech Corporation) were injected into the IRMS for computation of the $\delta^{13}C$ values of the eluting compounds. Analysis of the IRMS data was performed with Thermo Isodat 2.5 software. Stock solutions of the amino acids of interest were combined to make a standard mixture that was carried through the derivatization process and run daily on the GC-MS/IRMS. The individual, underivatized stock solutions or solid pure standards were also analyzed on a Costech ECS 4010 combustion elemental analyzer (EA) connected to the IRMS; this was necessary to correct for the carbon added during derivatization. The final $\delta^{13}C$ values of the amino acids in the samples and their precision were calculated as described elsewhere (Docherty et al., 2001; O'Brien et al., 2002; Elsila et al., 2009).

3.2.5. Solid-phase microextraction (SPME) analysis of monocarboxylic acids

Masses of 0.490 g of TL1, 0.500 g of TL4 and 0.640 g of TL10a were subsampled for carboxylic acid analyses and powdered using an alumina mortar and pestle. Both the subsampling and powdering steps were carried out in the subzero purified Ar glovebox to minimize the loss of volatile organic species and the powders were kept cold until their immediate transfer to 5 mL glass ampules as ~ 250 mg aliquots. 2 mL of water was added to each ampule, the ampules were flame-sealed and the samples were extracted at 100°C for 24 hours. The samples were subsequently removed from the oven and cooled to room temperature. The water extracts were transferred to centrifuge tubes and the residual solids were rinsed three times each with ~ 0.5 mL of water for each rinse. The water extracts were then centrifuged and the supernatants were transferred to round-bottom flasks. The precipitates were rinsed three times each with ~ 0.5 mL of water for each rinse. The pH of each sample was adjusted to ~11 using 6M NaOH (aq) in order to convert the carboxylic acids into non-volatile carboxylate salts. The solutions were then reduced to < 1 mL volumes using a rotary evaporator at 85°C. The pH of each concentrate was then adjusted to ~ 2−3 using 6M HCl (aq) in order to regenerate the carboxylic acids. Once the appropriate pH was reached, the final solvent volumes were measured and recorded and the solutions were analyzed via solid-phase microextraction (SPME) technique. Gas chromatography separation was performed on an Agilent 6890N using a Nukol^{TM} column (30 m length, 0.25 µm film thickness, 0.25 mm diameter) at MacEwan University. The SPME fiber (carbowax-polyethylene glycol (PEG), 23-gauge needle, 60 µm thickness, 1 cm length fiber) was soaked in a sample solution for 10 minutes prior to manual GC injection. The GC injection port was held at 210 °C and injection of the SPME adsorbed samples was performed using splitless mode. The initial oven temperature was set at 35 °C and held for 1 minute, after which the temperature was increased by 25 °C min^{-1} to 135 °C, then 1.5 °C min^{-1} to 185 °C, and then held at 185 °C for 10 minutes. Helium was the carrier gas at a constant flow rate of 1.0 mL min^{-1}. Detection was performed using an Agilent 5975C mass selective detector (MSD). Carboxylic acids were identified and quantified by comparison to a suite of reference standards and a standard calibration curve. A trace amount of formic acid and acetic acid was present in the procedural blanks. The abundances of formic acid and acetic acid in TL1 and TL4 were blank-corrected by subtracting these concentrations from the calculated abundances. Concentrations were not determined for the compounds in TL10a.

3.2.6. DCM solvent extractions

Masses of 0.500 g of TL1, 0.500 g of TL4 and 0.414 g of TL10a were subsampled and powdered in the subzero purified Ar glovebox and the powders were kept cold until their transfer to 20 mL vials. 15 mL of DCM was added to each vial and the samples were stirred at room temperature for 24 hours in order to extract weakly polar aliphatic and aromatic species. Following the extraction step, the DCM extracts were transferred to separate vials. The residual solid was rinsed three times with 0.5 mL of DCM for each rinse. The extracts were evaporated to 200 µL volumes under a stream of N_2 and then analyzed using GC-MS. Gas chromatography separation was performed on an Agilent 6890N using a HP-5MS column (30 m length, 0.25 µm film thickness, 250 µm diameter) at MacEwan University. The initial oven temperature was 50 °C and held for 1 minute, after which the temperature was increased by 10 °C min^{-1} to a final temperature of 250 °C. The temperature was held at 250 °C for 20 minutes for a total run time of 41 minutes. Helium was the carrier gas at a constant flow rate of 1.0 mL min^{-1}. Samples were injected using pulsed splitless mode at 275 °C. Detection was performed using an Agilent 5975C mass selective detector (MSD).

3.3. RESULTS

3.3.1. Amino acid distributions, $\delta^{13}C$ values and enantiomeric compositions

The absolute abundances of amino acids in the non-hydrolyzed extracts of TL1 and TL4 (“free” amino acids) and 6M HCl-hydrolyzed extracts of TL1, TL4 and TL10a (“total” amino acids) are reported in Table 3.1 and illustrated in Figures 3.2 and 3.3. TL1 was exceptionally rich in amino acids (~1877 ppb), while TL4 and TL10a were relatively depleted (~108 ppb and ~139 ppb, respectively). Acid hydrolysis resulted in similar increases in the abundance of glycine for both HCl-hydrolyzed samples (+133 ppb for TL1 and +72 ppb for TL4) (Figures 2 and 3). TL1 also showed a substantial increase in the abundance of γ-amino-n-butyric acid (γ-ABA) following acid hydrolysis (free γ-ABA abundance: 37.5 ppb; total γ-ABA abundance: 431.7 ppb). TL4 and TL10a contained very similar amino acid distributions, both dominated by glycine and containing relatively low levels of other amino acids, while the hydrolyzed extract of TL1 contained relatively high abundances of β-alanine and γ-ABA. Glycine, β-alanine, D,L-alanine and γ-ABA were present in sufficient abundances in TL1 to obtain their compound-specific $\delta^{13}C$ values (Table 3.2). The $\delta^{13}C$ values for these amino acids span a wide range of positive values with γ-ABA exhibiting the lowest value (+6‰), followed by β-alanine (+16 to +22‰), and with glycine and alanine exhibiting similarly high values (+31 to +47‰). The amino acid $\delta^{13}C$ values from the non-hydrolyzed and hydrolyzed TL1 extracts fall within error of one another for all measurements. Table 3.3 lists the measured enantiomeric ratios (D/L) for amino acids detected in TL1, TL4 and TL10a. Alanine, β-amino-n-butyric acid (β-ABA), and isovaline were near racemic (D/L ratios > 0.87) for all measurements. Glutamic acid exhibited a substantial excess of the L enantiomer for all measurements. Particularly low D/L ratios were measured for serine in all samples, and for valine in TL10a. Despite near-racemic values for alanine, β-ABA, and isovaline, the TL10a amino acids generally exhibited the lowest D/L ratios of the sample set.

Table 3.1. Amino acid abundances (ng/g) from non-hydrolyzed (“free”) and 6 M HCl-hydrolyzed (“total”) hot-water extracts.

	TL1		**TL4**		**TL10a**
	Free	**Total**	**Free**	**Total**	**Total[a]**
D-aspartic acid	5.87 ± 0.16	9.47 ± 0.36	< 0.01	2.02 ± 0.06	2.14± 0.09
L-aspartic acid	6.40 ± 0.27	11.41 ± 0.30	< 0.01	1.74 ± 0.06	4.07± 0.04
L-glutamic acid	1.57 ± 0.48	22.28 ± 0.53	< 0.01	1.78 ± 0.25	7.14± 1.20
D-glutamic acid	0.89 ± 0.20	16.80 ± 1.06	< 0.01	0.80 ± 0.10	4.07± 0.20
D-serine	1.14 ± 0.25	0.42 ± 0.04	< 0.01	0.04 ± 0.01	0.12± 0.01
L-serine	2.46 ± 0.45	4.24 ± 2.04	0.06 ± 0.03	< 0.01	0.83± 0.06
D-threonine	0.16 ± 0.08	< 0.01	< 0.01	0.36 ± 0.15	< 0.01
L-threonine	1.85 ± 1.42	1.13 ± 0.24	0.07 ± 0.01	0.10 ± 0.04	2.47± 0.78
Glycine	426.35 ± 41.58	559.44 ± 56.28	20.28 ± 1.63	92.39 ± 11.11	85.21± 7.03
β-alanine	308.28 ± 51.99	371.19 ± 66.05	1.15 ± 0.07	2.32 ± 0.10	5.16± 0.11
D-alanine	71.95 ± 8.26	72.74 ± 2.92	0.82 ± 0.03	1.77 ± 0.08	4.77± 0.46
L-alanine	70.23 ± 1.47	75.55 ± 2.56	0.75 ± 0.02	2.01 ± 0.06	5.26± 0.29
γ-ABA	37.45 ± 2.67	431.71 ± 15.43	0.10 ± 0.04	0.94 ± 0.09	6.12± 0.27
D-β-ABA	83.07 ± 3.64	71.40 ± 3.26	0.04 ± 0.00	0.04 ± 0.01	0.56± 0.01
L-β-ABA	83.76 ± 1.99	64.09 ± 1.38	0.04 ± 0.00	0.04 ± 0.01	0.51± 0.00
α-AIB	16.25 ± 0.87	11.51 ± 3.46	0.26 ± 0.04	0.80 ± 0.10	4.90± 0.06
D,L-α-ABA	30.38 ± 7.88	35.86 ± 6.00	0.24 ± 0.10	< 0.01	1.44± 0.54
ε-EACA	8.05 ± 0.66	23.09 ± 2.09	< 0.01	0.16 ± 0.04	3.19± 0.28
3-a-2,2-dmpa	1.72 ± 0.07	4.48 ± 0.17	0.01 ± 0.00	< 0.01	< 0.01
D,L-4-apa	5.28 ± 0.38	27.10 ± 1.21	< 0.01	< 0.01	< 0.01
D,L-4-a-3-mba	0.14 ± 0.01	2.41 ± 0.19	< 0.01	< 0.01	< 0.01
D,L-3-a-2-mba	4.39 ± 0.95	1.95 ± 0.12	< 0.01	< 0.01	< 0.01
D,L-3-a-2-epa	1.49 ± 0.15	1.38 ± 0.16	< 0.01	< 0.01	< 0.01
5-apa	1.51 ± 0.18	13.38 ± 1.19	< 0.01	< 0.01	< 0.01
D,L-4-a-2-mba	1.38 ± 0.18	35.73 ± 2.07	< 0.01	< 0.01	< 0.01
3-a-3-mba	< 0.01	< 0.01	< 0.01	< 0.01	< 0.01
D-isovaline	0.21 ± 0.02	< 0.01	< 0.01	< 0.01	0.27 ± 0.01
D,L-3-apa	5.81 ± 0.34	5.43 ± 0.36	< 0.01	< 0.01	< 0.01
L-isovaline	0.24 ± 0.02	< 0.01	< 0.01	< 0.01	0.27 ± 0.02
L-valine	0.62 ± 0.08	1.23 ± 0.05	< 0.01	0.43 ± 0.20	0.69 ± 0.03
D-valine	0.47 ± 0.11	1.28 ± 0.08	< 0.01	< 0.01	0.04 ± 0.00
D-norvaline	< 0.01	0.11 ± 0.05	< 0.01	< 0.01	< 0.01
L-norvaline	< 0.01	0.12 ± 0.05	< 0.01	< 0.01	< 0.01
Total abundance	**1179.4**	**1876.9**	**23.8**	**107.7**	**139.3**

[a] TL10a abundances are not blank-corrected values

Table 3.2. Compound-specific carbon isotopic measurements (‰ VPDB) of amino acids from the non-hydrolyzed ("free") and 6 M HCl-hydrolyzed ("total") hot-water extracts of Tagish Lake specimen TL1, compared to the previously analyzed specimens TL5b and TL11h (data from Glavin et al., 2012)

	TL1		**TL5b Total**	**TL11h Total**
Amino acid	Free	Total	*Glavin et al. (2012)*	*Glavin et al. (2012)*
Glycine	+ 31 ± 5	+ 39 ± 7	+ 39 ± 6	+ 19 ± 4
β-alanine	+ 22 ± 6[a]	+ 16 ± 5[a]	+ 30 ± 6	– 5 ± 4
D-alanine	+ 37 ± 3	+ 34 ± 13	+ 67 ± 7	+ 6 ± 3
L-alanine	+ 42 ± 7	+ 47 ± 4	+ 55 ± 3	+ 16 ± 4
γ-ABA	n.d.	+ 6 ± 5	n.d.	+ 4 ± 3

n.d. – not determined

[a] β-alanine contains some co-eluting D,L-β-ABA

Table 3.3. Amino acid enantiomeric ratio (D/L) measured in the non-hydrolyzed ("free") and 6 M HCl-hydrolyzed ("total") hot water extracts of TL1, TL4 and TL10a.

	TL1		**TL4**		**TL10a**
Amino acid	Free	Total	Free	Total	Total
Aspartic acid	0.92± 0.05	0.83± 0.04	n.d.	1.16± 0.05	0.53± 0.02
Glutamic acid	0.57± 0.22	0.75± 0.05	n.d.	0.45± 0.08	0.57± 0.10
Serine	0.46± 0.13	0.10± 0.05	0.10± 0.07	n.d.	0.14± 0.01
Alanine	1.02± 0.12	0.96± 0.05	1.10± 0.04	0.88± 0.05	0.91± 0.10
β-ABA	0.99± 0.05	1.11± 0.06	1.07± 0.07	1.06± 0.26	1.09± 0.02
Isovaline	0.87± 0.12	n.d.	n.d.	n.d.	1.00± 0.07
Valine	0.76± 0.20	1.03± 0.08	n.d.	n.d.	0.06± 0.01

n.d. – not determined

Non-protein amino acids are shown in italics.

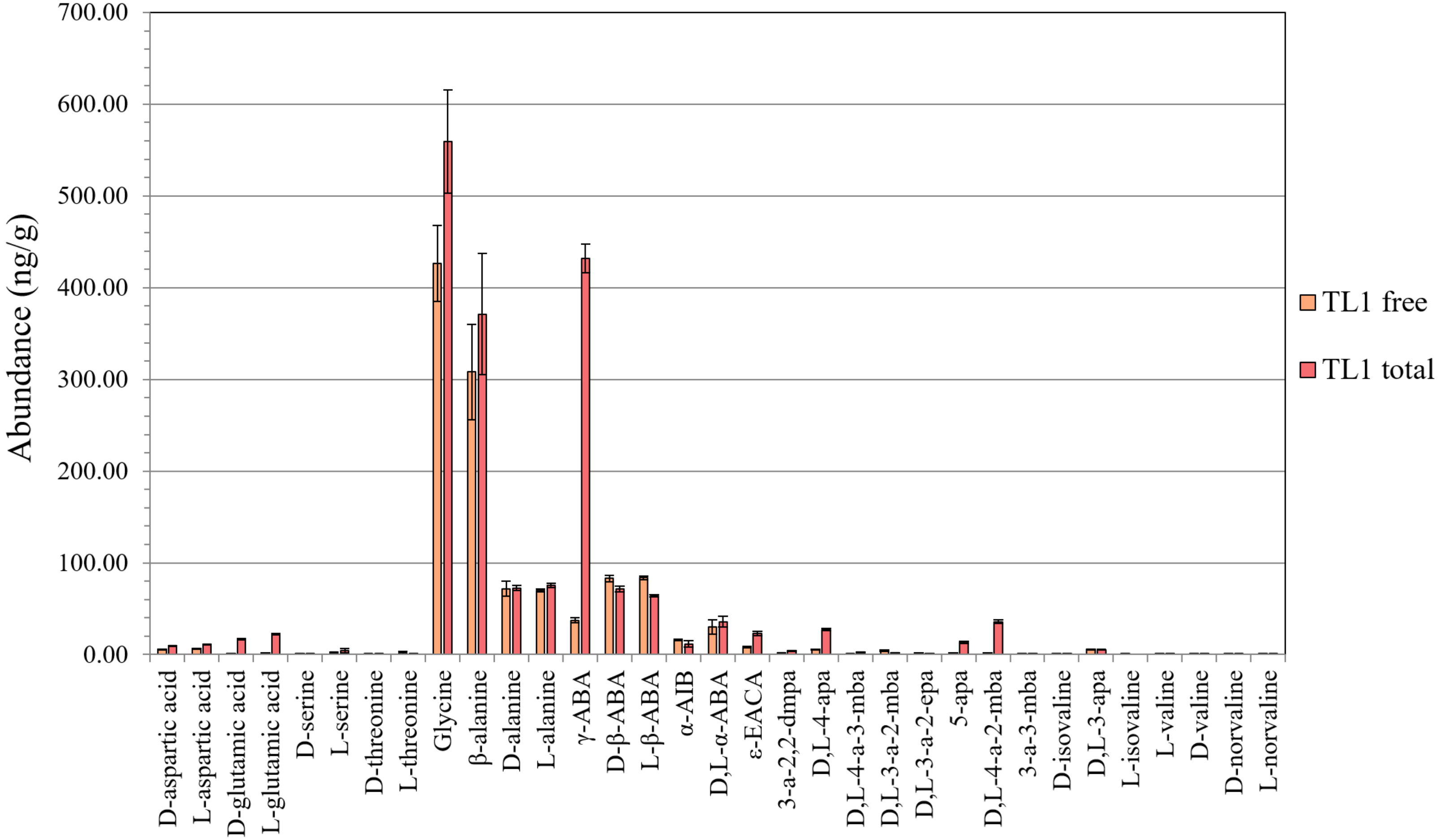

Figure 3.2. Absolute abundances (ng/g) of non-hydrolyzed (“free”) and 6 M HCl-hydrolyzed (“total”) amino acids in TL1. Error bars represent one standard deviation from the mean for triplicate runs.

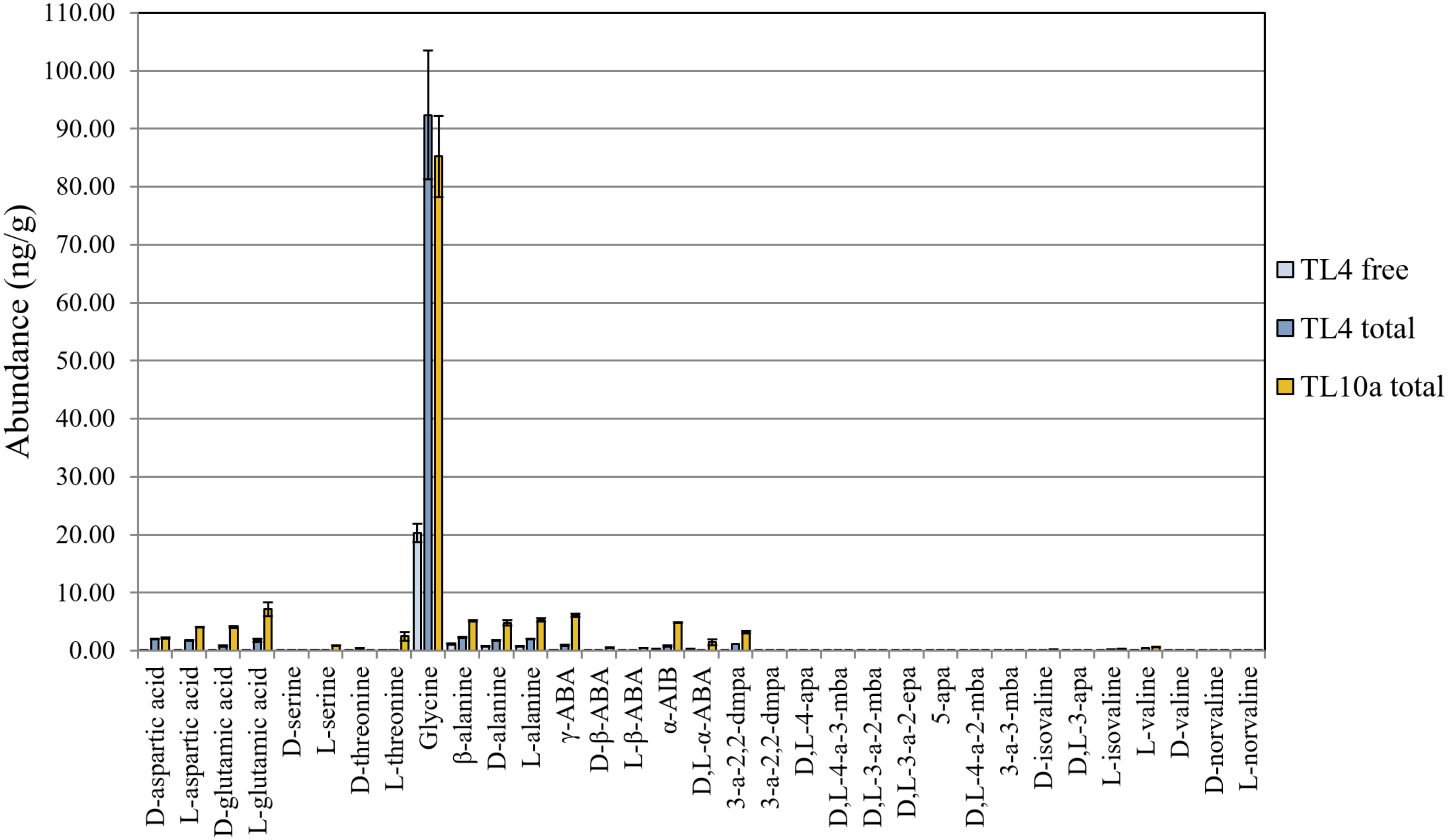

Figure 3.3. Absolute abundances (ng/g) of non-hydrolyzed (“free”) in TL4 and 6 M HCl-hydrolyzed (“total”) amino acids in TL4 and TL10a. Error bars represent one standard deviation from the mean for triplicate runs.

3.3.2. Aldehyde and ketone distributions and δ^{13}C compositions

The sum total abundances of aldehydes and ketones steadily decreased from TL1 to TL10a to TL4 (Table 3.4, Figure 3.4). The three specimens contained similar suites of carbonyl compounds, with the exception of the relatively high abundance of acetaldehyde detected in TL1 and the absence of butyraldehyde and acetophenone in TL10a. Formaldehyde, acetaldehyde and acetone were present in sufficient abundances in all three samples to obtain compound-specific δ^{13}C measurements (Table 3.4). Several of the carbonyl derivative peaks partially co-eluted with either the unreacted PFBHA reagent or unknown organic compounds present in the samples. These partial co-elutions are noted in Table 3.4. The aldehyde and ketone δ^{13}C values were highly ^{13}C-depleted in comparison to the amino acid δ^{13}C values. The formaldehyde δ^{13}C values, ranging from -51.5 to -34.6‰ were exceptionally ^{13}C-depleted. While the formaldehyde and acetone δ^{13}C values were relatively consistent across the Tagish Lake specimens, the acetaldehyde δ^{13}C values varied from -0.3 to -23.3‰, becoming progressively more ^{13}C-enriched from TL1 to TL10a to TL4.

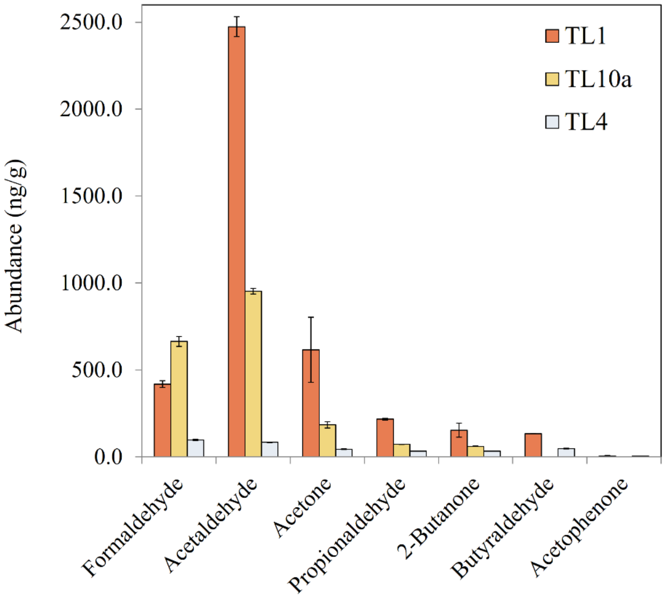

Figure 3.4. Abundances (ng/g) of aldehydes and ketones detected in water extracts from TL1, TL10a and TL4. Abundances represent the sum of the (*E*) and (*Z*) isomers, where applicable.

Table 3.4. Concentrations (ng/g) and compound-specific $\delta^{13}C$ compositions (‰ VPDB) for carbonyl compounds in hot-water extracts of samples TL1, TL4 and TL10a.

Compound	TL1		TL10a		TL4	
	Abundance (ng/g)	$\delta^{13}C$ (‰)	Abundance (ng/g)	$\delta^{13}C$ (‰)	Abundance (ng/g)	$\delta^{13}C$ (‰)
Aldehydes						
Formaldehyde	419.2 ± 18.7	-40.7[a] ± 4.2	664.5 ± 28.6	-34.6[a] ± 2.5	96.7 ± 3.7	-51.5[a] ± 7.9
(E)-Acetaldehyde	1107.0 ± 19.0	-0.3 ± 1.4	419.8 ± 7.0	-12.3 ± 0.7	45.4 ± 0.8	-23.3[b] ± 6.7
(Z)-Acetaldehyde	1367.1 ± 38.1	-3.9 ± 2.0	533.2 ± 13.7	-12.2 ± 0.9	38.7 ± 0.6	n.d.
Propionaldehyde	217.4 ± 4.5	n.d.	73.3 ± 0.4	n.d.	34.2 ± 0.5	n.d.
Butyraldehyde	134.7 ± 1.2	n.d.	n.d.	n.d.	48.4 ± 1.8	n.d.
Ketones						
Acetone	616.0 ± 187.1	-13.4[a] ±1.9	184.3 ± 18.0	-12.8[a] ± 2.4	44.9 ± 1.8	-19.1[a] ± 7.3
2-Butanone	154.4 ± 40.3	n.d.	61.8 ± 1.3	n.d.	33.7 ± 1.1	n.d.
Acetophenone	6.6 ± 0.9	n.d.	n.d.	n.d.	3.9 ± 0.6	n.d.
Total abundance	**4022.3 ± 285.7**		**1936.9 ± 64.8**		**282.8 ± 51.7**	

[a] Partially co-eluting with an unknown compound

[b] Partially co-eluting with unreacted PFBHA reagent

3.3.3. Monocarboxylic acids

Monocarboxylic acids were detected in all three Tagish Lake specimens (Figure 3.5, Table 3.5). The most abundant acids in samples TL1 and TL4 were quantified by comparison to a series of reference standard curves. TL1 contained a relatively higher total abundance (635 ppm) compared to TL4 (474 ppm). Despite having similar concentrations for formic acid, TL1 and TL4 contained different relative abundances of the other carboxylic acids. TL1 contained relatively high abundances of acetic acid (225 ppm), propanoic acid (34 ppm) and trace amounts of higher molecular weight acids, while TL4 was relatively depleted in acetic acid (94 ppm) and devoid of higher molecular weight compounds, aside from benzoic acid (2.0 ppm). These abundances have been corrected to account for the trace amounts of formic acid and acetic acid present in the corresponding procedural blanks. Unlike TL1 and TL4, the bulk of the monocarboxylic acids in the TL10a sample appeared to be primarily terrestrial in origin, as most of the acids identified in the sample were also present in the corresponding blanks. This observation is true for two separate analyses of TL10a (Table A2.1, Figure A2.1). Benzoic acid appears to be indigenous to TL10a as it was not present in the procedural blank and a similar result was observed for the repeat analysis (Table A2.1, Figure A2.1). No formic acid was detected in either of the two TL10a analyses.

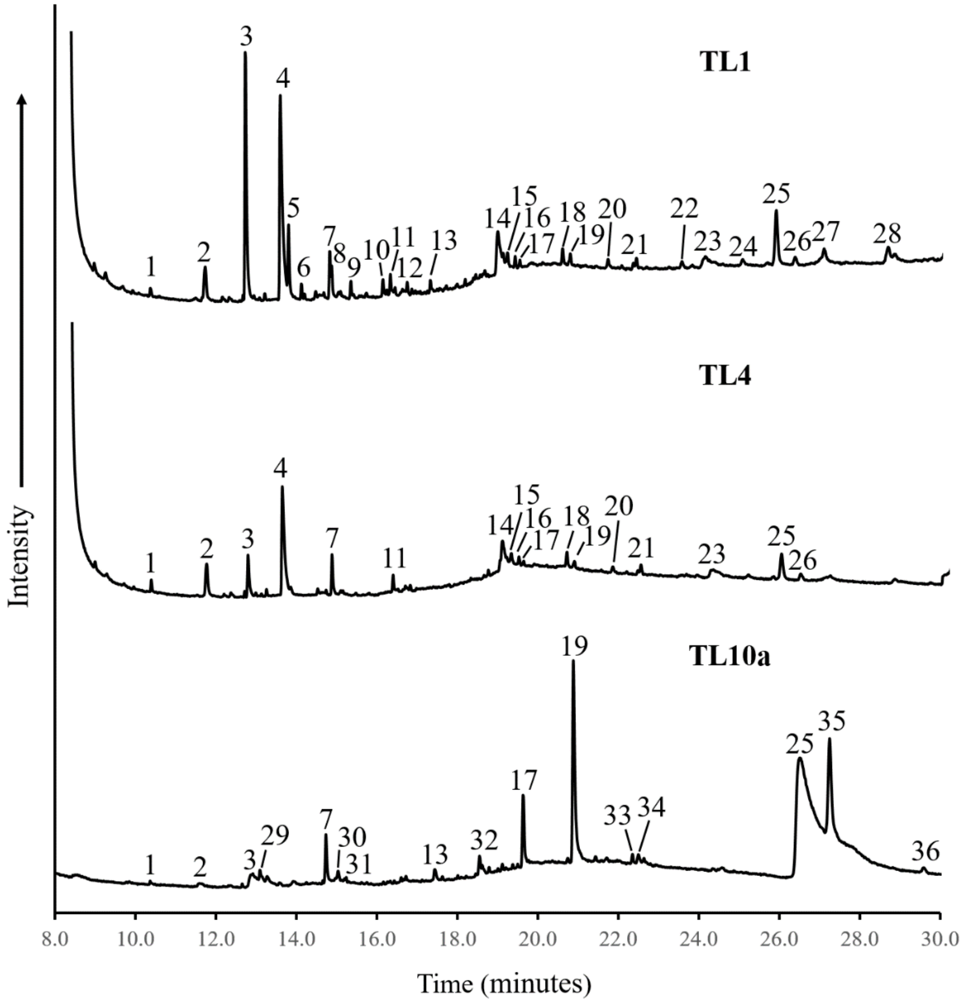

Figure 3.5. GC-MS chromatograms for SPME analyses of hot-water extracts of TL1, TL4 and TL10a. Water extractions were carried out on similar masses for the three specimens: 0.490 g of TL1, 0.500 g of TL4 and 0.640 g of TL10a. The final sample volumes are: 1.56 mL for TL1, 2.30 mL for TL4 and 1.52 mL for TL10a. Peak identifications: (1) Dodecamethyl-cyclohexasiloxane; (2) 2-chloroethanol; (3) acetic acid; (4) formic acid; (5) propanoic acid; (6) 2-methyl-propanoic acid; (7) 2-(2-ethoxyethoxy)-ethanol; (8) butanoic acid; (9) 2-methyl-butanoic acid; (10) pentanoic acid; (11) 2-(2-chloroethoxy)-ethanol; (12) 3-methyl-pentanoic acid; (13) hexanoic acid; (14) 2,2-oxybis-ethanol; (15) 2-[2-(2-ethoxyethoxy)ethoxy]-ethanol; (16) 1,4-dioxan-2-yl-hydroperoxide; (17) octanoic acid; (18) 2-[2-(2-chloroethoxy)ethoxy]-ethanol; (19) nonanoic acid; (20) 4-chloro-1-butanol; (21) tetraoxacyclododecanone; (22) 4-oxo-pentanoic acid; (23) triethylene glycol; (24) pentaoxadexadecanol; (25) benzoic acid; (26) indole; (27) 3-methyl-benzoic acid; (28) 3-methyl-benzoic acid; (29) phenyl-pentamethyl-disiloxane; (30) butyrolactone; (31) 1-chloro-dodecane; (32) heptanoic acid; (33) 1,1-oxybis-octane; (34) n-decanoic acid; (35) dodecanoic acid; (36) octadecanol.

Table 3.5. Abundances (µg/g) of soluble organic compounds, including carboxylic acids, identified in hot-water extracts of TL1, TL4, and TL10a using SPME GC-MS technique. GC-MS chromatograms with labeled peaks are illustrated in Figure 3.5. Probabilities (%) reported by the NIST Mass Spectral Library are reported in Table A2.2.

Sample TL1		**Sample TL4**		**Sample TL10a**	
Compound	µg/g	Compound	µg/g	Compound	µg/g
Dodecamethyl-cyclohexasiloxane[a]	n.d.	Dodecamethyl-cyclohexasiloxane[a]	n.d.	Dodecamethyl-cyclohexasiloxane[a]	n.d.
2-chloroethanol[a]	n.d.	2-chloroethanol[a]	n.d.	2-chloroethanol[a]	n.d.
Acetic acid[a]	225	Acetic acid[a]	94	Acetic acid	n.d.
Formic acid[a]	368	Formic acid[a]	378	Phenyl-pentamethyl-disiloxane	n.d.
Propanoic acid	34	2-(2-ethoxyethoxy)-ethanol[a]	n.d.	2-(2-ethoxyethoxy)-ethanol[a]	n.d.
2-methyl-propanoic acid	n.d.	2-(2-chloroethoxy)-ethanol[a]	n.d.	Butyrolactone[a]	n.d.
2-(2-ethoxyethoxy)-ethanol[a]	n.d.	2,2-oxybis-ethanol[a]	n.d.	1-chloro-dodecane	n.d.
Butanoic acid	n.d.	2-[2-(2-ethoxyethoxy)ethoxy]-ethanol[a]	n.d.	Hexanoic acid[a]	n.d.
2-methyl-butanoic acid	n.d.	1,4-dixoan-2-yl-hydroperoxide[a]	n.d.	Heptanoic acid[a]	n.d.
Pentanoic acid	n.d.	Octanoic acid	n.d.	Octanoic acid[a]	n.d.
2-(2-chloroethoxy)-ethanol[a]	n.d.	2-[2-(2-chloroethoxy)ethoxy]-ethanol[a]	n.d.	Nonanoic acid[a]	n.d.
3-methyl-pentanoic acid	n.d.	Nonanoic acid	n.d.	1,1-oxybis-octane[a]	n.d.
Hexanoic acid	2.8	4-chloro-1-butanol	n.d.	n-decanoic acid[a]	n.d.
2,2-oxybis-ethanol	n.d.	Tetraoxacyclododecanone[a]	n.d.	Benzoic acid	n.d.
2-[2-(2-ethoxyethoxy)ethoxy]-ethanol[a]	n.d.	Triethylene glycol	n.d.	Dodecanoic acid[a]	n.d.
1,4-dioxan-2-yl-hydroperoxide[a]	n.d.	Benzoic acid	2.4	Octadecanol	n.d.
Octanoic acid	1.7	Indole	n.d.		
2-[2-(2-chloroethoxy)ethoxy]-ethanol[a]	n.d.				
Nonanoic acid	1.6				
4-chloro-1-butanol	n.d.				
Tetraoxacyclododecanone[a]	n.d.				
4-oxo-pentanoic acid	n.d.				
Triethylene glycol	n.d.				
Pentaoxadexadecanol	n.d.				
Benzoic acid	2.0				
Indole	n.d.				
2-methyl-benzoic acid	n.d.				
3-methyl-benzoic acid	n.d.				

n.d. – not determined

[a] Detected in the procedural blank

3.3.4. DCM extractions

Table 3.6 lists the weakly polar aliphatic and aromatic species detected in DCM extracts of the Tagish Lake samples TL1, TL4, and TL10a. The GC-MS chromatograms for the three DCM extracts are illustrated in Figure 3.6 and the probabilities (%) reported by the NIST Mass Spectral Library are reported in Table A2.3. The compositions of TL1 and TL4 are essentially identical in terms of similar abundances of weakly polar aliphatic hydrocarbons. TL1 contained some PAHs (naphthalene, fluoranthene, pyrene) which were absent in both the TL4 and TL10a samples. The peaks identified by the NIST Mass Spectral Library as 3,5,5-trimethyl-2-hexene, 1,2,3,4,5-pentamethyl-cyclopentane, 2,4,4-trimethyl-1-hexene, undecane, and dodecane in the TL1 and TL4 samples were also present in similar abundances in the corresponding procedural blanks and are, therefore, presumed to be terrestrial contaminants. The TL10a sample was essentially devoid of aliphatic and aromatic compounds; the DCM extraction only yielded a large sulfur (S_8) peak and two small peaks identified as 4-methyl-2-pentanol and 2-ethyl-1-hexanol. These two peaks were observed in similar trace abundances in the corresponding procedural blanks and are assumed to be terrestrial in origin. Consistent with these results, a similar DCM extraction on a separate subsample of TL10a (0.414 g) yielded no detectable aliphatic or aromatic compounds (Figure A2.2).

Based on the GC-MS peak areas of S_8 (eluting at ~ 19.4 minutes), TL1 and TL10a yielded similar abundances of dissolved sulfur (S_8), while TL4 yielded a notably smaller abundance. The earlier DCM extraction and analysis of TL10a (Figure A2.2) yielded only a trace amount of S_8; however, this observation is likely due to dissolved S_8 precipitating from solution when the DCM extract was evaporated to dryness. The sulfur precipitate was visible as a yellow solid at the bottom of the glass vial containing the dried extract. The sulfur contained in all subsequent DCM extracts (TL1, TL4 and TL10a) appears to have remained in solution as these three subsequent extracts were evaporated to small volumes (~ 200 μL) rather than to complete dryness.

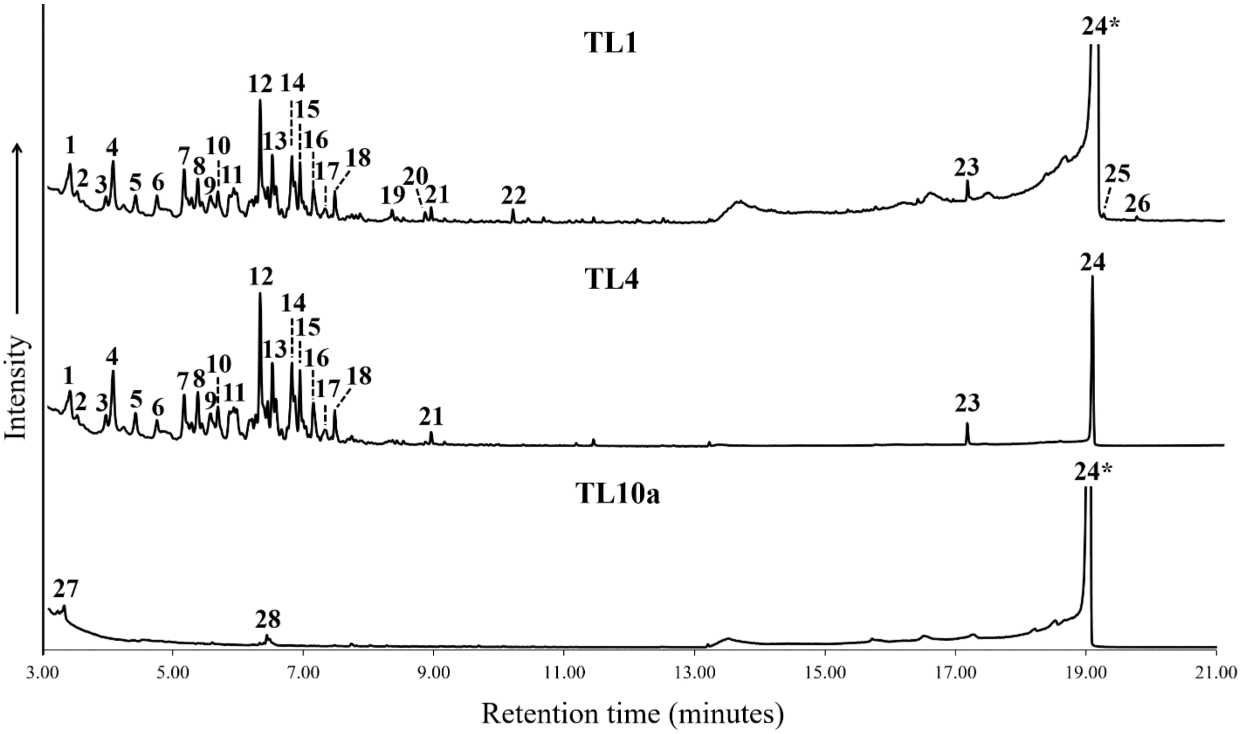

Figure 3.6. Stacked GC-MS chromatograms for DCM extracts of Tagish lake samples TL1, TL4 and TL10a (1 µL injections from 200 µL volumes). The cyclic octaatomic sulfur peaks$^{(*)}$ in Samples TL1 and TL10a have been truncated. Compound identifications are listed in Table 3.6.

Table 3.6. Weakly polar aliphatic and aromatic compounds and S_8 detected in DCM extracts of Tagish Lake samples TL1, TL4 and TL10a. Compound identifications are best matches reported by the NIST Mass Spectral Library.

Compound	Compound number	Compound	Compound number	Compound	Compound number
Sample TL1		**Sample TL4**		**Sample TL10a**	
3,5,5-trimethyl-2-hexene[a]	1	3,5,5-trimethyl-2-hexene[a]	1	4-methyl-2-pentanol[a]	27
3,5,5-trimethyl-2-hexene[a]	2	3,5,5-trimethyl-2-hexene[a]	2	2-ethyl-1-hexanol[a]	28
Ethylbenzene	3	Ethylbenzene	3	S_8	24
1,3-dimethyl-benzene	4	1,3-dimethyl-benzene	4		
p-xylene	5	p-xylene	5		
1,2,3,4,5-pentamethyl-cyclopentane[a]	6	1,2,3,4,5-pentamethyl-cyclopentane[a]	6		
2,4,4-trimethyl-1-hexene[a]	7	2,4,4-trimethyl-1-hexene[a]	7		
2,6-dimethyl-undecane	8	2,2,6-trimethyl-octane	8		
2,2,6-trimethyl-octane	9	2,2,6-trimethyl-octane	9		
2,2,6-trimethyl-octane	10	2,2,6-trimethyl-octane	10		
Mesistylene	11	Mesistylene	11		
2,2-dimethyl-decane	12	2,2-dimethyl-decane	12		
6-ethyl-2-methyl-octane	13	2,3,6,7-tetramethyl-octane	13		
5-ethyl-2,2,3-trimethyl-heptane	14	3-methyl-nonane	14		
2,6-dimethyl-octane	15	3,6-dimethyl-undecane	15		
3-methyl-undecane	16	2,6,10-trimethyl-dodecane	16		
3,7-dimethyl-decane	17	4-methyl-dodecane	17		
Undecane[a]	18	Undecane[a]	18		
1,2,4,5-tetramethyl-benzene	19	Dodecane[a]	21		
Naphthalene	20	1,2-benzene-dicarboxylic acid, bis(2-methylpropyl) ester	23		
Dodecane[a]	21	S_8	24		
Pentamethyl-benzene	22				
1,2-benzene-dicarboxylic acid, bis(2-methylpropyl) ester	23				
S_8	24				
Fluoranthene	25				
Pyrene	26				

[a] Terrestrial contaminant

3.4. DISCUSSION

3.4.1. Total soluble organic contents and general observations

The soluble organic data collected for the three newly analyzed Tagish Lake specimens can be described as two general groupings: (1) sample TL1, containing a relatively high overall soluble organic content and sharing compositional similarities with the previously analyzed Tagish Lake lithologies TL5b and TL11h (Herd et al., 2011; Glavin et al., 2012; Hilts et al., 2014); and (2) samples TL4 and TL10a, which are generally depleted in soluble organics, possibly due to very distinct alteration histories. Expanding the Tagish Lake dataset with these new results allows us to better evaluate the influence of aqueous alteration on the chemical synthesis and preservation of prebiotic organic compounds in the parent body asteroid. Previous studies have discussed the idea of a "sweet spot" of parent body aqueous alteration, whereby an intermediate level of alteration allows for optimal synthesis and preservation of soluble organics, while the lower and higher end-members of the alteration sequence either result in poor production or poor preservation of the compounds (Herd et al., 2011; Hilts et al., 2014). In the present study, we observe soluble organic compositions in the newly analyzed Tagish Lake specimens that appear to further support this theory. We also consider and discuss additional factors (e.g. presence or absence of key precursor compounds) that may have played a key role during prebiotic organic synthesis in Tagish Lake.

Based on our results, the composition of TL1 appears to reflect the "sweet spot" of aqueous alteration; for all quantifications (amino acids, carboxylic acids and carbonyl compounds), TL1 yielded much higher abundances of organics compared to TL4 and TL10a. The sum total of amino acids (~1877 ppb) and carboxylic acids (~635 ppm) in TL1 are intermediate between those of the previously analyzed TL5b and TL11h samples, which have previously been discussed as having experienced moderate levels of alteration (Table A2.4; Herd et al., 2011; Glavin et al., 2012; Hilts et al., 2014). Here, we discuss in detail the distribution of a range of compound classes in Tagish Lake, aiming to elucidate formation mechanisms and to gain insight into what factors played a role in synthesizing relatively high abundances of organics in TL1.

3.4.2. Amino acid synthesis and the influence of aqueous alteration

The amino acid content of the Tagish Lake meteorite has been previously shown to vary widely across the range of lithologies, not only in terms of total amino acid abundances, but also in terms of the amino acid distributions and their compound-specific carbon isotope compositions (Herd et al., 2011; Glavin et al., 2012; Hilts et al., 2014). The amino acid content of TL1 is unique in terms of its exceptionally high abundance of β-alanine and γ-ABA (Table 3.1); TL1 has the highest reported abundances for these two compounds in Tagish Lake so far. The bulk of the γ-ABA in TL1 was observed only in the acid-hydrolyzed sample, indicating that the compound was either minerally bound or present as a labile precursor that was converted to γ-ABA upon acid hydrolysis (Glavin et al., 2011). Unlike TL5b and TL11h, isovaline and α-AIB, common α-amino acids in CM chondrites, are present in only trace amounts in TL1. A similar amino acid composition has been observed for the CI chondrites Orgueil and Ivuna (Ehrenfreund et al., 2001); their relatively high abundances of β-alanine and γ-ABA and relatively low abundances of α-amino acids were attributed to amino acid synthesis in low temperature conditions and/or in the absence of Strecker α-amino acid precursors (e.g. HCN). The latter scenario is consistent with the relatively high abundance of aldehydes/ketones observed in TL1, as aldehydes/ketones would remain unreacted if the other Strecker precursors (e.g. HCN) were limiting in the system. The collective data suggest that Strecker synthesis was not the dominant reaction involved in amino acid production in TL1, but rather a process such as Michael addition or decarboxylation/deamination of dicarboxylic or diamino acids which would result in relatively higher abundances of β- and γ-amino acids, respectively (Elsila et al., 2016). In contrast, TL11h, dominated by α-amino acids, appears to have recorded a primarily Strecker synthesis source of amino acids, while TL5b has recorded a combination of multiple processes.

Although TL4 and TL10a resemble the previously analyzed TL11i sample in terms of their low total abundances of amino acids (Glavin et al., 2012), the relative abundances of the individual amino acids in these two samples are substantially different from those of TL11i. TL4 and TL10a are both dominated by glycine (at 90 and 70 mol%, respectively) whereas, in TL11i, glycine only comprises 27 mol% of the amino acid content. This observation implies that the low abundances of amino acids in TL4 and TL10a resulted from distinct processes than those which affected the composition of TL11i. This difference in composition is not surprising for TL4, as the TL4 specimen shows several characteristics (e.g. low abundance of phyllosilicates and high porosity) that imply that it has experienced very low levels of aqueous alteration compared to TL11i and has, therefore, experienced a very different alteration history. However, the amino acid composition of TL10a is more difficult to explain with minimal lithological context.

The amino acid compositions observed in the present study and previously for Tagish Lake samples exhibit some inconsistencies compared to general trends observed amongst carbonaceous chondrites (Figure 3.7). For example, the high relative abundances of γ-ABA and β-alanine observed in minimally-altered samples (TL1 and TL5b) is unusual; generally, higher relative abundances of β- and γ-amino acids are indicators of higher levels of alteration (Botta et al., 2002; Elsila et al., 2016). TL4 and TL10a are also unusual as their amino acid compositions are nearly identical, despite some apparent differences in their alteration histories and organic contents. Our amino acid data indicate that aqueous alteration may not have been the sole factor influencing the type, extent and duration of amino acid synthesis taking place in the Tagish Lake parent body asteroid and that, perhaps, the presence or absence of precursor molecules played the most significant role. The mobilization and, thus, the availability of key precursors compounds (e.g. aldehydes/ketones, HCN/NH_4, aliphatic hydrocarbons) would have been directly affected by aqueous alteration processes, so these potential influences would have been interconnected to some extent. However, our results suggest that a particular degree of aqueous alteration does not necessarily dictate the types of amino acids that are synthesized and that some mechanisms of amino acid synthesis may be de-coupled from aqueous alteration processes.

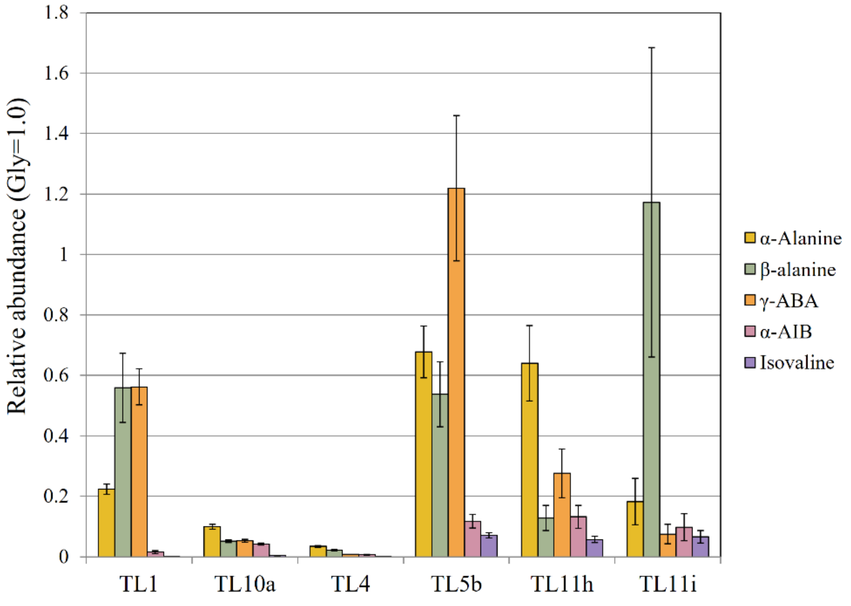

Figure 3.7. Molar relative abundances (Gly = 1.0) of amino acids in hydrolyzed samples of TL1, TL10a and TL4 (this study) compared to abundances for hydrolyzed samples of TL5b, TL11h and TL11i by Glavin et al. (2012). All values are blank-subtracted, with the exception of those of TL10a (see Section 3.2.4 for details).

The D/L enantiomeric ratios for the amino acids in TL1, TL4 and TL10a (Table 3.3) are generally consistent with what has been observed previously for Tagish Lake samples (Glavin et al., 2012). Both TL5b and TL11h have been previously shown to exhibit near-racemic values for alanine, β-ABA and isovaline and low D/L ratios for glutamic acid, serine and valine (Glavin et al., 2012). Unlike TL5b and TL11h, however, TL1 and TL4 both exhibit near-racemic D/L ratios for aspartic acid. The consistent observation of low D/L ratios for glutamic acid, serine and valine across Tagish Lake specimens supports the theory that these L-enantiomeric excesses are derived from extraterrestrial processes (e.g. amplification of conglomerate crystals; Glavin et al., 2012) and are not indicators of terrestrial contamination. The relatively high D/L ratios observed for aspartic acid in TL1 and TL4 compared to previously analyzed specimens may reflect a lower degree of aqueous alteration experienced by these two samples, as L-enantiomeric excesses are thought to be amplified via aqueous alteration (Glavin and Dworkin, 2009).

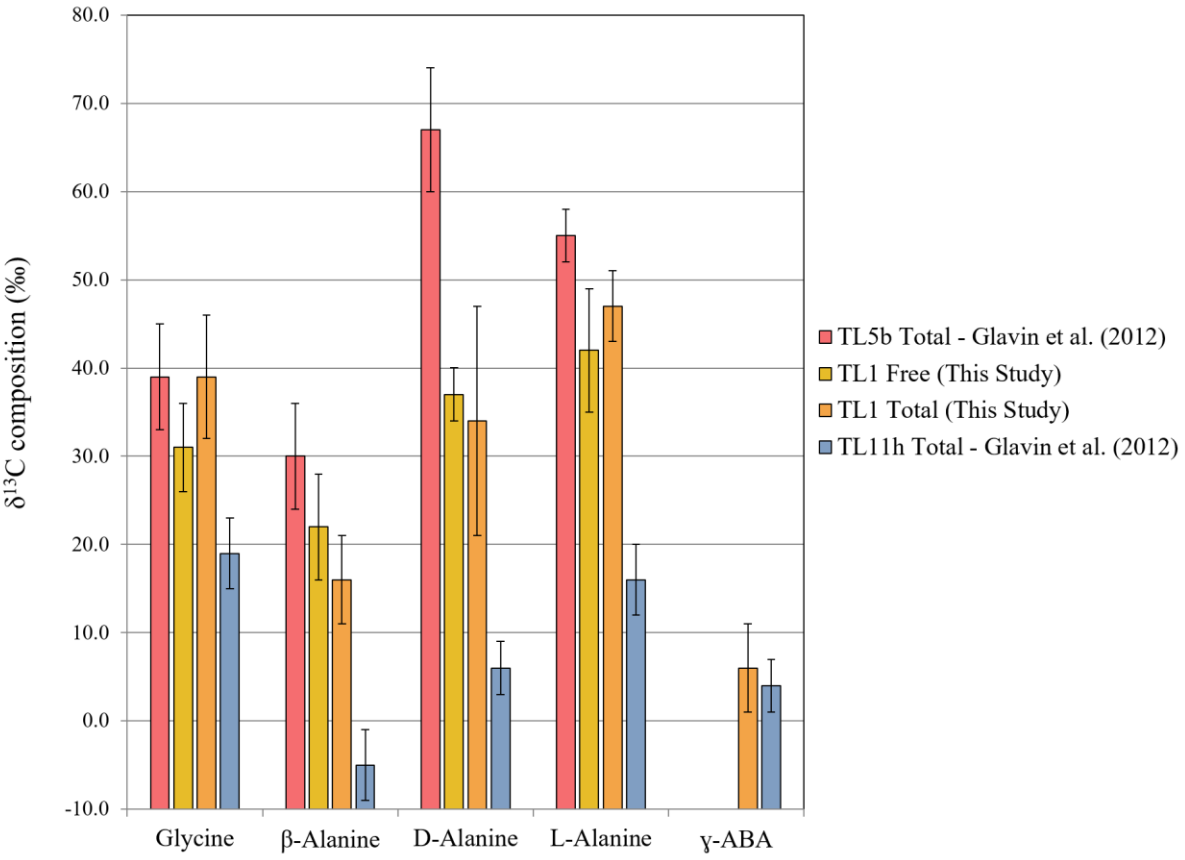

Figure 3.8. Stable carbon isotope ratios for amino acids in hydrolyzed and non-hydrolyzed samples of TL1 (this study) compared to values reported by Glavin et al. (2012) for hydrolyzed samples of TL5b and TL11h.

Figure 3.8 compares the compound-specific carbon isotope compositions of amino acids in TL1 with previous measurements from samples TL5b and TL11h (Glavin et al., 2012). Similar to the total amino acid abundances, several of the TL1 amino acid $\delta^{13}C$ values fall intermediate between those of TL5b and TL11h. The $\delta^{13}C$ values exhibit a general trend towards more ^{13}C-depleted compositions from TL5b to TL1 to TL11h (Figure 3.8). Exceptions to this trend are the glycine and hydrolyzed β-alanine values of TL5b which overlap with TL1 values within error, and the γ-ABA values for TL1 and TL11h, which also overlap within error. The differences in amino acid $\delta^{13}C$ values between TL5b and TL11h have been previously discussed by Glavin et al. (2012); the more ^{13}C-depleted values were interpreted as indicating more extensive aqueous alteration and/or a secondary pulse of alteration. However, there are several other possible explanations for the differences observed. Relatively ^{13}C-depleted amino acid compositions (e.g. in TL11h) could indicate a ^{13}C-depleted source/precursor (e.g. ^{13}C-depleted aldehydes, ketones, imines and/or HCN). The relatively ^{13}C-depleted amino acids in TL11h could also indicate a larger kinetic isotope fractionation effect associated with the reaction due to lower temperature conditions (Sephton and Gilmour, 2001). Alternatively, the TL11h amino acids may have been synthesized first, followed by TL1 and then TL5b; in theory, as preferentially ^{13}C-depleted amino acids are synthesized (e.g. amino acids in TL11h), the isotopic composition of the Strecker source/precursor would shift towards a more ^{13}C-enriched composition and the subsequently synthesized amino acids would reflect that shift (e.g. amino acids in TL1 and TL5b). This scenario, however, is only applicable if TL1, TL5b and TL11h were all part of highly interconnected closed system. Lastly, the $\delta^{13}C$ values could indicate that the amino acids in TL1 and TL5b were fractionated (shifted towards more ^{13}C-enriched compositions) as ^{12}C-containing amino acids were preferentially consumed or degraded during subsequent chemical reactions. The fact that the TL1 and TL11h γ-ABA values share a common carbon isotope composition is consistent with this theory, as the bulk of the γ-ABA detected in both specimens was released during hydrolysis, indicating that the γ-ABA may have been minerally-bound and not be chemically available for post-synthesis reactions

3.4.3. The origin of aldehydes and ketones in the Tagish Lake meteorite

The relative abundances of aldehydes and ketones in the Tagish Lake specimens (Figure 3.4) are similar to the distribution observed for the Murchison meteorite (Chapter 2); although the $\delta^{13}C$ values, ranging from -51.5‰ to -0.34‰, are highly ^{13}C-depleted compared to those measured from Murchison (+5.3 to +29.1‰, Chapter 2). The Tagish Lake formaldehyde values, ranging from -51.5‰ to -34.6‰, are the most exceptionally ^{13}C-depleted, even more so than the terrestrial formaldehyde δ^{13}C value measured for the procedural blanks (-28.1‰). The highly ^{13}C-depleted values in Tagish Lake suggest that these compounds are not primordial, as interstellar aldehydes and ketones are expected to be highly ^{13}C-enriched (δ^{13}C > +117‰; Wirström et al., 2012; Henkel et al., 1982; Chapter 2). As was proposed for aldehydes and ketones in the Murchison meteorite, the meteoritic carbonyl compounds detected here are likely derived from secondary formation processes during aqueous alteration in the asteroid. The relative ^{13}C-depletion of the Tagish Lake samples compared to the Murchison sample indicate that Tagish Lake has experienced more excessive chemical processing via secondary aqueous alteration reactions and/or that the Tagish Lake alteration temperatures were lower, resulting in greater isotopic fractionations.

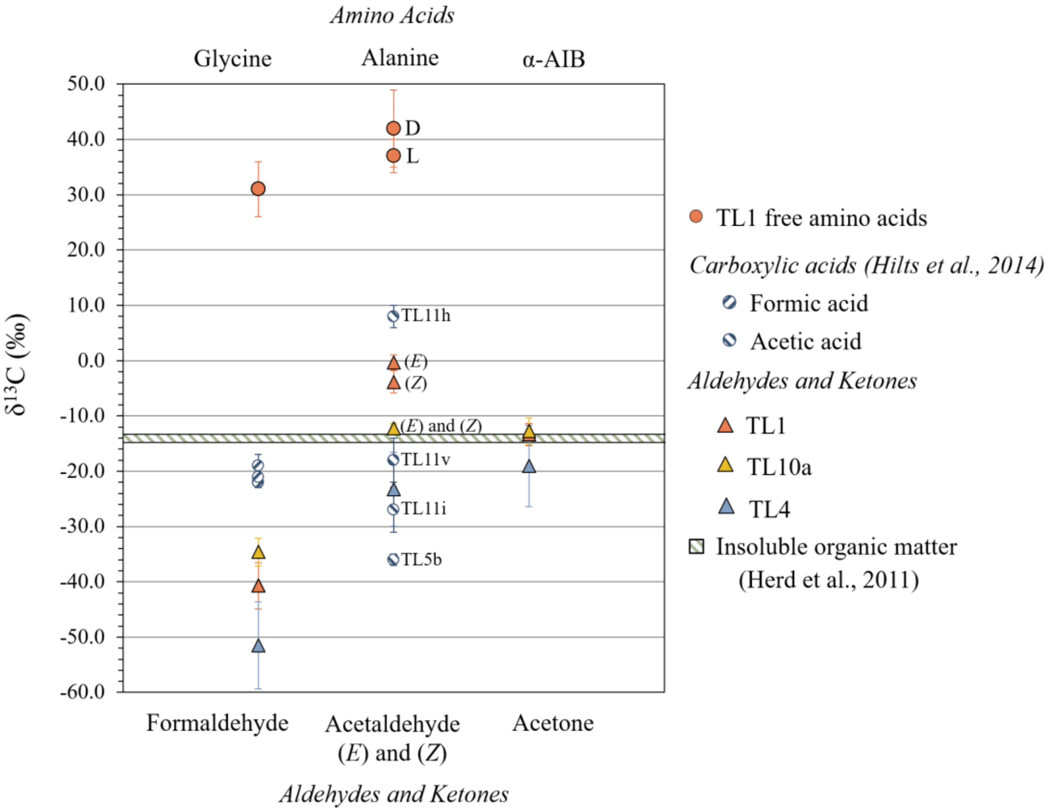

Figure 3.9. Carbon stable isotope compositions (‰ VPDB) of aldehydes and ketones in TL1, TL4 and TL10a (this study), the corresponding amino acids for TL1 (this study), carboxylic acids (Hilts et al., 2014) and insoluble organic matter (Herd et al., 2011). Two acetaldehyde data points represent the (*E*) and (*Z*) isomers. Two alanine data points represent the D- and L-enantiomers.

If Strecker synthesis reactions involve significant kinetic isotope fractionation effects, the amino acids products would be expected to be relatively ^{13}C-depleted in comparison to their aldehyde and ketone precursors. Based on their relatively high δ^{13}C (Figure 3.9), glycine and alanine detected in TL1 are not products of Strecker synthesis reactions involving the formaldehyde and acetaldehyde detected in the TL1 specimen. Similar to the results for the Murchison meteorite (Chapter 2), the Tagish Lake δ^{13}C values suggest that the aldehydes and ketones are either derived from the decomposition of the amino acids or from the oxidation of the IOM. In contrast to the Murchison results, the isotopic separations between the TL1 amino acid δ^{13}C ratios and the corresponding TL1 aldehyde and ketone δ^{13}C ratios are large (Δ(glycine-formaldehyde) ~ 70‰ and Δ(alanine-acetaldehyde) ~ 40‰). The fact that the aldehyde and ketone δ^{13}C ratios are more ^{13}C-depleted than the corresponding α-amino acids is consistent with what we would expect for amino acid decomposition, though we are limited in our ability to assess whether the magnitude of the isotopic separation is consistent with this theory. The aldehydes and ketones, particularly formaldehyde, may also be derived from oxidation of the IOM (Cody and Alexander, 2005). The isotopic separation between the formaldehyde δ^{13}C values and previous bulk IOM carbon isotope measurements is consistent with this theory. The amounts of oily residue present in the water extracts (Figure 3.1) also seem to correlate with the total abundances of aldehydes and ketones measured for each specimen, suggesting that there may be relationship between the IOM/aromatic carbon content and carbonyl content for these samples.

The δ^{13}C values for the aldehydes and ketones vary across the three Tagish Lake specimens but these differences between samples should be interpreted with caution as many of the values overlap within error and the carbon isotope analyses were likely affected to some extent by partially-coeluting peaks in the spectrum (Table 3.4). The lower the abundance of an aldehyde or ketone (i.e. the smaller the peak area), the greater the influence a co-eluting peak is expected to have on an isotopic analysis, as the overlap between peaks will comprise a larger proportion of the aldehyde or ketone peak area. As such, the variations in δ^{13}C values observed across the three specimens may be a result of varying concentrations of aldehydes and ketones. It does appear, however, that the TL1 $\delta^{13}C_{\text{acetaldehyde}}$ values are slightly more ^{13}C-enriched than those of TL4 and TL10a. This suggests that the acetaldehyde in TL1 is derived from a more ^{13}C-enriched source. Alternatively, its composition may have shifted towards a more ^{13}C-enriched value due to preferential reaction of relatively ^{13}C-depleted acetaldehyde molecules during subsequent chemical reactions. In any case, the apparent variation in $\delta^{13}C$ values observed for acetaldehyde across the TL1, TL4 and TL10a specimens is consistent with the wide range of $\delta^{13}C$ values observed for the structurally analogous carboxylic acid (acetic acid) in previously analyzed Tagish Lake specimens (Figure 3.9), suggesting that the synthesis and/or reactivity of acetaldehyde and acetic acid are highly influenced by parent body aqueous alteration processes.

3.4.4. Monocarboxylic acids

The monocarboxylic acid content of the Tagish Lake samples, specifically the abundance of acetic acid, may be used to group the samples into two categories: specimens with high abundances of acetic acid (225-293 ppm; TL5b, TL1 and TL11h) and specimens with low abundances of acetic acid (71-94 ppm; TL4, TL11i and TL11v) (Herd et al., 2011; Hilts et al., 2014; Table 3.7). Once again, the data suggest that there may be a sweet spot of alteration that allows for optimal synthesis and preservation of carboxylic acids, as the moderately altered specimens (TL1, TL5b, TL11h) exhibited the highest total abundances, while the end-members (TL4, TL11i, TL11v) yielded lower total abundances. These observations suggest that at least a proportion of the monocarboxylic acids are derived from alteration-driven reactions, such as oxidation of aldehydes (Corey et al., 1968) or oxidation of the macromolecular organic matter (Oba and Naraoka, 2006).

Table 3.7. Comparison of monocarboxylic acid abundances (ppm) of TL1 and TL4 (this study) compared to abundances (ppm) for TL5b, TL11h, TL11i, TL11v reported by Hilts et al. (2014).

	This Study		*Hilts et al. (2014)*			
	TL1	**TL4**	**TL5b**	**TL11h**	**TL11i**	**TL11v**
Formic	368	378	209	340	260	309
Acetic	**225**	94	**293**	**240**	92	71
Propanoic	34	n.d.	9	57	4	5
Hexanoic	2.8	n.d.	n.d.	3	0.9	0.6
Octanoic	1.7	n.d.	2	2	0.2	0.1
Nonanoic	1.6	n.d.	1	0.4	0.9	0.3
Benzoic	2.0	2.4	n.d.	n.d.	n.d.	n.d.
Total[a]	*635.1*	*474.4*	*533*	*656*	*359*	*387*

n.d. – not determined

[a] Total abundances for TL5b, TL11h, TL11i and TL11v include monocarboxylic acids that were not detected in TL1 and TL4 (not listed here).

Acetic acid is commonly the most abundant monocarboxylic acid detected in hot-water extracts of carbonaceous chondrite samples (Krishnamurthy et al., 1992; Naraoka et al., 1999;

Huang et al., 2005; Oba and Naraoka, 2006). The Tagish Lake specimens, however, exhibited relatively higher abundances of formic acid, which is likely attributable to their low-temperature storage conditions (Hilts et al., 2014). TL1 and TL4 contained the highest abundances of formic acid observed to date for the Tagish Lake meteorite. The relatively high concentrations of formic acid detected in these newly analyzed Tagish Lake specimens may reflect the importance of maintaining low-temperature storage conditions during subsampling and powdering. The Tagish Lake specimens analyzed in the present study were kept cold right up until the water extraction step, including the powdering step, unlike previous analyses. TL10a did not contain any detectable formic acid in either of the two water extracts, despite the care taken to keep the sample cold during subsampling and powdering, suggesting that the specimen does not contain indigenous formic acid. In fact, the bulk of the monocarboxylic acids detected in the TL10a samples may be terrestrial in origin based on comparisons with the procedural blanks, suggesting that TL10a is essentially devoid of carboxylic acids, with the exception of benzoic acid and potentially a trace amount of acetic acid. These observations alone suggest that TL10a is a relatively highly altered sample and that the lower molecular weight carboxylic acids degraded and/or were mobilized during parent body aqueous alteration. The presence of benzoic acid is consistent with this theory, as it is relatively less labile/less soluble in water in comparison to the carboxylic acids detected and is less likely to be mobilized by liquid water during periods of alteration. We also consider the possibility that the lack of monocarboxylic acids in TL10a is due to the absence of key precursor compounds (see Section 3.4.5).

3.4.5. Weakly polar aliphatic and aromatic compounds

The DCM solvent extractions and analyses of TL1, TL4 and TL10a yielded two notable differences in their organic contents (Figure 3.6, Table 3.6): (1) TL1 contained several PAHs (naphthalene, fluoranthene, pyrene), while free PAHs were absent from both TL4 and TL10a. This observation is consistent with the relatively higher abundance of an oily residue in water extracts of TL1 (Figure 3.1); and (2) two separate DCM extractions (Figures 6, A2) revealed that the TL10a specimen has a unique composition that is essentially devoid of weakly polar aliphatic hydrocarbons.

The presence of PAHs in TL1 and the absence in TL4/TL10a may provide some important insight into the alteration history of these three samples. PAHs are most often discussed as having a pre-accretionary origin, synthesized in low temperature interstellar clouds or circumstellar environments prior to the formation of the solar system (Gilmour, 2003). However, PAHs may also be derived from oxidation of the IOM during aqueous alteration on the parent body asteroid (Wing and Bada, 1992). The absence of PAHs in TL4, which appears to be minimally aqueously altered, suggests that the PAHs in the Tagish Lake meteorite were primarily synthesized during aqueous alteration; if the PAHs were pre-accretionary in origin, we would expect them to be detectable in the minimally-altered samples as well. For a comparison to other Tagish Lake lithologies, the previously analyzed TL5b specimen contained many PAHs (e.g. branched isomers of naphthalene, and pyrene), while TL11h contained naphthalene only, and TL11i contained no PAHs at all (Hilts et al., 2014). The presence of PAHs in the mid-sequence samples (TL1, TL5b, TL11h) and the absence of PAHs in the end-member samples (TL4, TL11i and possibly TL10a) suggests that, similar to other organic compound classes, there may be "sweet spot" for the production and preservation of free PAHs via aqueous alteration that is reflected in TL1, TL5b and TL11h. The relatively high free PAH content observed for TL1, TL5b, and TL11h may have played a role in yielding alteration-derived organics (e.g. carboxylic acids or aldehydes/ketones) in these three specimens.

The unusually "clean" GC-MS spectra observed for both TL10a DCM extracts suggest that this specimen has a unique history of aqueous alteration and chemical synthesis. It appears as though the weakly polar aliphatic and aromatic hydrocarbons have been essentially washed out of the sample during parent body aqueous alteration. The removal of these compounds during a period of aqueous alteration would be expected to influence subsequent chemical reactions, as the absence of low molecular weight straight-chain hydrocarbons and PAHs might preclude the formation of other soluble organics.

3.4.6. Implications for aqueous alteration on the Tagish Lake parent body asteroid

Collectively, the absence of weakly polar aliphatic hydrocarbons, PAHs and indigenous carboxylic acids, and the presence of amino acids, aldehydes, and ketones (in low abundances) in TL10a suggests that TL10a has a unique and unusual alteration history. The alteration processes in TL10a appear to have favored the production and/or preservation of amino acids and aldehydes/ketones over other compound classes. Without carbon isotope analyses for the amino acids in TL10a, it is difficult to assess the origins of these compounds and whether the amino acids, aldehydes and ketones in TL10a share a common synthetic relationship. However, it appears that, at some point, TL10a experienced a pulse of aqueous alteration at elevated temperatures or with a high water/rock ratio that resulted in the degradation and/or mobilization of most soluble organics, as reflected by the "clean" GC-MS spectra for this specimen. The amino acids, aldehydes, and ketones detected in TL10a may have been introduced to TL10a via mobilization from another region of the asteroid. Alternatively, the amino acids may not be as directly influenced by aqueous alteration as previously thought; it's possible that these compounds were synthesized via a mechanism that does not require the presence of liquid water, though the presence of aldehydes and ketones in TL10a is more difficult to interpret without an alteration-driven reaction.

The high abundances of soluble organics present in TL1 and the low abundances observed for TL4 support the idea of an optimal degree of aqueous alteration for producing and preserving high abundances of prebiotic compounds. Our data are also consistent with the parent body asteroid being an interconnected system that has experienced some fluid flow (rather than static aqueous alteration), as we seem to have observed some loss or mobilization of organics across Tagish Lake specimens (e.g. TL10a). Further interpretation may require some specificity about what exactly is implied by the "degree" of parent body aqueous alteration, as variations in water/rock ratios, durations of alteration and alteration temperatures may have very different effects on the soluble organic chemistry.

3.5. CONCLUSIONS

The three newly analyzed Tagish Lake specimens yielded unique soluble organic contents that suggest distinct parent body alteration histories. The distribution and abundances of amino acids, carboxylic acids and weakly polar aliphatic and aromatic hydrocarbons in TL1 resembled the soluble organic contents of the previously analyzed TL5b and TL11h (Herd et al., 2011; Glavin et al., 2012; Hilts et al., 2014); TL1 exhibited relatively high abundances soluble organic compounds and appears to reflect a "sweet spot" of aqueous alteration that did not result in the degradation or loss of alteration-derived organics. TL4, which appears to be a minimally-altered sample, yielded very low abundances of organics, supporting the theory that many of the soluble organics observed in the Tagish Lake meteorite are primarily generated via alteration-driven reactions. Specimen TL10a was found to be essentially devoid of monocarboxylic acids and weakly polar aliphatic and aromatic compounds. TL10a contained low abundances of amino acids, dominated by glycine, and low abundances aldehydes and ketones, which we propose may be derived from a different portion of the asteroid via mobilization during fluid flow.

3.6. REFERENCES

Bland, P. A., G. Cressey, and O. N. Menzies (2004) Modal mineralogy of carbonaceous chondrites by X-ray diffraction and Mossbauer spectroscopy. *Meteoritics & Planetary Science* **39**, 3-16.

Blinova, A. I., C. D. K. Herd, and M. J. M. Duke (2014a) Testing variations within the Tagish Lake meteorite - II: Whole-rock geochemistry of pristine samples. *Meteoritics & Planetary Science* **49** (6), 1100-1118.

Blinova, A. I., T. J. Zega, C. D. K. Herd and R. M. Stroud (2014b) Testing variations within the Tagish Lake meteorite - I: Mineralogy and petrology of pristine samples. *Meteoritics & Planetary Science* **49** (4), 473-502.

Botta, O., D. P. Glavin, G. Kminek, and J. L. Bada (2002) Relative amino acid concentrations as a signature for parent body processes of carbonaceous chondrites. *Origins of Life and Evolution of the Biosphere* **32**, 143-163.

Botta, O. and J. L. Bada (2002) Extraterrestrial organic compounds in meteorites. *Surveys in Geophysics* **23**, 411–467.

Brown, P. G., A. R. Hildebrand, M. E. Zolensky, M. Grady, R. N. Clayton, T. K. Mayeda, E. Tagliaferri, R. Spalding, N. D. MacRae, E. L. Hoffman, D. W. Mittlefehldt, J. F. Wacker, J. A. Bird, M. D. Campbell, R. Carpenter, H. Gingerich, M. Glatiotis, E. Greiner, M. J. Mazur, P. J. A. McCausland, H. Plotkin, T. R. Mazur (2000) The fall, recovery, orbit, and composition of the Tagish Lake meteorite: A new type of carbonaceous chondrite. *Science* **290**, 320-325.

Cancho, B., F. Ventura and M. T. Galceran (2001) Determination of aldehydes in drinking water using pentafluorobenzylhydroxylamine derivatization and solid-phase microextraction. *Journal of Chromatography* **943**, 1-13.

Cody, G. D., and C. M. O'D. Alexander (2005) NMR studies of chemical structural variation of insoluble organic matter from different carbonaceous chondrite groups. *Geochimica et Cosmochimica Acta* **69**, 1085-1097.

Docherty, G., V. Jones, and R. P. Evershed (2001) Practical and theoretical considerations in the gas chromatography/combustion/isotope ratio mass spectrometry $\delta^{13}C$ analysis of small polyfunctional compounds. *Rapid Communications in Mass Spectrometry* **15**, 730-738.

Ehrenfreund, P., D. P. Glavin, O. Botta, G. Cooper, and J. L. Bada (2001) Extraterrestrial amino acids in Orgueil and Ivuna: Tracing the parent body of CI type carbonaceous chondrites. *PNAS* **98** (5), 2138-2141.

Elsila, J. E., D. P. Glavin, and J. P. Dworkin (2009) Cometary glycine detected in samples returned by Starbust. *Meteoritics & Planetary Science* **44**, 1323-1330.

Elsila, J. E., S. B. Charnley, A. S. Burton, D. P. Glavin, and J. P. Dworkin (2012) Compound-specific carbon, nitrogen, and hydrogen isotopic ratios for amino acids in CM and CR chondrites and their use in evaluating potential formation pathways. *Meteoritics & Planetary Sciences* **47** (9), 1517-1536.

Elsila, J. E., J. C. Aponte, D. G. Blackmond, A. S. Burton, J. P. Dworkin, and D. P. Glavin (2016) Meteoritic amino acids: diversity in compositions reflects parent body histories. *ACS Central Science* **2** (6), 370-379.

Gilmour, I. (2003) Structural and isotopic analysis of organic matter in carbonaceous chondrites. *Treatise on Geochemistry 1st Edition*, H.D. Holland and K. K. Turekian, Eds. (Elsevier, 2004) vo1. 1, p. 269-290.

Gilmour, C. (2017) Economic significance of platinum group elements and water in asteroids: Insights from chondritic meteorites (Master's thesis), University of Alberta.

Glavin, D. P., J. P. Dworkin, A. Aubrey, O. Botta, J. H. Dotty III, Z. Martins, and J. L. Bada (2006) Amino acid analyses of Antarctic CM2 meteorites using liquid chromatography – time of flight – mass spectrometry. *Meteoritics & Planetary Science* **41** (6), 899-902.

Glavin, D. P., J. E. Elsila, A. S. Burton, M. P. Callahan, J. P. Dworkin, R. W. Hilts, and C. D. K. Herd (2012) Unusual nonterrestrial L-proteinogenic amino acid excesses in the Tagish Lake meteorite. *Meteoritics & Planetary Science* **47** (8), 1347-1364.

Glavin, D. P., and J. P. Dworkin (2009) Enrichment of the amino acid L-isovaline by aqueous alteration on CI and CM meteorite parent bodies. *PNAS* **106**, 5487-5492.

Henkel, C., T. L. Wilson, and J. Bieging (1982) Further ($^{12}C/^{13}C$) ratios from formaldehyde: A variation with distance from the galactic center. *Astronomy & Astrophysics* **109**, 344–351.

Herd, C. D. K, A. Blinova, D. N. Simkus, Y. Huang, R. Tarozo, C. M. O'D. Alexander, F. Gyngard, L. R. Nittler, G. D. Cody, M. L. Fogel, Y. Kebukawa, A. L. D. Kilcoyne, R. W. Hilts, G. F. Slater, D. P. Glavin, J. P. Dworkin, M. P. Callahan, J. E. Elsila, B. T. De Gregorio, and

R. M. Stroud (2011) Origin and evolution of prebiotic organic matter as inferred from the Tagish Lake meteorite. *Science* **332**, 1304-1307.

Herd, C. D. K., R. W. Hilts, A. W. Skelhorne, and D. N. Simkus (2016) Cold curation of pristine astromaterials: Insights from the Tagish Lake meteorite. *The Meteoritical Society* **51**, 499-519.

Hilts, R. W, C. D. K. Herd, D. N. Simkus, and G. F. Slater (2014) Soluble organic compounds in the Tagish Lake meteorite. *Meteoritics & Planetary Science* **49** (4), 526-549.

Huang, Y., Y. Wang, M. R. Alexandre, T. Lee, C. Rose-Petruck, M. Fuller, and S. Pizzarello (2005) Molecular and compound-specific isotopic characterization of monocarboxylic acids in carbonaceous chondrites. *Geochimica et Cosmochimica Acta* **69** (4), 1073-1084.

Kminek, G., O. Botta, D. P. Glavin, and J. L. Bada (2002) Amino acids in the Tagish Lake meteorite. *Meteoritics & Planetary Science* **37**, 697-701.

Krishnamurthy, R. V., S. Epstein, J. R. Cronin, S. Pizzarello and G. U. Yuen (1992) Isotopic and molecular analyses of hydrocarbons and monocarboxylic acids of the Murchison meteorite. *Geochimica et Cosmochimica Acta* **56**, 4045-4058.

Naraoka, H., A. Shimoyama, and K. Harada (1999) Molecular distribution of monocarboxylic acids in Asuka carbonaceous chondrites from Antarctica. *Origins of Life and Evolution of the Biosphere* **29**, 187-201.

Oba, Y. and H. Naraoka (2006) Carbon isotopic composition of acetic acid generated by hydrous pyrolysis of macromolecular organic matter from the Murchison meteorite. *Meteoritics & Planetary Science* **41** (8), 1175-1181.

O'Brien, D. M., M. L. Fogel, and C. L. Boggs (2002) Renewable and nonrenewable resources: Amino acid turnover and allocation to reproduction in Lepidoptera. *PNAS* **99**, 4413-4418.

Ralchenko, M., D. T. Britt, C. Samson, C. D. K. Herd, R. K. Herd, and P. J. A. McCausland (2014) Bulk physical properties of the Tagish Lake meteorite frozen pristine fragments. *LPSC XIV*, # 1021.

Sephton, M. A. (2002) Organic compounds in carbonaceous meteorites. *Natural Product Reports* **19**, 292-311.

Wing, M. R. and J. L. Bada (1992) The origin of the polycyclic aromatic hydrocarbons in meteorites. *Origins of Life and Evolution of the Biosphere* **21**, 375-383.

Wirström, E. S., S. B. Charnley, W. D. Geppert, and C. M. Persson (2012) Observations of carbon isotopic fractionation in interstellar formaldehyde. *43rd Lunar and Planetary Science Conference,* #1611.

Zolensky, M. E., K. Nakamura, M. Gounelle, T. Mikouchi, T. Kasama, O. Tachikawa, and E. Tonui (2002) Mineralogy of Tagish Lake: An ungrouped type 2 carbonaceous chondrite

CHAPTER 4:

TIME-OF-FLIGHT SECONDARY ION MASS SPECTROMETRY (TOF-SIMS) ANALYSIS OF AMINO ACIDS IN THE MURCHISON AND TAGISH LAKE METEORITES

4.1. INTRODUCTION

The soluble organic content of carbonaceous chondrite meteorites records a history of abiotic chemical processes that took place throughout early solar system formation and during aqueous alteration on asteroidal parent bodies. Several classes of prebiotic organic compounds, including amino acids – the building blocks of protein in living systems – have been detected and studied across a wide range of carbonaceous chondrite samples (Sephton, 2014). Investigations of the soluble organic content of carbonaceous chondrites, most often focusing on their prebiotic organic compounds, are generally carried out as solvent extractions of bulk meteorite samples. Compound identifications and quantifications are achieved using gas chromatography mass spectrometry (GC-MS), high performance liquid chromatography (HPLC), or liquid chromatography-mass spectrometry (LC-MS). These methods offer information about the structure, abundance and potential origins of organic matter in meteorites; however, bulk analyses alone cannot address whether organic compounds are distributed homogeneously throughout the meteorite samples or whether they are concentrated in association with certain mineral grains or textures. Furthermore, the solvent extraction step itself could potentially result in the modification or production of organic compounds, which may result in a misrepresentation of the indigenous organic matter. Investigating the distribution of organic compounds on a micrometer scale and identifying compound-mineral associations can provide valuable insight into the synthesis and possible migration of prebiotic organic compounds in asteroid parent bodies throughout their alteration histories.

Secondary ion mass spectrometry (SIMS) is an in-situ analytical technique that provides a detailed chemical composition of a sample by sputtering the surface with a primary ion beam and generating a mass spectrum from the secondary ionized particles that are emitted (Vickerman, 2013). Time-of-flight secondary ion mass spectrometry (TOF-SIMS) is a variant of this technique that measures the "time-of-flight" from the moment a primary ion impacts the sample surface to the moment that a secondary ionized particle reaches the detector. Measured on the scale of nanoseconds, the “time-of-flight” approach for differentiating ionized species provides high mass resolution. One of the other main advantages of TOF-SIMS is that it allows for the quasi-simultaneous detection of all secondary ion species (organic and inorganic) of one polarity. As such, the method is particularly valuable when analyzing rare astromaterials, as it provides a wealth of information about the composition of a sample through a single analysis. The pulsing of the primary ion beam also minimizes destruction of the sample. TOF-SIMS is highly sensitive and is suitable for the analysis of small samples due to high lateral resolution (~0.2 μm) (Stephan, 2001).

Over the past ~ 20 years, research has demonstrated the utility of TOF-SIMS as a powerful tool for investigating the chemical composition of astromaterials, including elemental distributions and mineral identification for carbonaceous chondrites, Martian meteorites, interplanetary dust particles (IDPs), presolar grains, and particle impact residues from space probes (see review and references therein: Stephan, 2001). TOF-SIMS investigations of organics in astromaterials have focused primarily on polyaromatic species (e.g. polycyclic aromatic hydrocarbons (PAHs) in the Martian meteorite Allan Hills 84001 (Stephan et al., 2003)). Lower molecular weight organic compounds, such as amino acids, have not been a priority target for TOF-SIMS analyses of astromaterials, despite their prebiotic significance, likely due to challenges associated with obtaining confident compound identifications. Henkel and Lyon (2015, 2016) recently analyzed the Murchison meteorite using C_{60}^+-TOF-SIMS in search for indigenous amino acids but concluded that the suite of amino acids detected were not present above background levels and could not be conclusively characterized as indigenous to the meteorite. Detecting amino acids in situ on meteorite fresh fracture surfaces and identifying potential compound-mineral associations would provide valuable insights into the geochemical conditions and mechanisms involved in the synthesis of these compounds in space.

The objectives of the present study were threefold: (1) to establish a database of expected fragmentation patterns for standard amino acid compounds analyzed by Bi_1^+ and Bi_3^+-TOF-SIMS and develop a basis for identifying amino acids in situ on meteorite samples; (2) to analyze fresh fracture surfaces of the Murchison and Tagish Lake carbonaceous chondrites to evaluate the utility of TOF-SIMS for the analysis of indigenous amino acids in astromaterials; and (3) to investigate the distribution of organic compounds across fresh fracture surfaces of the Murchison and Tagish

Lake meteorite samples to determine whether there are any spatial associations between the organics and specific mineral grains or textures. We utilized the information gained from solvent extraction analyses of the Murchison and Tagish Lake meteorites to build a list of target organic compounds for TOF-SIMS analyses of these two carbonaceous chondrites. The Murchison meteorite is often used as a reference standard for investigating the organic content of other carbonaceous chondrites, due to the large dataset available from nearly 50 years of research (Botta and Bada, 2002; Sephton, 2014). The Tagish Lake meteorite is exceptionally pristine as it was collected shortly after its fall without direct hand contact and has been stored in clean, cold (< 0°C) conditions (Herd et al., 2016). Tagish Lake is particularly well-suited for in-situ analyses as it has been shown to exhibit a unique heterogeneity that may be present on the micrometer scale (Herd et al., 2011). The specific Tagish Lake specimen analyzed in this study (TL1) contains indigenous amino acids in relatively high abundances (Chapter 3) and is, therefore, a good target for detecting these types of compounds. Table 4.1 summarizes the concentrations of the ten most abundant amino acids in the Murchison and Tagish Lake meteorites, based on solvent extraction analyses. In the present study, we focus our standard analyses and compound identifications on amino acids that are specifically abundant in the Tagish Lake meteorite: glycine, β-alanine, γ-amino-n-butyric acid (γ-ABA), α-alanine, β-amino-n-butyric acid (β-ABA), α-amino-n-butyric acid (α-ABA), glutamic acid, aspartic acid, and α-aminoisobutyric acid (α-AIB). These compounds are all found in relatively high abundances in the Murchison meteorite as well (Table 4.1).

Table 4.1. Concentrations (ppb) of the ten most abundant amino acids detected in the Murchison meteorite and in the Tagish Lake TL1 specimen, based on solvent extraction analyses.

Murchison[a]		Tagish Lake[b]	
Amino acid	**Abundance[c]**	**Amino acid**	**Abundance[c]**
Glycine	2919	Glycine	559
α-AIB	2901	γ-ABA	432
α-Alanine	1676	β-Alanine	371
Glutamic acid	1338	α-Alanine	148
γ-ABA	1331	β-ABA	136
β-Alanine	1269	Glutamic acid	39
Isovaline	808	α-ABA	36
β-ABA	708	4-a-2-mba	36
α-ABA	642	Aspartic acid	21
Aspartic acid	442	α-AIB	12

[a] Murchison amino acid data is from Botta et al. (2002)
[b] Tagish Lake (TL1) amino acid data is from Chapter 3 of this Ph.D. thesis
[c] Amino acid abundances are "total" (HCl-hydrolyzed) abundances

4.2. MATERIALS AND METHODS

4.2.1. Laboratory reagents and materials

Amino acid standards were purchased from Sigma Aldrich and Fisher Scientific. Ultrapure water (Millipore Direct Q3 UV, 18.2 MΩ, 3 ppb total organic carbon; hereafter referred to as "water") was used for all standard solutions. All glass and metal laboratory materials used for preparing and transferring samples were wrapped in aluminum foil and combusted at 450 °C for at least 6 hours prior to use to remove any potential terrestrial organic contaminants. Nitrile gloves were worn at all times during sample preparation to prevent contamination.

4.2.2. Analysis of amino acid standards

Silicon wafers were sectioned into small (~ 1 cm^2) pieces and placed within a glass petri dish, which was subsequently wrapped in aluminum foil and combusted at 450°C for > 6 hours to remove any organic contaminants. Amino acid standards were dissolved in Millipore water. For each amino acid standard, one droplet of solution was placed on the surface of a wafer piece in the fume hood. Once the solution was evaporated, usually within 1-2 minutes, a separate clean wafer piece was placed on top of the dried solution to contain the sample and prevent cross-contamination between wafers. This process was repeated for each of the standards. The wafers with their wafer covers were transferred to the TOF-SIMS sample holder within the fume hood. Once all wafers were transferred, the wafer covers were removed and the sample holder was immediately loaded into the TOF-SIMS machine. The wafers were exposed to laboratory air for less than 30 seconds during this process. Bismuth was used as the primary ion source to achieve high yields of organic ions with minimal molecular fragmentation (Touboul et al., 2005; Tyler et al., 2011). The standards were analyzed using two separate bismuth primary ion beams, Bi_1^+ and Bi_3^+, to compare the associated mass fragmentation patterns. The Bi_1^+ and Bi_3^+ analyses for a single amino acid standard were both run on the same day to minimize any temporal variations derived from instrumental effects. The analyses were run with the same instrumental parameters as the meteorite samples: high current bunched mode, 10 shots/pixel, 256 x 256 pixels, with charge compensation. Each analysis was run for 10 minutes. Negative ion spectra were generated for five of the amino acids – glycine, β-alanine, α-AIB, glutamic acid, aspartic acid – but were found to be relatively uninformative compared to the positive ion spectra; relatively small peaks corresponding to the quasi-molecular ions $[M-H]^-$ were present but the spectra were otherwise dominated by inorganic ions. A similar result has been observed for other studies (e.g. Mantus et al., 1993; Samuel et al., 2001). All further standard analyses were carried out for positive ion spectra only.

4.2.3. TOF-SIMS analysis of the Murchison meteorite

Two separate Murchison meteorite samples were analyzed for this study. The first sample, USNM 5360, provided by the Department of Mineral Sciences at the Smithsonian Institution, had been sealed in a jar since 1971 (Figure 4.1) and was fully enveloped by a fusion crust. The sample was removed from the jar in a laminar flow hood and immediately wrapped in previously combusted aluminum foil. A small corner of the rock was split off using a clean, miniature rock splitter. The aluminum foil was removed from the sample and the small chip was quickly mounted onto the TOF-SIMS sample holder using carbon tape on the outer surface as an adhesive. The fresh fracture surface of the meteorite chip did not encounter the carbon tape adhesive or any other external surfaces. The sample holder with the Murchison chip was loaded into the ION-TOF GmbH TOF-SIMS IV instrument at the Smithsonian Institution for analysis. Five 500 x 500 μm^2 sample areas of the fresh fracture surface were analyzed using a 25 keV Bi_3^+ beam at a pulsed current of 0.3 pA. The five areas chosen for analysis were those that provided the highest and most homogeneously distributed total ion yield, reflecting the flattest surface topographies. An electron flood gun was used for charge compensation; this process provides low energy electrons (10-20 eV) to the insulating sample surface to compensate for any positive surface charge build-up (Hagenhoff et al., 1989). The instrument was optimized for high mass resolution by carrying out the analyses using high current bunched mode (m/Δm of at least ~5,000 at m/z 30) and negative secondary ion distribution images were generated for each section, with 256 x 256-pixel resolution. Each scan consisted of 10 primary ion shots per pixel. The analyses were run until 100 total scans of the area were completed, or until a dose density limit of 10^3 counts per pixel was reached.

The second Murchison sample, MET11544, provided by the University of Alberta Meteorite Collection was subsampled at room temperature in a purified Ar glovebox in the University of Alberta Subzero Facility for Curation of Astromaterials (Herd et al., 2016). The objective for this analysis was to compare Bi_1^+ and Bi_3^+ analyses across the same sample areas to observe any differences in secondary ion yields and mass fragmentation patterns derived from the two methods. The sample was split within the glovebox using a clean rock splitter and an interior chip with a relatively flat fresh fracture surface was collected for analysis. The sample was removed from the glovebox and quickly transferred with clean tweezers to the TOF-SIMS sample holder, using carbon tape as an adhesive on the outer surface of the meteorite chip. The fresh fracture surface of the chip did not encounter the carbon tape or any other external surface. The sample holder containing the meteorite chip was loaded into the ION-TOF GmbH TOF-SIMS IV instrument in the nanoFAB laboratory at the University of Alberta for analysis. The electron flood gun was used for charge compensation. Two 500 x 500 μm^2 sample areas were analyzed, both by Bi_1^+ and Bi_3^+, using the same instrumental parameters that were used for the Murchison (USNM 5360) analyses: high current bunched mode, 256 x 256-pixel resolution, 10 shots/pixel, 500 x 500 μm^2 sample areas, 100 scans each. For the first sample area, the order of analyses was Bi_1^+-TOF-SIMS followed by Bi_3^+-TOF-SIMS. For the second sample area, the order of analyses was Bi_3^+-TOF-SIMS followed by Bi_1^+-TOF-SIMS.

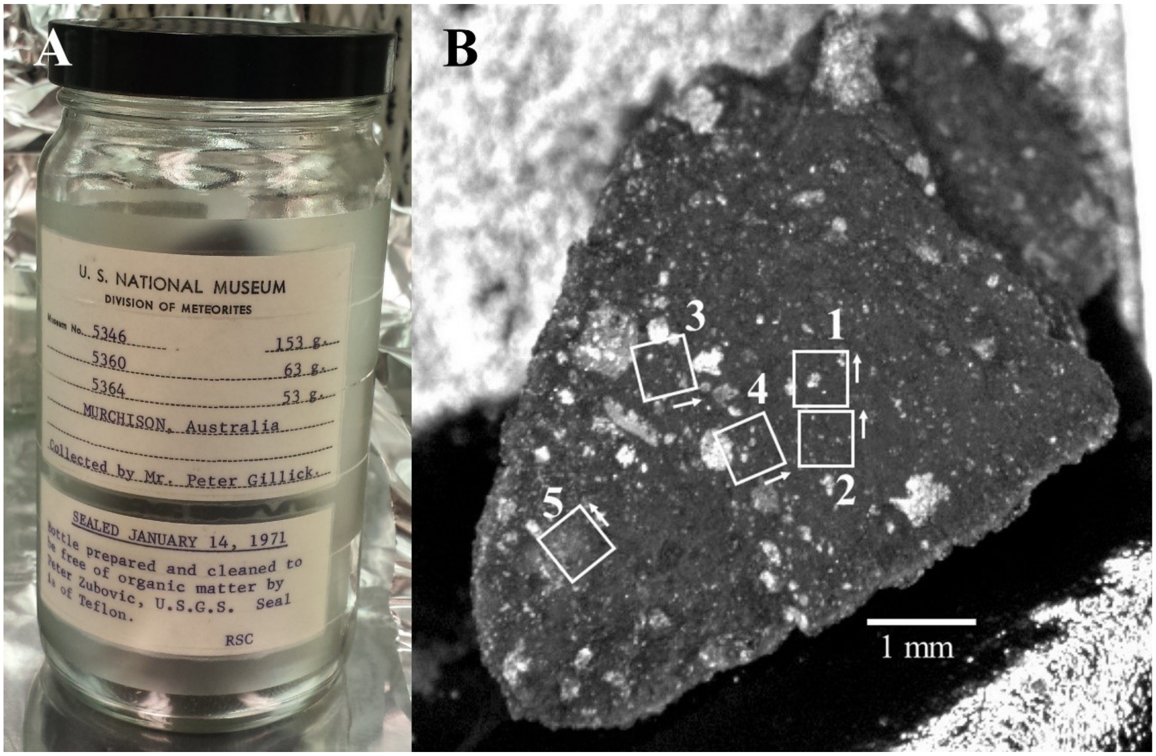

Figure 4.1. **A.** Storage container for the Murchison sample (USNM 5360). **B.** The fresh fracture surface and five 500 x 500 μm^2 sample areas analyzed by Bi_3^+-TOF-SIMS. Arrows indicate the upwards orientation of the secondary ion distribution images generated for each sample area (Figure 4.5).

4.2.4. TOF-SIMS analysis of the Tagish Lake meteorite

Subsampling of the Tagish Lake sample (TL1) was carried out in the University of Alberta Subzero Facility for Curation of Astromaterials (Herd et al., 2016), in a purified Ar glovebox contained within a walk-in freezer (< -10°C). A small chip of TL1 was broken off from the main mass using a clean scalpel to expose a fresh fracture surface of the meteorite. The outer side of the chip was entirely fusion crust. The sample was brought to room temperature within a clean, covered petri dish in the Class 1000 clean room and was transferred to the TOF-SIMS sample holder using a clean pair of tweezers and carbon tape as an adhesive on the fusion crust side of the chip. No external surfaces came into contact with the fresh fracture surface of the sample. The sample holder was transferred to the TOF-SIMS lab inside a storage container filled with cleanroom air. The sample was re-adjusted slightly before transferring the stage into the TOF-SIMS machine, but the sample was exposed to lab air for less than a minute and the fresh fracture surface remained untouched. The TL1 chip was analyzed using the same instrumental parameters that were used for the Murchison analyses: high current bunched mode, 256 x 256-pixel resolution, 10 shots/pixel, 500 x 500 μm^2 sample areas, 100 scans each. The electron flood gun was used for charge compensation. Only positive ion spectra were obtained for the TL1 samples. Seven 500 x 500 μm^2 sample areas were analyzed. The signal varied widely between each sample area due to topographic variations. Sample areas 1-4 had the highest and most uniform total ion yield, indicating relatively flat topographies.

Two additional fresh fracture surfaces of the Tagish Lake TL1 specimen were analyzed using Bi_1^+-TOF-SIMS for this study (refer to Section A3.1 of the Appendix). The goal of this second analysis was to break open a meteorite chip and analyze the two mirror-image fresh fracture surfaces of the meteorite to compare the resulting secondary ion distribution images and look for similarities in the distribution of the organics between mirroring sample areas (Figure A3.1). Unfortunately, due to the rough surface topography of the two fracture surfaces, both TL1 chips yielded low and irregular total ion yields. For many sample areas, the spectra exhibited broad doublet peaks; mass resolution was insufficient to properly identify molecular ions in five of the ten sample areas. The results are reported in the Appendix (Table A3.1) along with details of the subsampling and analytical procedure.

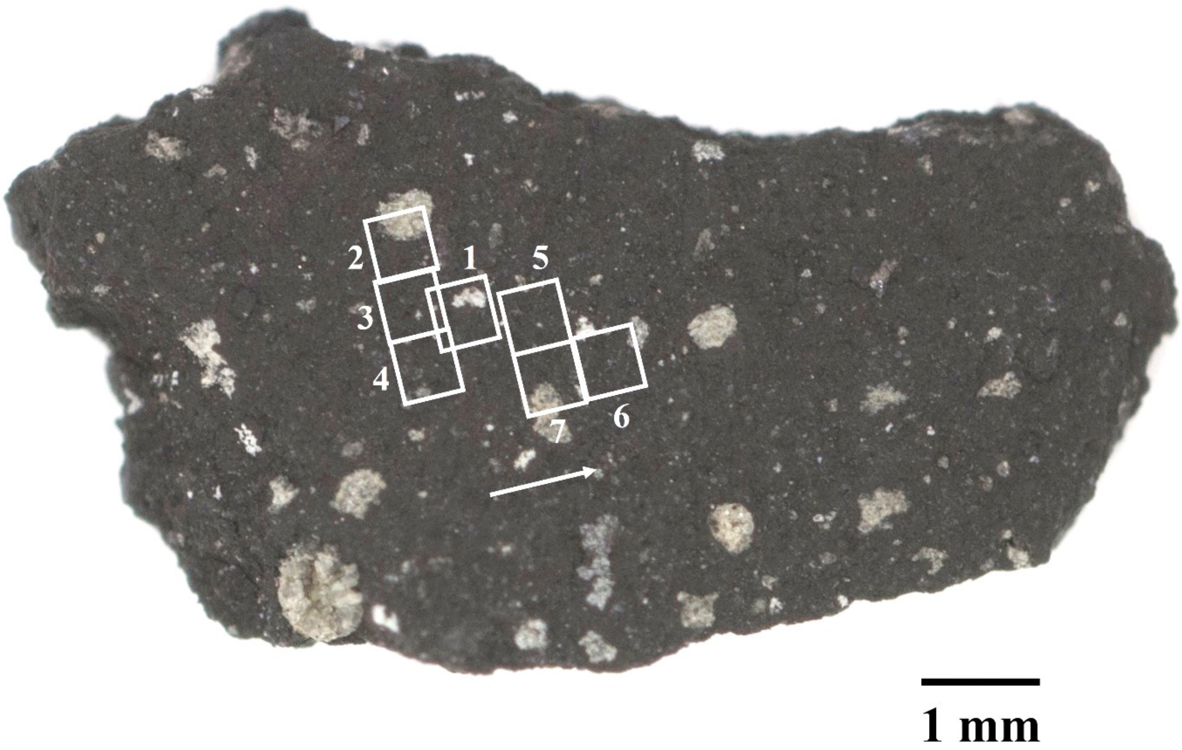

Figure 4.2. Fresh fracture surface of the Tagish Lake TL1 specimen and seven 500 x 500 µm^2 areas analyzed via Bi_1^+-TOF-SIMS. Arrow indicates the upwards orientation of the secondary ion distribution images for the sample areas.

4.2.5. Compound identifications and secondary ion distribution images

All TOF-SIMS data were acquired and processed using SurfaceLab 6 Version 6.1 software. The "detection" or "non-detection" of a molecular ion on a sample surface is based on the software's best match for the nominal mass of interest and is therefore reliant on the quality of the mass resolution and accuracy of the mass calibration. Molecular ion identifications for organic compounds can be particularly challenging due to mass interferences between countless possible combinations of C, H, O and N, as well as the presence of cationized organic species (Briggs and Fletcher, 2013). For this reason, we have chosen to carry out analyses using high current bunched mode, optimizing the instrumental parameters for high mass resolution. This paper only reports specific molecular ions as "detected" if the ion is the best match reported by the software (i.e. if the particular molecular ion has the lowest deviation from the mass and has a 100% explained variance). The detection of both the intact ion and molecular fragments derived from the parent molecule add confidence to the identification of specific organic compounds. All nominal masses have both an inorganic and an organic component; all of the elemental isotopes with masses greater than that of ^{16}O (m = 15.9949) have masses that are slightly below the nominal mass, while organic fragments, composed mostly of ^{12}C (12.0000) and ^{1}H (m = 1.0078), have masses that are slightly above the nominal mass. For this reason, all nominal masses in the TOF-SIMS spectra are composed of two peaks, which are distinguishable given a reasonable mass resolution (Figure 4.3).

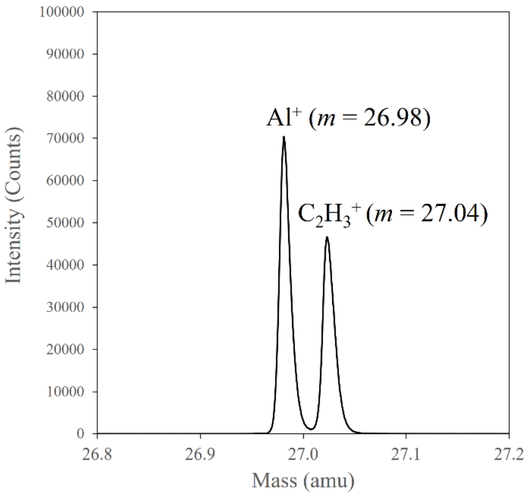

Figure 4.3. Example of two peaks detected at the approximate mass 27 in a mass spectrum obtained from the Bi_1^+-TOF-SIMS analysis of the Murchison meteorite (MET11544), representing the inorganic (Al$^+$) and organic ($C_2H_3^+$) component of this particular nominal mass.

Poly-dimethyl-siloxane (PDMS), trimethylsilane, and di-iso-octyl phthalate (DOP) are common laboratory contaminants and can be identified on sample surfaces by characteristic patterns of prominent peaks in the positive ion spectra: PDMS: m/z = 28$^+$, 43$^+$, 73$^+$, 133$^+$, 147$^+$, 207$^+$, 221$^+$, 281$^+$; trimethylsilane: m/z = 28$^+$, 43$^+$, 58$^+$, 59$^+$, 73$^+$; DOP: 149$^+$, 261$^+$, 279$^+$, 391$^+$ (Oran et al., 2004; Reich, 2013). Although prominent peaks were observed at m/z = 28$^+$ and 133$^+$ for most standards and samples, these two peaks (identified by the software as Si$^+$ and Cs$^+$) are unlikely derived from PDMS, as the other characteristic PDMS peaks were absent. The prominent m/z = 133$^+$ peak observed in most sample areas (identified as Cs$^+$) is not indigenous to the samples, however. Cs$^+$ from the pulsed ion beam was deposited onto the sample surfaces as the extractor gradually warmed up during long-duration analyses. A similar effect has been reported previously for other TOF-SIMS studies (Briggs and Fletcher, 2013; Naraoka et al., 2015) and is not expected to have introduced any other contaminants (organic or inorganic) onto the sample surfaces.

Although the Cs^+ abundance in the sample areas increased over time (as the ion beam gradually warmed up throughout a set of sample analyses), other molecular ions measured in the analyses remained constant.

4.3. RESULTS AND DISCUSSION

4.3.1. Standard analyses and expected fragmentation patterns

For each of the amino acid standards, a quasi-molecular ion $[M+H]^+$ (where M is the molecular weight) was generated in the positive ion spectra as expected (Briggs and Fletcher, 2013), as well as characteristic mass fragments (Table 4.2; Figure 4.4). All amino acid standards, with the exception of glycine, yielded relatively large NH_4 peaks indicating cleavage at the C-N bonds, as was observed by Henkel and Lyon (2016). C-N bonds have generally weaker bond strengths than C-C bonds and would be expected to be primary sites of cleavage during ion bombardment. However, in contrast to the results from Henkel and Lyon (2016), the amino acid mass fragmentation patterns observed in the present study indicate that all nine amino acid standards were also cleaved at C-C bonds (Table 4.2, Figure 4.4). In most cases, the molecular ions generated from C-C bond breakage (e.g. CH_4N^+, $C_2H_6N^+$, $C_3H_8N^+$) generated the highest signal amongst the secondary ions (Figure 4.4). This fragmentation pattern, whereby the most abundant fragment is the immonium ion (H_2N^+–CH–R), is expected for the individual amino acids (Michel and Castner, 2006) and is also consistent with fragmentation patterns observed from Cs^+-TOF-SIMS analysis of poly-amino acids (Samuel et al., 2001) and Bi_3^+-TOF-SIMS analysis of protein samples (Tyler et al., 2011). The amino acid standards in the present study, analyzed as dried solutions on silicon wafers, likely crystallize during the evaporation process, potentially yielding poly-amino acid crystalline structures. As such, we take into consideration that the fragmentation patterns generated from indigenous meteoritic amino acids may result in different relative yields of the individual fragments, compared to our standards.

The relatively large peak detected at *m/z* = 149^+ on the silicon wafer blanks (identified by the software as $C_8H_5O_3^+$, corresponding to phthalic anhydride) is most likely derived from the common airborne laboratory contaminant di-iso-octyl phthalate (DOP), as both silicon wafer blanks also contained the characteristic masses for DOP at 149^+, 261^+, 279^+, and 391^+ (Reich, 2013). DOP is a plasticizer, potentially derived from sample preparation of the amino acid standards (e.g. from the pipette bulbs or silicon wafers). The absence of characteristic DOP peaks in the Murchison and Tagish Lake sample areas (Sections 4.3.2 and 4.3.3) indicates that the source of DOP for the silicon blanks did not similarly affect the meteorite sample surfaces.

The two bismuth primary ion beams (Bi_1^+ and Bi_3^+) yielded similar molecular fragments for the amino acid standards, though they produced different relative ion yields (Table 4.2, Figure 4.4). For instance, it appears that Bi_1^+ resulted in less fragmentation for the lower molecular weight amino acids; for glycine, alanine and β-alanine, the Bi_1^+ analyses resulted in relatively higher yields of the intact ($[M+H]^+$) masses, while the Bi_3^+ analyses resulted in relatively higher yields of the characteristic fragments (CH_4N^+ and $C_2H_6N^+$) (Figure 4.4). For α-AIB, α-ABA, and β-ABA, the relative yields for the intact masses vs. characteristic fragments were similar between Bi_1^+-TOF-SIMS and Bi_3^+-TOF-SIMS. The analysis of γ-ABA by Bi_3^+ resulted in relatively higher yields of the molecular fragments (CH_4N^+, $C_4H_5O^+$, and $C_4H_8NO^+$) compared to the Bi_1^+ results. Aspartic acid and glutamic acid were highly fragmented from both the Bi_1^+ and Bi_3^+ analyses. In general, the NH_4^+ peak had a relatively higher intensity for the Bi_3^+ analyses in comparison to the Bi_1^+. These collective data indicate that, for our purposes, as we are focusing on identifying the lower molecular weight amino acids (glycine, α-alanine, β-alanine and γ-ABA), Bi_1^+ may be more beneficial in that it results in relatively higher yields for those specific intact molecules. However, the Bi_3^+ analyses resulted in higher total ion yields, indicating that there are observable benefits to both methods. Consistent with these results, cluster ions such as Bi_3^+ and C_{60}^+ have been shown to result in higher secondary ion yields compared to monoatomic primary ions, especially for higher mass compounds (Kollmer, 2004; Dubey et al., 2011).

Table 4.2. Amino acid standards and their chemical formulae, molecular weights (g/mol) and characteristic molecular ions generated during Bi_1^+/Bi_3^+-TOF-SIMS analysis of dried standard solutions on clean silicon wafers.

Standard compound	**Molecular weight (g/mol)**	**Molecular ion**	**Nominal Mass**
Glycine ($C_2H_5NO_2$)	75.06	CH_4N^+	30
		$C_2H_6NO_2^+$	76
Alanine ($C_3H_7NO_2$)	89.09	NH_4^+	18
		$C_2H_6N^+$	44
		$C_3H_8NO_2^+$	90
β-Alanine ($C_3H_7NO_2$)	89.09	NH_4^+	18
		CH_4N^+	30
		$C_3H_8NO_2^+$	90
α-AIB ($C_4H_9NO_2$)	103.12	NH_4^+	18
		$C_3H_5^+$	41
		$C_3H_8N^+$	58
		$C_4H_{10}NO_2^+$	104
α-Amino-n-butyric acid ($C_4H_9NO_2$)	103.12	NH_4^+	18
		$C_2H_3^+$	27
		$C_3H_5^+$	41
		$C_3H_8N^+$	58
		$C_4H_{10}NO_2^+$	104
β-Amino-n-butyric acid ($C_4H_9NO_2$)	103.12	NH_4^+	18
		$C_2H_6N^+$	44
		$C_3H_8N^+$	58
		$C_4H_{10}NO_2^+$	104
γ-Amino-n-butyric acid ($C_4H_9NO_2$)	103.12	NH_4^+	18
		CH_4N^+	30
		$C_3H_5^+$	41
		$C_4H_5O^+$	69
		$C_4H_8NO^+$	86
		$C_4H_{10}NO_2^+$	104
Aspartic acid ($C_4H_7NO_4$)	133.11	NH_4^+	18
		$C_2H_3^+$	27
		$C_3H_5^+$	41
		$C_2H_6N^+$	44
		$C_3H_4NO^+$	70
		$C_2H_4NO_2^+$	74
		$C_3H_6NO_2^+$	88
		$C_4H_{10}NO_2^+$	104
		$C_4H_8NO_4^+$	134
Glutamic acid ($C_5H_9NO_4$)	147.13	NH_4^+	18
		$C_3H_6N^+$	56
		$C_4H_6NO^+$	84
		$C_4H_8NO_2^+$	102
		$C_5H_{10}NO_4^+$	148

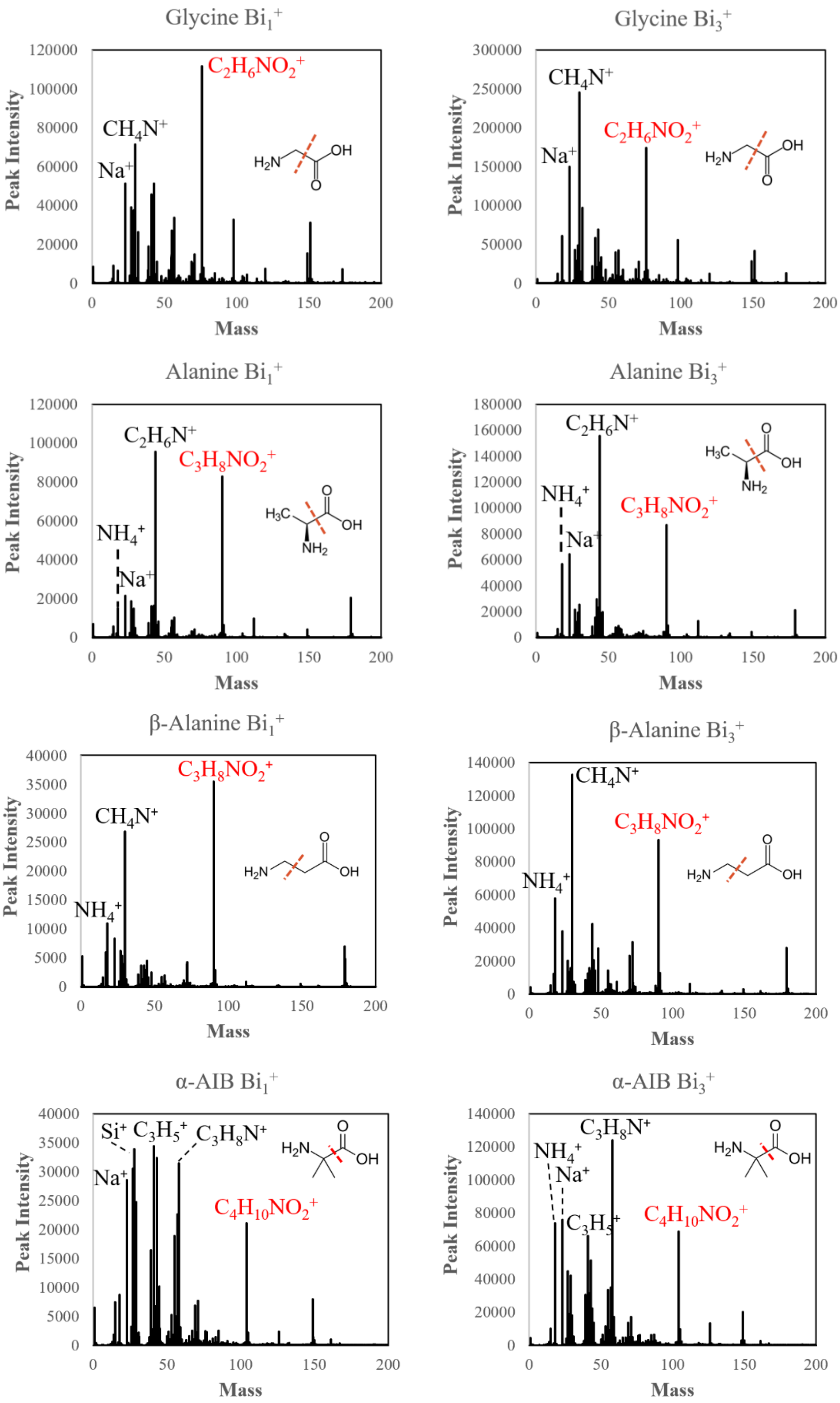

Glycine Bi$_1^+$
Peak Intensity
Mass
CH$_4$N$^+$
Na$^+$
C$_2$H$_6$NO$_2^+$
H$_2$N
OH
O
0
20000
40000
60000
80000
100000
120000
0
50
100
150
200
Glycine Bi$_3^+$
CH$_4$N$^+$
Na$^+$
C$_2$H$_6$NO$_2^+$
0
50000
100000
150000
200000
250000
300000
Alanine Bi$_1^+$
C$_2$H$_6$N$^+$
C$_3$H$_8$NO$_2^+$
NH$_4^+$
Na$^+$
H$_3$C
NH$_2$
Alanine Bi$_3^+$
140000
160000
180000
β-Alanine Bi$_1^+$
C$_3$H$_8$NO$_2^+$
CH$_4$N$^+$
NH$_4^+$
5000
10000
15000
20000
25000
30000
35000
40000
β-Alanine Bi$_3^+$
CH$_4$N$^+$
C$_3$H$_8$NO$_2^+$
NH$_4^+$
α-AIB Bi$_1^+$
Si$^+$
C$_3$H$_5^+$
C$_3$H$_8$N$^+$
Na$^+$
C$_4$H$_{10}$NO$_2^+$
α-AIB Bi$_3^+$
C$_3$H$_8$N$^+$
NH$_4^+$
Na$^+$
C$_3$H$_5^+$
C$_4$H$_{10}$NO$_2^+$

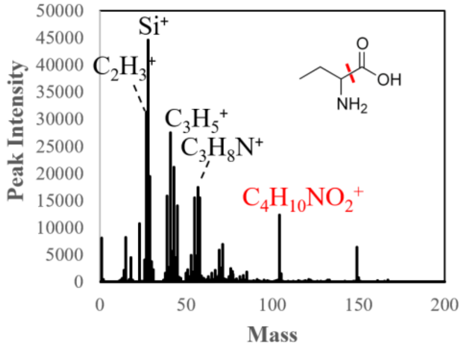
α-ABA Bi_1^+

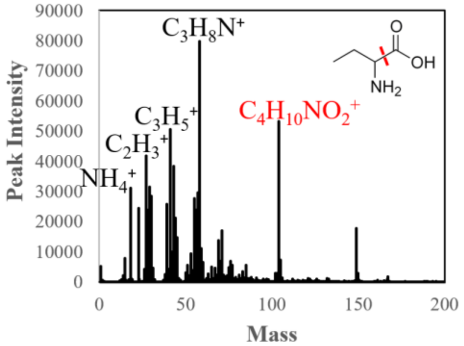
α-ABA Bi_3^+

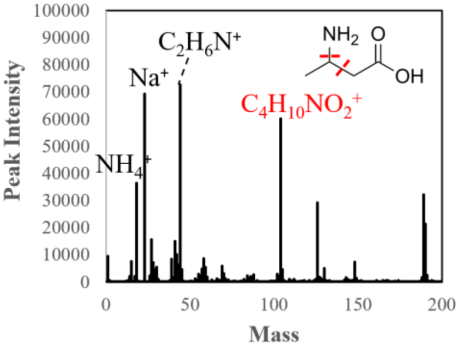
β-ABA Bi_1^+

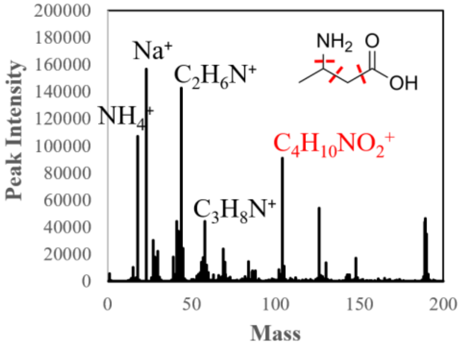
β-ABA Bi_3^+

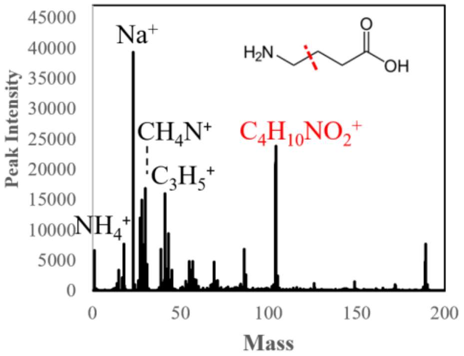
γ-ABA Bi_1^+

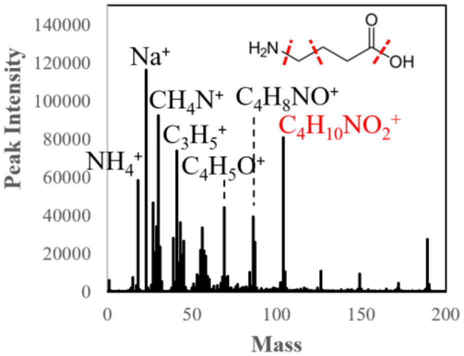
γ-ABA Bi_3^+

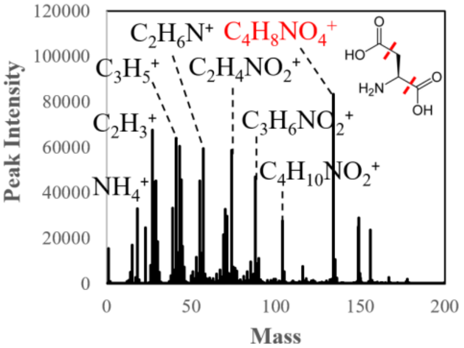
Aspartic Acid Bi_1^+

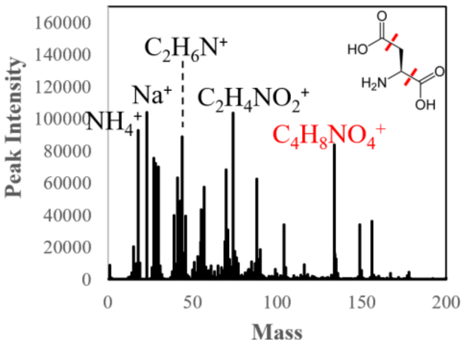
Aspartic Acid Bi_3^+

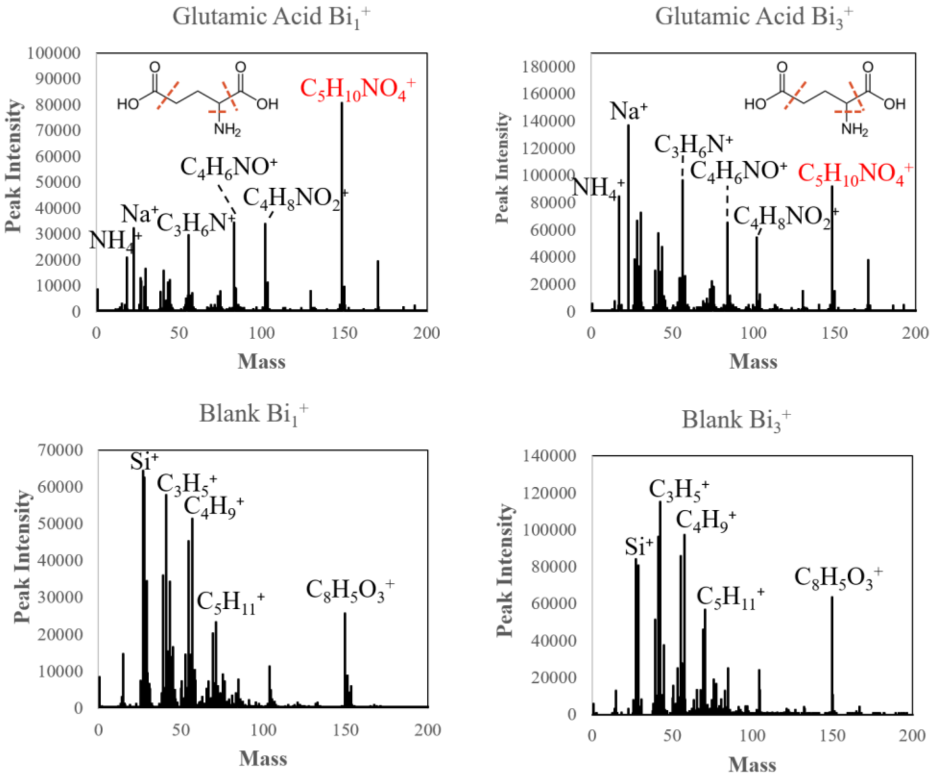

Figure 4.4. Positive secondary ions detected from amino acid standards and silicon wafer blanks using Bi_1^+- and Bi_3^+-TOF-SIMS. Molecular ions labeled in red are the corresponding intact amino acids ($[M+H]^+$, where M is the molecular weight). Abbreviations: α-AIB – α-aminoisobutyric acid; α-ABA – α-amino-n-butyric acid; β-ABA – β-amino-n-butyric acid; γ-ABA – γ-amino-n-butyric acid.

4.3.2. TOF-SIMS analysis of the Murchison meteorite

Intact amino acids were not detected in any of the five sample areas of the Murchison (USNM 5360) fresh fractures surface (Table 4.3). Some characteristic amino acids fragments (CH_4N^+, $C_2H_6N^+$, $C_3H_8N^+$) were detected in all sample areas (Table 4.3); however, the signals were low and it is unclear whether these ions were present above background levels. Similarly, Henkel and Lyon (2016) did not detect any intact amino acids or amino acid fragments above background levels in Murchison via TOF-SIMS. Solvent extraction analyses of the Murchison meteorite have found Murchison to contain relatively high abundances of indigenous amino acids, so the apparent absence of amino acids in the TOF-SIMS data is surprising (Botta and Bada, 2002; Sephton, 2014). The non-detection of intact amino acids in Murchison via TOF-SIMS could have resulted from mass interferences, as the complexity of the organic content of the Murchison meteorite may have resulted in some overlap between peaks in the spectra, which would have masked the signal of the individual amino acids. Alternatively, the lack of an in-situ detection of intact amino acids may indicate that the amino acids that are commonly detected in solvent extracts of the Murchison meteorite are present in the meteorite in a different chemical form and are only converted to amino acids during the solvent extraction procedure. The latter explanation seems less likely, as free amino acids are commonly identified in high abundances in the Murchison meteorite water extracts.

Table 4.3. Amino acid-associated molecular ions and their detection (Y) or non-detection (N) for a Bi_3^+-TOF-SIMS analysis of five 500 x 500 μm^2 sample areas on a fresh fracture surface of the Murchison meteorite (USNM 5360). Sample area locations are shown in Figure 4.1.

Molecular ion	Amino acid(s)	Area 1	Area 2	Area 3	Area 4	Area 5
NH_4^+	Ala, β-Ala, α-AIB, α-ABA, β-ABA, γ-ABA, Asp, Glu	Y	Y	Y	Y	Y
$C_2H_3^+$	α-ABA, Asp	Y	Y	Y	Y	Y
CH_4N^+	Gly, β-Ala, γ-ABA	Y	Y	N	N	Y
$C_3H_5^+$	α-AIB, γ-ABA, Asp	Y	Y	Y	Y	Y
$C_2H_6N^+$	Ala, β-ABA, Asp	Y	Y	N	N	N
$C_3H_6N^+$	Glu	N	N	N	N	N
$C_3H_8N^+$	α-AIB, α-ABA, β-ABA	Y	Y	Y	Y	N
$C_4H_5O^+$	γ-ABA	N	N	N	N	N
$C_3H_4NO^+$	Asp	N	N	N	N	N
$C_2H_4NO_2^+$	Asp	N	N	N	N	N
$^{a}C_2H_6NO_2^+$	Gly	N	N	N	N	N
$C_4H_6NO^+$	Glu	N	N	N	N	N
$C_4H_8NO^+$	γ-ABA	N	N	N	N	N
$C_3H_6NO_2^+$	Asp	N	N	N	N	N
$^{a}C_3H_8NO_2^+$	Ala, β-Ala	N	N	N	N	N
$C_4H_8NO_2^+$	Glu	N	N	N	N	N
$^{a}C_4H_{10}NO_2^+$	α-AIB, α-ABA, β-ABA, γ-ABA, Asp	N	N	N	N	N
$^{a}C_4H_8NO_4^+$	Asp	N	N	N	N	N
$^{a}C_5H_{10}NO_4^+$	Glu	N	N	N	N	N

^{a}Intact amino acids – $[M+H]^+$ (where M is the molecular weight)

Murchison – USNM 5360 – Area 1

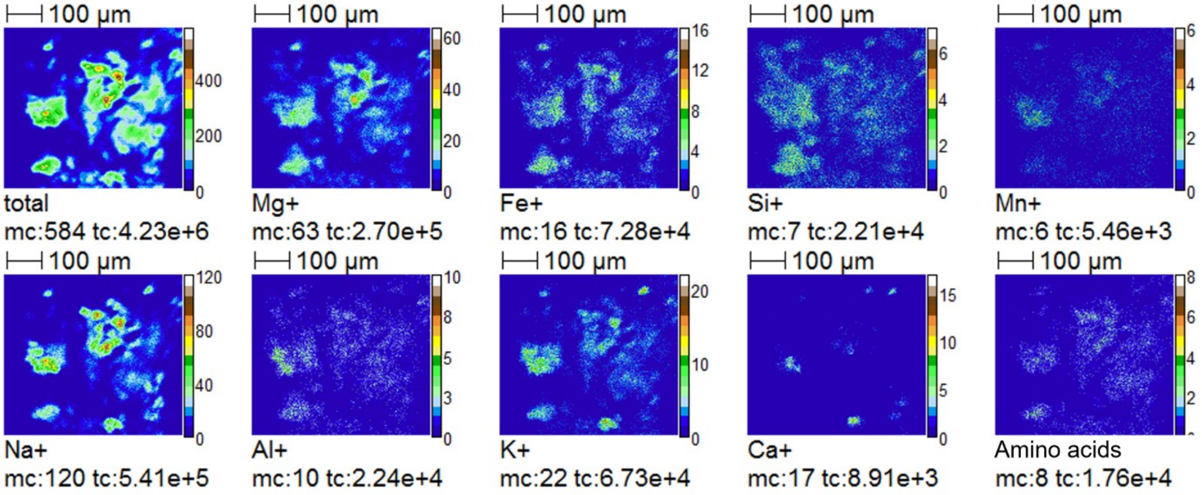

Murchison – USNM 5360 – Area 2

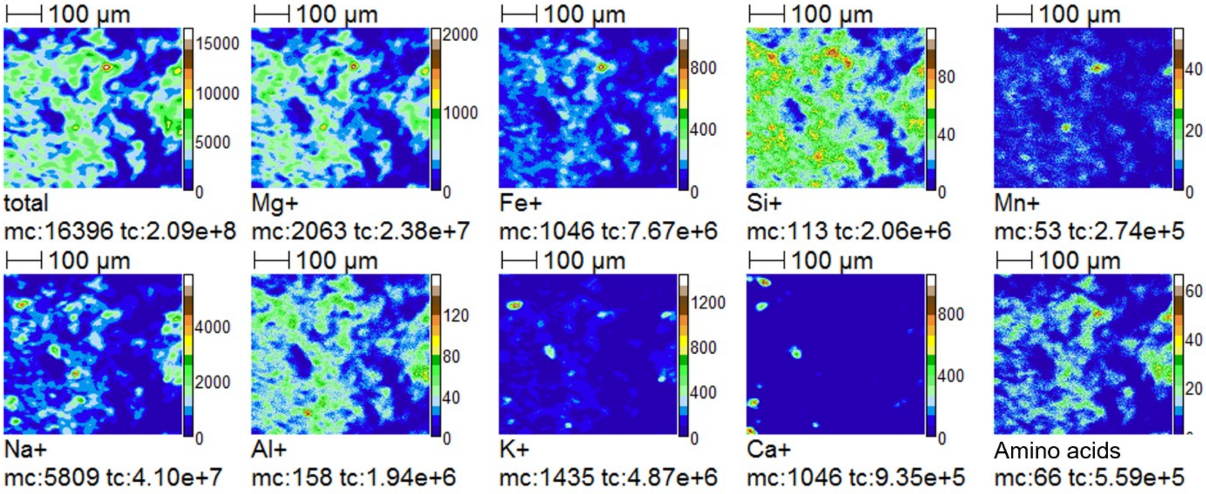

Murchison – USNM 5360 – Area 3

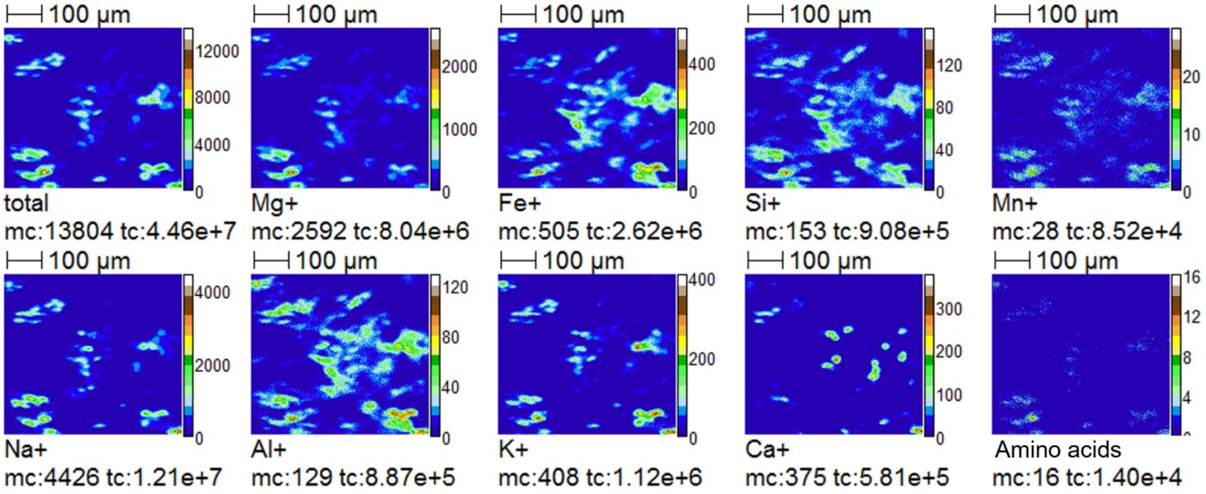

Murchison – USNM 5360 – Area 4

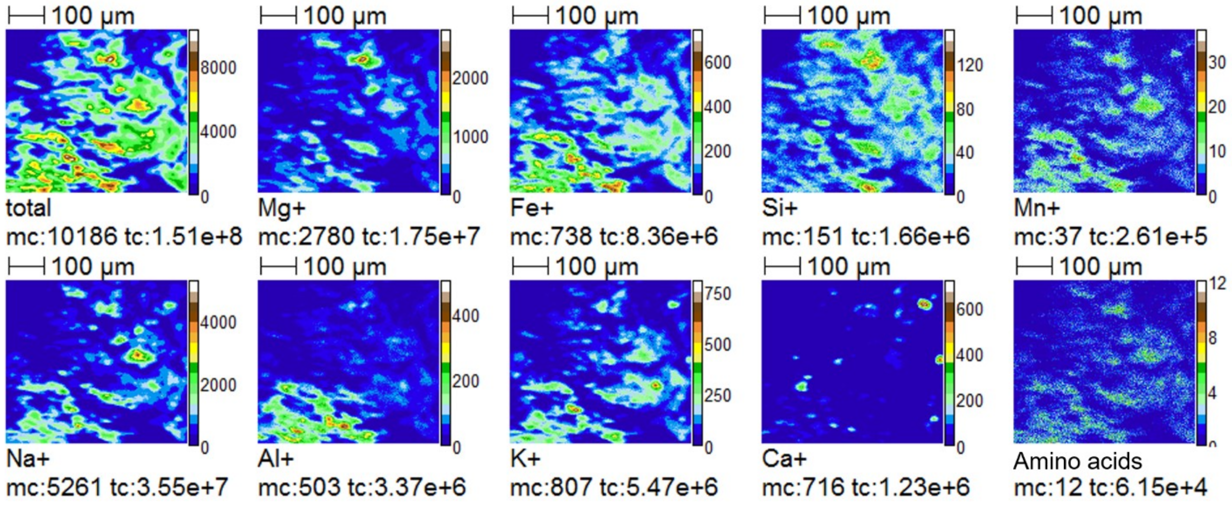

Murchison – USNM 5360 – Area 5

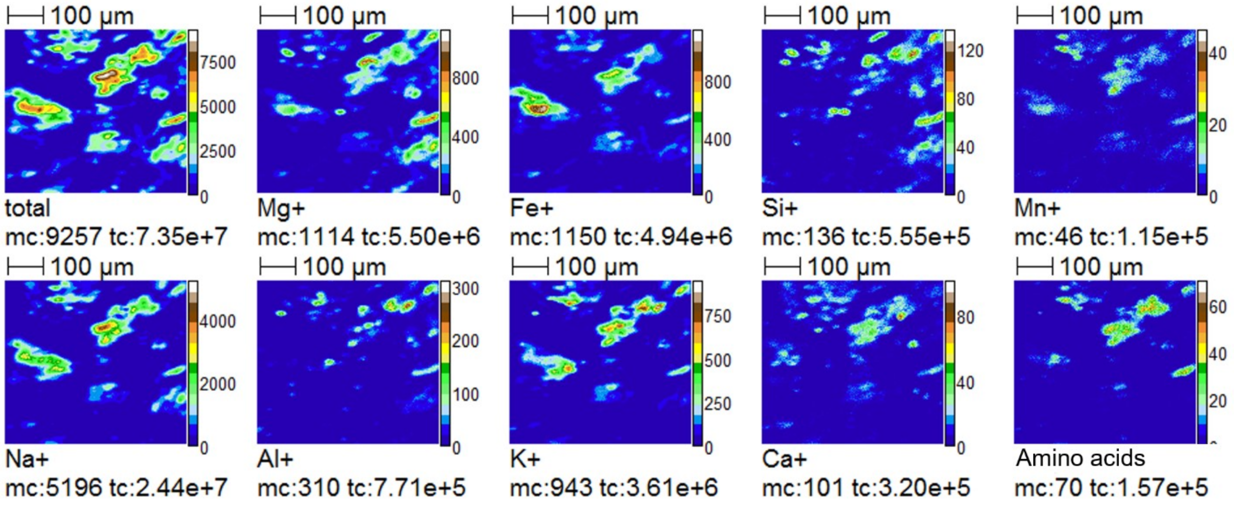

Figure 4.5. Secondary ion distribution images for positive ions for five 500 x 500 µm^2 sample areas on a fresh fracture surface of the Murchison meteorite (USNM 5360). The “amino acid” images do not include NH_4^+, $C_2H_3^+$ or $C_3H_5^+$, as these fragments may also be derived from other organic compound classes and both $C_2H_3^+$ and $C_3H_5^+$ are commonly observed in the blanks.

Table 4.4 compares the results from the Bi_1^+- and Bi_3^+-TOF-SIMS analysis of the Murchison MET11544 sample. Overall, the two ion beams generated comparable results in terms of yields of amino acid-associated molecular ions; analyzing the Murchison sample with the two types of bismuth beams did not result in the detection of intact amino acids in either sample area, though characteristic molecular fragments of the amino acid aspartic acid were detected in Area 1 with both beams. The corresponding secondary ion distribution images generated for the two areas show that the Bi_3^+-TOF-SIMS analysis resulted in a higher overall ion yield, which allowed for better spatial resolution, as has been previously shown (e.g. Dubey et al., 2011) (Figure 4.6).

Table 4.4. Amino acid-associated molecular ions and their detection (Y) or non-detection (N) within two 500 x 500 μm^2 sample areas on a fresh fracture surface of the Murchison meteorite (MET11544), using Bi_1^+ and Bi_3^+ primary ion beams.

		Area 1		Area 2		Blank	
Molecular ion	Amino acid(s)	Bi_1^+	Bi_3^+	Bi_1^+	Bi_3^+	Bi_1^+	Bi_3^+
NH_4^+	Ala, β-Ala, α-AIB, α-ABA, β-ABA, γ-ABA, Asp, Glu	Y	Y	Y	Y	Y	Y
$C_2H_3^+$	α-ABA, Asp	Y	Y	Y	Y	Y	Y
CH_4N^+	Gly, β-Ala, γ-ABA	N	N	N	N	N	N
$C_3H_5^+$	α-AIB, γ-ABA, Asp	Y	Y	Y	Y	Y	Y
$C_2H_6N^+$	Ala, β-ABA, Asp	N	N	N	N	N	N
$C_3H_6N^+$	Glu	N	N	N	N	N	N
$C_3H_8N^+$	α-AIB, α-ABA, β-ABA	N	N	N	N	N	N
$C_4H_5O^+$	γ-ABA	N	N	N	N	N	N
$C_3H_4NO^+$	Asp	N	N	N	N	N	N
$C_2H_4NO_2^+$	Asp	Y	Y	N	N	N	N
${}^aC_2H_6NO_2^+$	Gly	N	N	N	N	N	N
$C_4H_6NO^+$	Glu	N	N	N	N	N	N
$C_4H_8NO^+$	γ-ABA	N	N	N	N	N	N
$C_3H_6NO_2^+$	Asp	Y	Y	N	N	N	N
${}^aC_3H_8NO_2^+$	Ala, β-Ala	N	N	N	N	N	N
$C_4H_8NO_2^+$	Glu	N	N	N	N	N	N
${}^aC_4H_{10}NO_2^+$	α-AIB, α-ABA, β-ABA, γ-ABA, Asp	N	N	N	N	N	N
${}^aC_4H_8NO_4^+$	Asp	N	N	N	N	N	N
${}^aC_5H_{10}NO_4^+$	Glu	N	N	N	N	N	N

[a]Intact amino acids – $[M+H]^+$ (where M is the molecular weight)

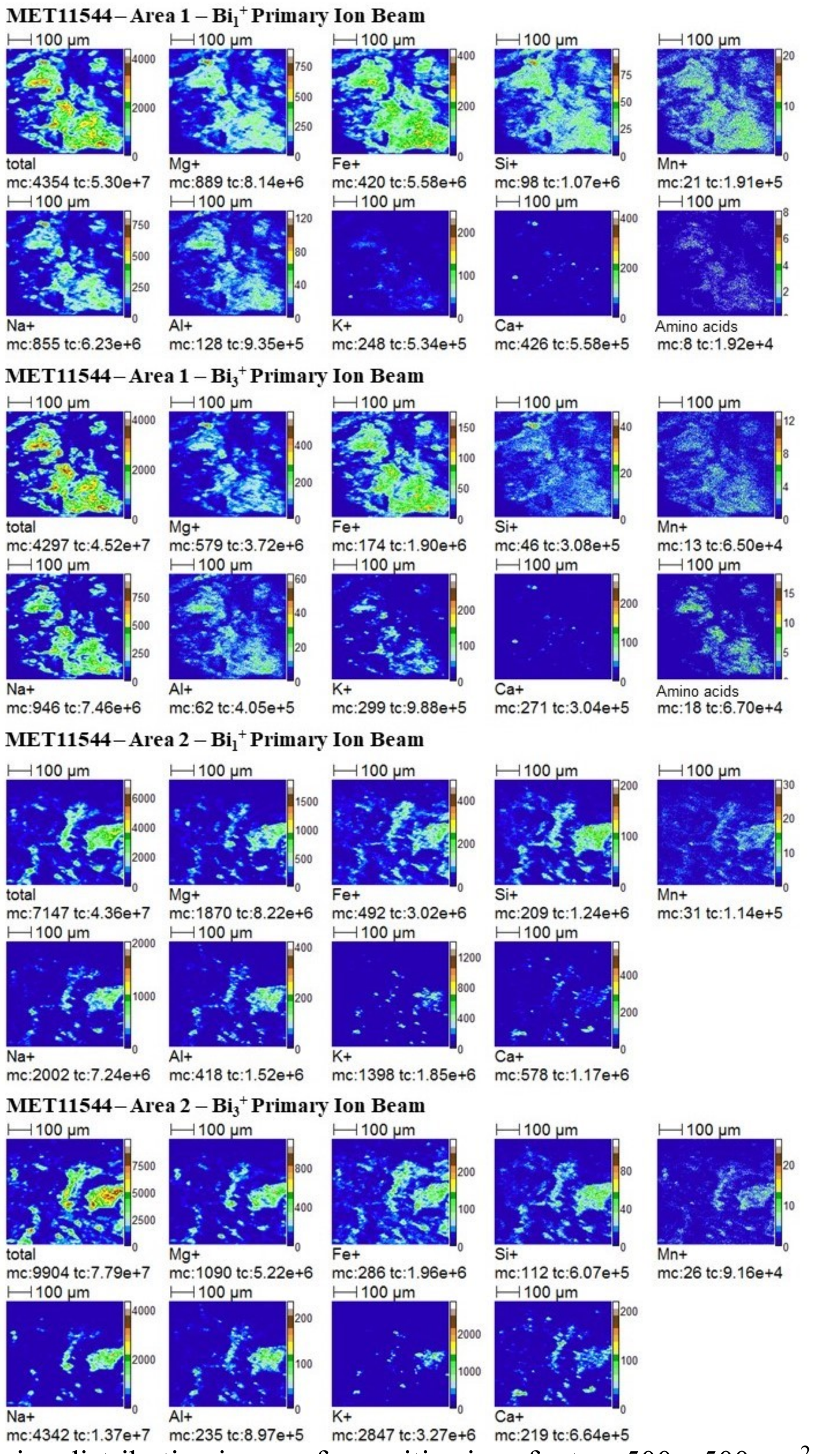

Figure 4.6. Secondary ion distribution images for positive ions for two 500 x 500 µm^2 sample areas on a fresh fracture surface of the Murchison meteorite (MET11544) analyzed by both Bi_1^+ and Bi_3^+-TOF-SIMS. The "amino acid" images only illustrate the distribution of amino acid-associated molecular ions that were detected in the corresponding sample areas and that were not present in the procedural blanks. For the sample area 2, no amino acid images are shown, as the amino acid-associated fragments detected (NH_4^+, $C_2H_3^+$, and $C_3H_5^+$) may be derived from other organics and both $C_2H_3^+$and $C_3H_5^+$ are also present in the blanks.

Low-molecular weight aldehydes (formaldehyde, CH_2O; acetaldehyde, C_2H_4O; benzaldehyde, C_7H_6O), carboxylic acids (formic acid, CH_2O_2; acetic acid, $C_2H_4O_2$), and amines (methylamine, CH_5N; ethylamine, C_2H_7N; propylamine, C_3H_9N), known to be present in the Murchison meteorite (Huang et al., 2005; Pizzarello and Holmes, 2009; Aponte et al., 2014) were not detected at the nominal masses (M) or at the masses of the expected quasi-molecular ions $[M+H]^+$ in either of the Murchison samples. Henkel and Lyon (2016) detected methylamine, ethylamine and propylamine above background levels in Murchison using C_{60}^+-TOF-SIMS, potentially indicating a relatively higher sensitivity for these types of compounds associated with using a C_{60}^+ primary ion beam.

4.3.3. TOF-SIMS analysis of the Tagish Lake meteorite

For the Tagish Lake fresh fracture surface, small peaks corresponding to intact glycine ($C_2H_6NO_2^+$) and alanine/β-alanine ($C_3H_8NO_2^+$) were observed in five of the seven sample areas. $C_4H_{10}NO_2^+$, corresponding to intact α-AIB/α-ABA/β-ABA/γ-ABA, was detected in only one of the seven sample areas. Intact amino acids were not observed on any of the Si wafer blanks. There were relatively small peaks in the procedural blank samples with *m/z* values similar to the amino acid nominal masses (*m/z* = 76^+, 90^+ 104^+ 134^+, 148^+) but the software identified these peaks as $C_6H_4^+$, $SiCH_8N_3^+$, $SiCH_6N_3O^+$, $C_6H_4N_3O^+$, and $C_8H_4O_3^+$, respectively. Amino acid-associated molecular fragments (CH_4N^+, $C_2H_6N^+$ and $C_3H_8N^+$) were also detected in nearly all seven Tagish Lake sample areas. Solvent extraction analyses indicate that the amino acid content of TL1 is dominated by glycine, γ-ABA and β-alanine (Table 4.5; Chapter 3). However, the bulk of the γ-ABA detected in the solvent extract of TL1 was derived from the acid-hydrolyzed fraction, indicating that γ-ABA is likely minerally-bound within the meteorite or present in the meteorite in a different chemical form (Chapter 3). The TOF-SIMS detection of intact glycine and β-alanine and their molecular fragments in nearly all Tagish Lake sample areas and the absence of intact γ-ABA from nearly all sample areas is consistent with these observations.

A relatively large peak was observed at *m/z* = 91^+ in all seven Tagish Lake sample areas (Figure 4.8) which the TOF-SIMS software identifies as $C_3H_9NO_2^+$, the molecular formula for the amino alcohol aminopropanediol. To the best of our knowledge, neither aminopropanediol ($C_3H_9NO_2$) nor $C_3H_8NO_2$ ($[M + H^+] - H^+$) have been detected in meteorite samples to date. There are a few possible explanations for the presence of a relatively large *m/z* = 91^+ peak in Tagish

Lake: (1) the *m/z* = 91^+ peak in the Tagish Lake sample areas corresponds to $C_7H_7^+$ (benzyl radical; *m* = 91.05), a molecule which would be expected to be present in relatively high abundances in the meteorite, as benzene rings are a component of many aromatic and polyaromatic organic species; or (2) the *m/z* = 91^+ peak in the Tagish Lake sample areas is in fact $C_3H_9NO_2^+$ (*m* = 91.06) and its absence from solvent extraction analyses can be attributed to method limitations; or (3) the *m/z* = 91^+ peak is a molecular fragment from a larger organic molecule. A peak at this approximate mass was also observed in the corresponding silicon wafer blanks and in the Murchison sample areas; however, these *m/z* = 91^+ peaks are consistently identified as $C_7H_7^+$. The *m/z* = 91^+ peaks in the Murchison sample areas are most likely part of a series of aromatic peaks (characteristic aromatic peaks: *m/*z = 77^+, 91^+, 105^+, 128^+, 141^+, and 165^+; Poleunis et al., 2000). It is unclear whether the *m/z* = 91^+ peak in the Tagish Lake samples is part of an aromatic series, as the other characteristic masses for aromatic species (77^+, 105^+, 128^+, 141^+, and 165^+) did not exhibit similarly large peaks. Nevertheless, assigning the *m/z* = 91^+ peak to $C_7H_7^+$ in the Tagish Lake sample areas for the mass calibration did not affect the identification of amino acid-associated molecular ions in any of the sample areas. Whether this *m/z* = 91^+ peak is $C_3H_9NO_2^+$ or $C_7H_7^+$, it appears to be an organic compound that is indigenous to the meteorite and it is the most abundant organic peak in the Tagish Lake sample areas, aside from the simple aliphatic hydrocarbons ($C_2H_3^+$, $C_3H_5^+$, $C_3H_7^+$, $C_3H_9^+$, etc.).

Based on the secondary ion distribution images generated for positive secondary ions measured from the seven Tagish Lake sample areas, the amino acids do not appear to be associated with specific mineral grains or textures in the meteorite. Rather, they appear to be homogeneously distributed throughout the matrix, as the intact amino acids and their molecular fragments generally follow the same distribution as the total ion yield, which reflects the topography of the sample surface. Although these observations contrast with the results from Yesiltas and Kebukawa (2016), who observed a spatial correlation between organic compounds and phyllosilicates in the Tagish Lake meteorite, the bulk of the organic content of the Tagish Lake meteorite (which they were likely detecting) is in the form of insoluble organic matter (IOM). Our results suggest that amino acids in the Tagish Lake meteorite follow a distribution that is independent of the bulk IOM, at least for Tagish Lake specimen TL1.

4.3.4. Non-detection of intact amino acids in Murchison and method limitations

The non-detection of intact amino acids in the Murchison meteorite is surprising, considering the high abundances of amino acids detected via solvent extraction analyses; however, it seems most likely that mass interferences between amino acids and other organic species precluded the detection of the intact compounds. Consistent with this theory, the full TOF-SIMS positive ion spectra for the Murchison and Tagish Lake samples (1-150 *m/z*; Figure 4.8) illustrate some observable differences in their compositions as evidenced by relatively higher abundances of hydrocarbons ($C_xH_y^+$) in the Murchison sample areas compared to the Tagish Lake spectrum. These observations are consistent with the generally higher abundances of soluble organic compounds present in the Murchison meteorite (Pizzarello et al., 2006). The complexity of the Murchison organic content, combined with method limitations resulting from mass interferences and topographic effects, may have hindered the detection of intact amino acids.

One of the main limitations presented by TOF-SIMS analysis of astromaterials is the requirement for a relatively flat sample surface in order to achieve reliable and informative spectra and secondary ion distribution images. Uneven sample surfaces can result in variable ion yields and poor mass resolution. Optimizing parameters for high mass resolution is possible, but obtaining sufficient mass resolution while analyzing samples with uneven surface topography can result in a very weak ion signal (Gilmore, 2013). A flat surface topography can be achieved by cutting and polishing the meteorite sample, but this process risks introducing terrestrial contaminants onto the sample surface. Astromaterials are limited in number and highly valuable, and minimizing contamination is crucial, particularly when investigating indigenous extraterrestrial organic compounds. Long analysis times, averaging at approximately two hours per 500 x 500 μm^2 sample area, also limit one's ability to obtain a complete analysis of a sample surface. Each analysis generates thousands of peaks, so not only do specific sample areas need to be targeted for flat topographies, but a pre-determined list of target organic compounds is also highly beneficial.

Table 4.5. Amino acid-associated molecular ions and their detection (Y) or non-detection (N) within seven 500 x 500 μm^2 sample areas on a fresh fracture surface of the Tagish Lake meteorite. The procedural blank sample was a clean Si wafer (combusted at 450°C > 6 hours). Secondary ion distribution images for the seven areas are shown in Figure 4.7.

Molecular ion	Amino acid(s)	Area 1	Area 2	Area 3	Area 4	Area 5	Area 6	Area 7	Blank
NH_4^+	Ala, β-Ala, α-AIB, α-ABA, β-ABA, γ-ABA, Asp, Glu	Y	Y	Y	Y	Y	Y	Y	Y
$C_2H_3^+$	α-ABA, Asp	Y	Y	Y	Y	Y	Y	Y	Y
CH_4N^+	Gly, β-Ala, γ-ABA	Y	N	Y	Y	Y	Y	N	N
$C_3H_5^+$	α-AIB, γ-ABA, Asp	Y	Y	Y	Y	Y	Y	Y	Y
$C_2H_6N^+$	Ala, β-ABA, Asp	Y	Y	Y	Y	Y	Y	N	N
$C_3H_6N^+$	Glu	Y	N	N	N	Y	N	N	N
$C_3H_8N^+$	α-AIB, α-ABA, β-ABA	Y	Y	Y	Y	Y	Y	N	N
$C_4H_5O^+$	γ-ABA	N	N	N	N	N	N	N	N
$C_3H_4NO^+$	Asp	N	N	N	N	N	N	N	N
$C_2H_4NO_2^+$	Asp	Y	Y	Y	Y	N	N	Y	N
[a]$C_2H_6NO_2^+$	Gly	Y	Y	Y	Y	N	N	Y	N
$C_4H_6NO^+$	Glu	N	N	N	N	N	N	N	N
$C_4H_8NO^+$	γ-ABA	N	N	N	N	N	N	N	N
$C_3H_6NO_2^+$	Asp	Y	Y	Y	Y	N	N	Y	N
[a]$C_3H_8NO_2^+$	Ala, β-Ala	Y	Y	Y	Y	N	N	Y	N
$C_4H_8NO_2^+$	Glu	N	N	N	N	N	N	N	N
[a]$C_4H_{10}NO_2^+$	α-AIB, α-ABA, β-ABA, γ-ABA, Asp	Y	N	N	N	N	N	N	N
[a]$C_4H_8NO_4^+$	Asp	N	N	N	N	N	N	N	N
[a]$C_5H_{10}NO_4^+$	Glu	N	N	N	N	N	N	N	N

[a] Intact amino acids – $[M+H]^+$ (where M is the molecular weight)

Tagish Lake – Area 1

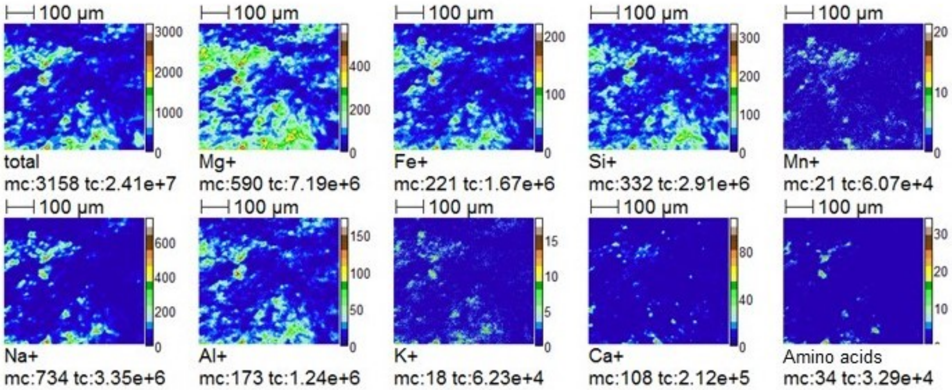

Tagish Lake – Area 2

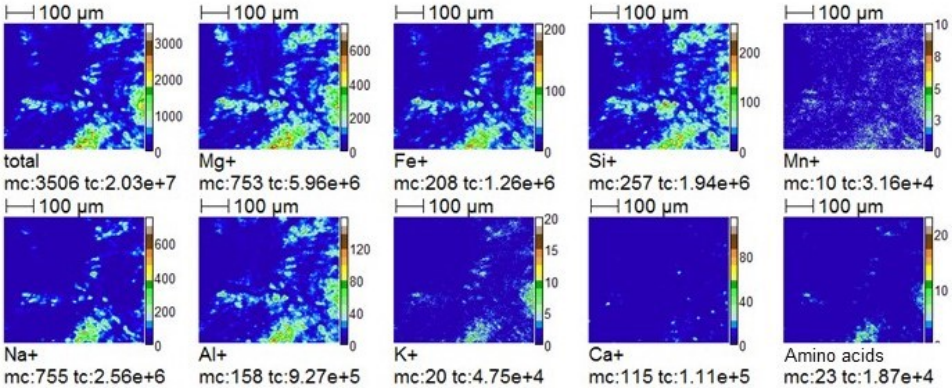

Tagish Lake – Area 3

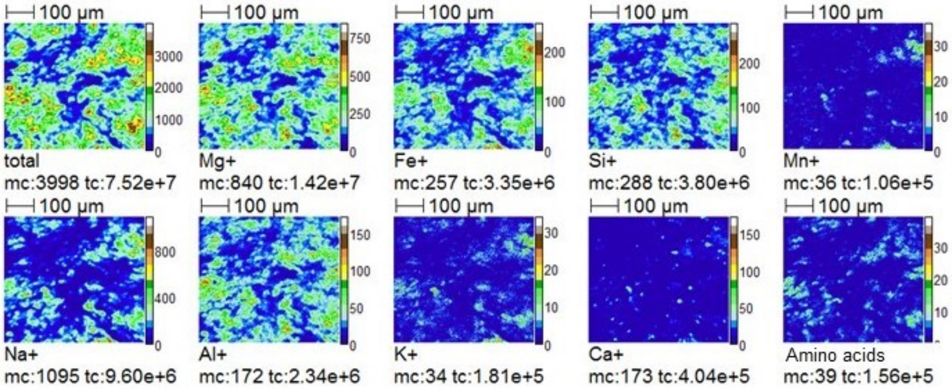

Tagish Lake – Area 4

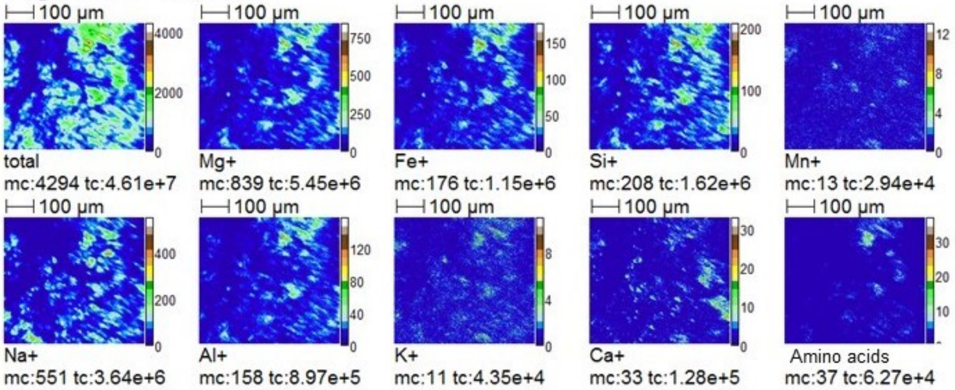

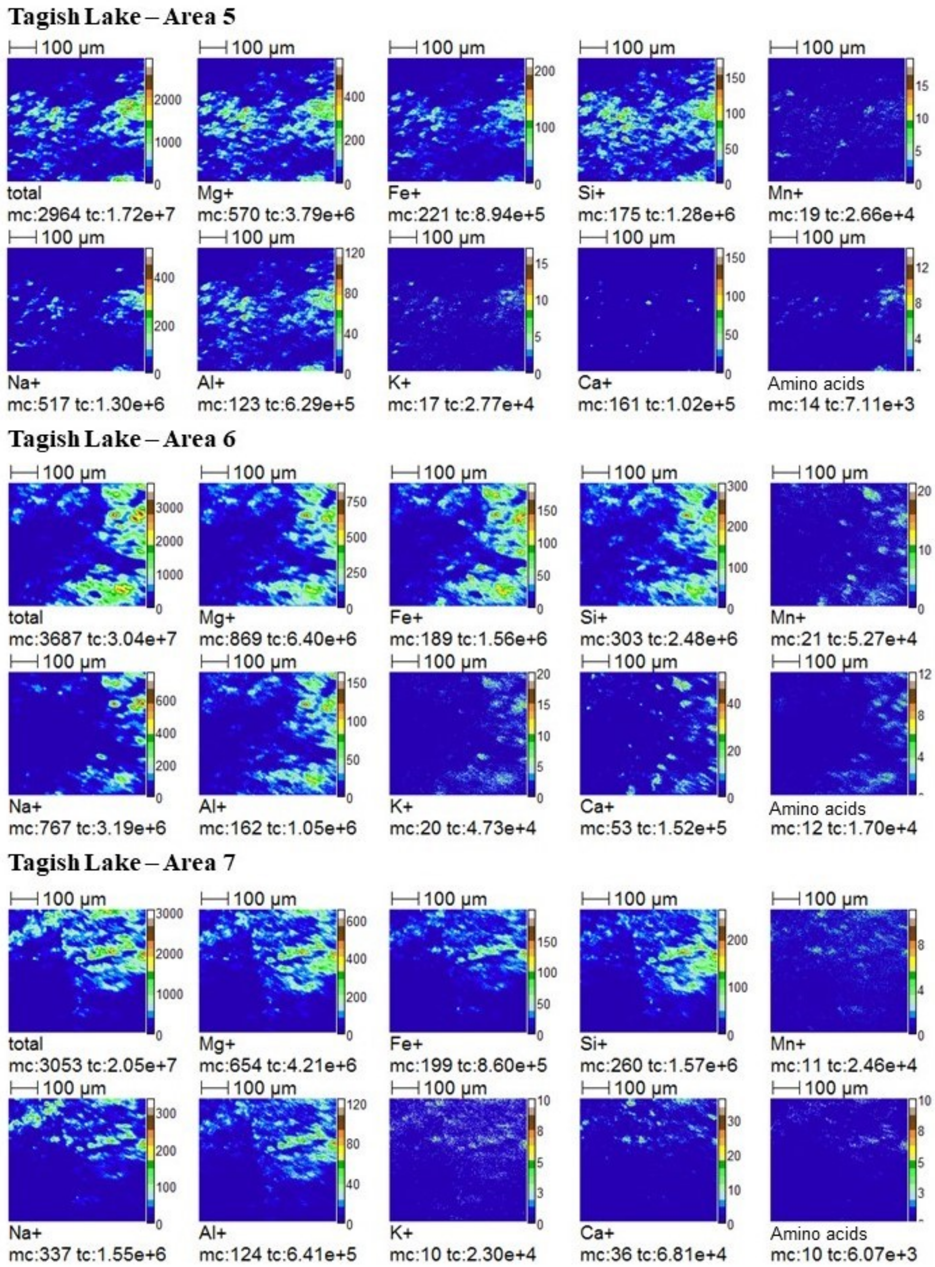

Figure 4.7. Secondary ion distribution images for positive ions for seven 500 x 500 μm^2 sample areas on a fresh fracture surface of the Tagish Lake meteorite, analyzed by Bi_1^+-TOF-SIMS. The "amino acid" images do not include NH_4^+, $C_2H_3^+$ or $C_3H_5^+$, as these fragments can be derived from other organic compound classes, and both $C_2H_3^+$ and $C_3H_5^+$ are commonly observed in the blanks.

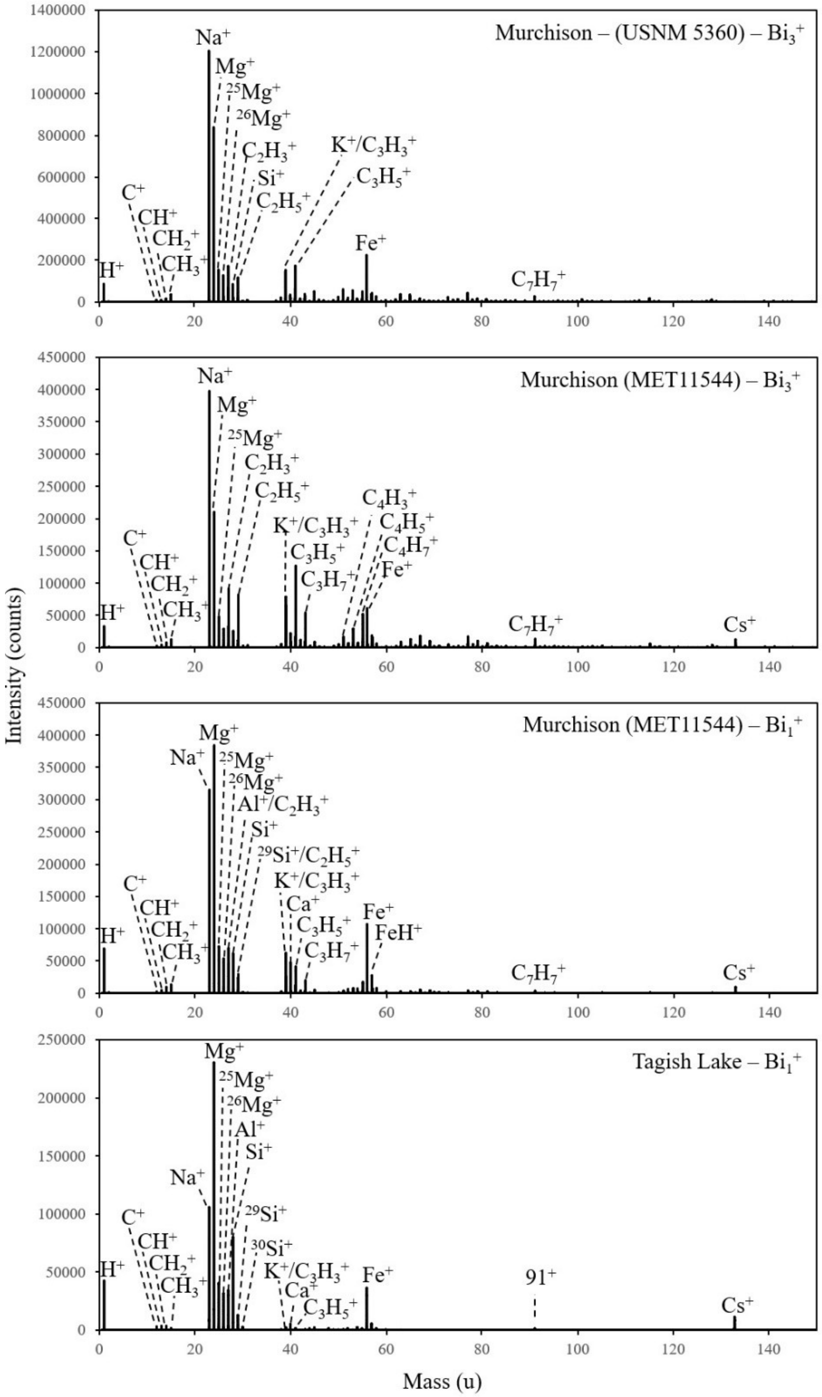

Figure 4.8. Mass spectra (1-150 *m/z*) of positive secondary ions measured by TOF-SIMS analyses of Murchison (Bi_1^+ and Bi_3^+) and Tagish Lake (Bi_1^+) samples. Cs^+ is a contaminant deposited from the Cs^+ pulsed ion beam in the TOF-SIMS instrument. Although the full spectra span from 1-750 *m/z*, peaks above *m/z* = 133^+ were too small to be observed in the figure and were not included.

4.4. CONCLUSIONS

This study reports the first positive identifications of amino acids and characteristic amino acid mass fragments on a meteorite fresh fracture surface via TOF-SIMS. Amino acid-associated ions were detected in most sample areas of the Tagish Lake meteorite. Intact amino acids were not detected in the Murchison meteorite and few characteristic amino acid fragments were detected in low abundances. We conclude that the non-detection of amino acids in Murchison was either due to mass interferences between organic species or due to an insufficiently flat sample surface topography, or a combination of the two effects. The detection of amino acids on the Tagish Lake sample surface illustrates the potential utility of the TOF-SIMS technique for detecting soluble organic compounds in situ in astromaterials. However, the analyses also demonstrated several challenges and limitations associated with the method. Target compounds of interest need to be present in sufficiently high abundances and a flat surface topography is essential in order to accurately evaluate the distribution of organic compounds across mineral grains and textures.

4.5. REFERENCES

Aponte, J. C., J. P. Dworkin, and J. E. Elsila (2014) Assessing the origins of aliphatic amines in the Murchison meteorite from their compound-specific carbon isotopic and enantiomeric composition. *Geochimica et Cosmochimica Acta* **141**, 331-345.

Botta, O. and J. Bada (2002) Extraterrestrial compounds in meteorites. *Surveys in Geophysics* **23**, 411-467.

Briggs, D. and I. W. Fletcher (2013) Qualitative interpretation of spectra. *In TOF-SIMS: Materials Analysis by Mass Spectrometry, 2nd Edition*, J. C. Vickerman and D. Briggs, Eds. (IM Publications LLP and SurfaceSpectra Limited, 2013) p. 417-448.

Cronin, J. R. and S. Pizzarello (1983) Amino acids in meteorites. *Advances in Space Research* **3** (9), 5-18.

Dubey, M., J. Brison, D. W. Grainger, and D. G. Castner (2011) Comparison of Bi_1^+, Bi_3^+ and C_{60}^+ primary ion sources for TOF-SIMS imaging of patterned protein samples. *Surface and Interface Analysis* **43** (1-2), 261-264.

Gilmore, I. (2013) Role of operating conditions in TOF-SIMS. *In TOF-SIMS: Materials Analysis by Mass Spectrometry, 2nd Edition*, J. C. Vickerman and D. Briggs, Eds. (IM Publications LLP and SurfaceSpectra Limited, 2013) p. 335-359.

Hagenhoff, B., D. Van Leyen, E. Niehuis, and A. Benninghoven (1989) Time-of-flight secondary ion mass spectrometry of insulators with pulsed charge compensation by low-energy electrons. *Journal of Vacuum Science and Technology A: Vacuum, Surfaces and Films* **7**, 3056-3064.

Henderson, A. (2013) Multivariate analysis of SIMS spectra. *In TOF-SIMS: Materials Analysis by Mass Spectrometry, 2nd Edition*, J. C. Vickerman and D. Briggs, Eds. (IM Publications LLP and SurfaceSpectra Limited, 2013) p. 449-483.

Henkel, T. and L. C. Lyon (2015) First in-situ analysis of amino acids in the Murchison meteorite with C_{60}-TOFSIMS. *78th Annual Meeting of the Meteoritical Society*, #5256.

Henkel, T. and L. C. Lyon (2016) Extended in-situ search of amino acids in the Murchison meteorite. *79th Annual Meeting of the Meteoritical Society*, #6437.

Herd, C. D. K, A. Blinova, D. N. Simkus, Y. Huang, R. Tarozo, C. M. O'D. Alexander, F. Gyngard, L. R. Nittler, G. D. Cody, M. L. Fogel, Y. Kebukawa, A. L. D. Kilcoyne, R. W. Hilts, G.

F. Slater, D. P. Glavin, J. P. Dworkin, M. P. Callahan, J. E. Elsila, B. T. De Gregorio, and R. M. Stroud (2011) Origin and evolution of prebiotic organic matter as inferred from the Tagish Lake meteorite. *Science* **332**, 1304-1307.

Herd, C. D. K., R. W. Hilts, A. W. Skelhorne and D. N. Simkus (2016) Cold curation of pristine astromaterials: Insights from the Tagish Lake meteorite. *The Meteoritical Society* **51**, 499-519.

Huang, Y., Y. Wang, M. R. Alexandre, T. Lee, C. Rose-Petruck, M. Fuller, and S. Pizzarello (2005) Molecular and compound-specific isotopic characterization of monocarboxylic acids in carbonaceous chondrite meteorites. *Geochimica et Cosmochimica Acta* **69** (4), 1073-1084.

Keenan, M. R. and P. G. Kotula (2004) Accounting for Poisson noise in the multivariate analysis of TOF-SIMS spectrum images. *Surface and Interface Analysis* **36**, 203-212.

Kollmer, F. (2004) Cluster primary ion bombardment of organic materials. *Applied Surface Science* **231-232**, 153-158.

Mantus, D. S., B. D. Ratner, B. A. Carlson, and J. F. Moulder (1993) Static secondary ion mass spectrometry of adsorbed proteins. *Analytical Chemistry* **65**, 1431-1438.

Michel, R. and D. G. Castner (2006) Advances in time-of-flight secondary ion mass spectrometry analysis of protein films. *Surface and Interface Analysis* **38**, 1386-1392.

Naraoka, H., D. Aoki, K. Fukushima, M. Uesugi, M. Ito, F. Kitajima, H. Mita, H. Yabuta, Y. Takano, T. Yada, Y. Ishibashi, Y. Karouji, T. Okada, and M. Abe (2015) TOF-SIMS analysis of carbonaceous particles in the sample catcher of the Hayabusa spacecraft. *Earth, Planets and Space* **67**, 1-9.

Oran, U., E. Ünveren, T. Wirth, and W. E. S. Unger (2004) Poly-dimethyl-siloxane (PDMS) contamination of polystyrene (PS) oligomer samples: a comparison of time-of-flight static secondary ion mass spectrometry (TOF-SSIMS) and X-ray photoelectron spectroscopy (XPS) results. *Applied Surface Science* **227**, 318-324.

Pizzarello, S., G. W. Cooper, and G. J. Flynn (2006) The nature and distribution of the organic material in carbonaceous chondrites and interplanetary dust particles. *In Meteorites and the Early Solar System II.* D. S. Lauretta and H. Y. McSween Jr. (Eds.) (University of Arizona Press, Tucson, 2006), p. 625-651.

Pizzarello, S. and W. Holmes (2009) Nitrogen-containing compounds in two CR2 meteorites: ^{15}N composition, molecular distribution and precursor molecules. *Geochimica et Cosmochimica Acta* **73**, 2150-2162.

Reich, F. (2013) Sample handling for TOF-SIMS. *In TOF-SIMS: Materials Analysis by Mass Spectrometry, 2nd Edition*, J. C. Vickerman and D. Briggs, Eds. (IM Publications LLP and SurfaceSpectra Limited, 2013) p. 397-416.

Samuel, N. T, M. S. Wagner, K. D. Dornfeld, and D. G. Castner (2001) Analysis of poly(amino acids) by static time-of-flight secondary ion mass spectrometry (TOF-SIMS). *Surface Science Spectra* **8**, 163-184.

Sephton, M. A. (2014) Organic geochemistry of meteorites. *Treatise on Geochemistry 2nd Edition*, H. D. Holland and K. K. Turekian, Eds. (Elsevier, 2014) vo1. 12, p. 1-31.

Stephan, T. (2001) TOF-SIMS in cosmochemistry. *Planetary and Space Science* **49**, 859-906.

Stephan, T., E. K. Jessberger, C. H. Heiss, and D. Rost (2003) TOF-SIMS analysis of polycyclic aromatic hydrocarbons in Allan Hills 84001. *Meteoritics & Planetary Science* **38** (1), 109-116.

Touboul, D., F. Kollmer, E. Niehuis, A. Brunelle, O. Laprevote (2005) Improvement of biological time-of-flight secondary ion mass spectrometry imaging with a bismuth cluster ion source. *Journal of the American Society for Mass Spectrometry* **16**, 1608-1618.

Tyler, B. J., C. Bruening, S. Rangaranjan, and H. F. Arlinghaus (2011) TOF-SIMS imaging of adsorbed proteins on topographically complex surfaces with Bi_3^+ primary ions.

Vickerman, J. C. (2013) TOF-SIMS – An evolving mass spectrometry of materials. *In TOF-SIMS: Materials Analysis by Mass Spectrometry, 2nd Edition*, J. C. Vickerman and D. Briggs, Eds. (IM Publications LLP and SurfaceSpectra Limited, 2013) p. 1-37.

Yesiltas, M. and Y. Kebukawa (2016) Associations of organic matter with minerals in Tagish Lake meteorite via high spatial resolution synchrotron-based FTIR microspectroscopy. *Meteoritics & Planetary Science* **51**, 584-595.

CHAPTER 5

CONCLUSIONS: THESIS SUMMARY AND FUTURE RESEARCH

5.1. THESIS SUMMARY

The soluble organic contents of carbonaceous chondrite meteorites record a history of abiotic synthesis reactions that took place in the interstellar medium, during early solar system formation, and on asteroid parent bodies. Elucidating these formation mechanisms provides us with insight into the origin of early solar system prebiotic organic compounds that may have contributed to the origin of life on Earth. This Ph.D. thesis project applied method development experiments and meteorite sample analyses to the investigation of prebiotic organic synthesis in astromaterials. The main outcomes of this research project were: (1) the first reports of compound-specific carbon isotope analyses of meteoritic aldehydes and ketones (Chapters 2 and 3), (2) an expanded evaluation of the influence of aqueous alteration on the soluble organic content of the Tagish Lake meteorite (Chapter 3), and (3) the successful in-situ detection of amino acids in the Tagish Lake meteorite using TOF-SIMS technique (Chapter 4). Detailed summaries of each thesis chapter are outlined below.

5.1.1. Chapter 2 – "Compound-Specific Carbon Isotope Compositions of Aldehydes and Ketones in the Murchison Meteorite"

A PFBHA derivatization method was optimized for the identification, quantification, and compound-specific carbon isotope analysis of meteoritic aldehydes and ketones and the optimized procedure was applied to the analysis of aldehydes and ketones in the Murchison meteorite. The results are generally consistent with the distribution of carbonyl compounds identified by Pizzarello and Holmes (2009), though the changes to the method in the present study appear to have favoured the recovery of lower molecular weight compounds. Compound-specific carbon isotope analyses of formaldehyde, acetaldehyde and acetone from Murchison reflect a secondary origin of aldehydes and ketones. The lack of highly ^{13}C-enriched δ^{13}C ratios indicates that these compounds are not primordial Strecker precursors from the interstellar medium. Rather, they are likely derived from a post-accretionary alteration-driven reaction (e.g. oxidation of the IOM or amino acid degradation on the parent body asteroid).

5.1.2. Chapter 3 – "Assessing the Role of Parent Body Aqueous Alteration During Prebiotic Organic Synthesis in the Tagish Lake Meteorite"

Chapter 3 explored the soluble organic contents of three previously unstudied Tagish Lake specimens (TL1, TL4, and TL10a) and included the first compound-specific carbon isotope analyses of aldehydes and ketones in the Tagish Lake meteorite. The soluble organic analyses of TL1, TL4 and TL10a reveal three very different compositions, likely indicating three distinct alteration histories. Based on comparisons with previously analyzed Tagish Lake lithologies (Herd et al., 2011; Glavin et al., 2012; Hilts et al., 2014), TL1 appears to be a moderately altered specimen, exhibiting relatively high abundances of organics and a composition similar to the previously analyzed TL5b and TL11h specimens. In contrast, TL4, which was found to contain exceptionally low abundances of amino acids, aldehydes, ketones and carboxylic acids was presumed to be a minimally altered specimen. It appears as though the synthesis of soluble organics in TL4 was precluded by the lack/absence of water-rock interactions. Lastly, the TL10a specimen is unusual in that it appears to be devoid of aliphatic and aromatic hydrocarbons and does not contain indigenous carboxylic acids (with the exception of benzoic acid). We conclude that TL10a lost soluble organic compounds via aqueous alteration reactions and the amino acids, aldehydes and ketones detected are likely not indigenous to the specimen, but rather introduced via mobilization during parent body aqueous alteration. Overall, the results from these analyses suggest that aqueous alteration in the Tagish Lake parent body asteroid was not a static process but involved the redistribution of organic compounds during fluid movement. The aldehyde and ketone $\delta^{13}C$ values are highly ^{13}C-depleted, even more so than the Murchison aldehyde and ketone values (Chapter 2), indicating either a greater isotope fractionation effect (potentially due to lower temperatures or a higher degree of alteration in the Tagish Lake meteorite) or a relatively ^{13}C-depleted source of aldehydes and ketones (e.g. relatively ^{13}C-depleted IOM).

5.1.3. Chapter 4 – "Time-of-Flight Secondary Ion Mass Spectrometry (TOF-SIMS) Analysis of Amino Acids in the Murchison and Tagish Lake Meteorites"

TOF-SIMS analysis of a suite of amino acid standards was used to generate a database of expected amino acid fragmentation patterns for both Bi_1^+- and Bi_3^+-TOF-SIMS. Using the standard analyses as a guide, amino acids and characteristic amino acid molecular fragments were detected in several sample areas of a Tagish Lake meteorite fresh fracture surface. The amino acids did not appear to be associated with specific mineral grains or textures in the meteorite, as they appeared to be homogeneously dispersed throughout the matrix. Intact amino acids were not detected in any of the Murchison sample areas. The non-detection of amino acids in the Murchison meteorite was puzzling, though we consider that the indigenous amino acids may have been masked by the signal of other organic compounds.

5.2. IMPLICATIONS FOR PREBIOTIC ORGANIC SYNTHESIS IN THE TAGISH LAKE AND MURCHISON PARENT BODIES

This thesis project identified several notable differences between the soluble organic contents of the Tagish Lake and Murchison meteorites. Although the analyses identified a similar suite of aldehydes and ketones in the two carbonaceous chondrites, the Murchison meteorite yielded a much higher total abundance of aldehydes and ketones (~ 12000 ng/g) compared to the Tagish Lake specimens (~ 4000 ng/g for TL1, ~ 2000 ng/g for TL10a and ~ 300 ng/g for TL4). This observation is consistent with a relatively higher abundance of precursor materials (e.g. IOM, amino acids) present within the Murchison meteorite (Botta and Bada, 2002). The relative ^{13}C-depletion of the Tagish Lake aldehyde and ketone δ^{13}C values compared to the Murchison values indicate either a greater isotope fractionation effect associated with the synthesis mechanism (e.g., due to lower temperature conditions), or a more ^{13}C-depleted source of precursor carbon. The TOF-SIMS analyses of the Murchison meteorite reveal a more diverse organic composition compared to the Tagish Lake samples, potentially indicating a longer duration of organic synthesis on the parent body asteroid or a more complex suite of precursor materials. Lastly, this collection of new Tagish Lake soluble organic data demonstrates the particularly heterogeneous nature of the meteorite compared to Murchison and other carbonaceous chondrites.

The Tagish Lake meteorite has been proposed to have originated from a D- or P-type asteroid located in the outer asteroid belt (Brown et al., 2000; Hiroi et al., 2001) and its composition is commonly compared to CM and CI carbonaceous chondrites as the meteorite shares affinities with both chondrite groups. However, the unusual composition of the Tagish Lake meteorite indicates that it has a unique and distinct origin that may include some incorporation of cometary material (Izawa et al., 2010). It has recently been proposed that the Tagish Lake parent body asteroid may, in fact, be a captured cometary body from the Kuiper Belt region of the solar system (Vokrouhlicky et al., 2016). The high porosity, friability and heterogeneity of the Tagish Lake meteorite may be consistent with a cometary origin and the highly ^{13}C-depleted carbon isotope compositions for soluble organics in the Tagish Lake meteorite are consistent with episodic low-temperature alteration reactions that would take place during melting of cometary ice.

5.3. FUTURE RESEARCH DIRECTIONS

Chapters 2 and 3 of this thesis reported the first carbon isotope analyses of aldehydes and ketones in meteorite samples and the values obtained in these studies indicated alteration-driven reactions as sources for these compounds. An in-depth interpretation of the δ^{13}C values was limited, however, due to low abundances of soluble organics. Low abundances of aldehydes and ketones precluded the carbon isotope analysis of the higher molecular weight compounds (e.g. propionaldehyde, butyraldehyde, 2-butanone, 2-pentanone) and low abundances of amino acids in both TL4 and TL10a precluded their compound-specific carbon isotope analyses entirely. In order to gain a full understanding of the origin of meteoritic aldehydes and ketones and their relationship to other meteoritic compound classes (e.g., amino acids), carbon isotope analyses need to be obtained for a larger series of compounds. This can be achieved by analyzing larger meteorite sample masses, and now that soluble organic abundances have been obtained for TL1, TL4 and TL10a, the minimum sample masses required for accurate measurements can be determined and targeted. Though beyond the scope of this thesis, the soluble organic analyses would also greatly benefit from an in-depth investigation of the mineralogy and petrology of the Tagish Lake specimens TL1, TL4 and TL10a, as was carried out previously by Blinova et al. (2014a,b) for TL5b, TL11h, TL11i and TL11v. Combining the present soluble organic data, and the associated interpretations, with information about the geologic history of the Tagish Lake specimens would help shed light on whether or not the organic chemistry records an alteration history that is consistent with the mineralogical/petrological data.

Other prebiotic organic compounds of interest for soluble organic analyses of carbonaceous chondrites are aliphatic alcohols, which are potentially structurally related to aldehydes, ketones, amines and, indirectly, amino acids, hydroxy acids and carboxylic acids. Despite their biological significance, the distribution of alcohols in meteorites have only been investigated in two studies (Studier et al., 1965; Jungclaus et al., 1976) and neither their enantiomeric compositions nor their compound-specific δ^{13}C values have been measured to date. Obtaining carbon isotope analyses for meteoritic alcohols would provide further insight into the origin of aldehydes, ketones and amines in meteorites. Determining whether chiral meteoritic alcohols are racemic or exhibit L-enantiomeric excesses would shed light on the origin of L-enantiomeric excesses observed for meteoritic amino acids.

Lastly, the hypothesis of a cometary origin for the Tagish Lake meteorite may be tested by investigating bulk hydrogen isotope compositions of Tagish Lake specimens in comparison to known cometary values. The possibility of a synthetic relationship would be best tested by obtaining hand samples of cometary material, investigating their mineralogy, petrology, soluble organic contents and isotopic compositions. Comparing and contrasting the results with the present data and identifying a similarly heterogeneous composition with highly ^{13}C-depleted carbon isotope compositions and similar water hydrogen isotope compositions may help to shed light on a genetic relationship between the Tagish Lake meteorite and cometary nuclei.

5.4. REFERENCES

Blinova, A. I., C. D. K. Herd, and M. J. M. Duke (2014a) Testing variations within the Tagish Lake meteorite - II: Whole-rock geochemistry of pristine samples. *Meteoritics & Planetary Science* **49** (6), 1100-1118.

Blinova, A. I., T. J. Zega, C. D. K. Herd and R. M. Stroud (2014b) Testing variations within the Tagish Lake meteorite - I: Mineralogy and petrology of pristine samples. *Meteoritics & Planetary Science* **49** (4), 473-502.

Botta, O. and J. L. Bada (2002) Extraterrestrial organic compounds in meteorites. *Surveys in Geophysics* **23**, 411−467.

Brown, P. G., A. R. Hildebrand, M. E. Zolensky, M. Grady, R. N. Clayton, T. K. Mayeda, E. Tagliaferri, R. Spalding, N. D. MacRae, E. L. Hoffman, D. W. Mittlefehldt, J. F. Wacker, J. A. Bird, M. D. Campbell, R. Carpenter, H. Gingerich, M. Glatiotis, E. Greiner, M. J. Mazur, P. J. A. McCausland, H. Plotkin, T. R. Mazur (2000) The fall, recovery, orbit, and composition of the Tagish Lake meteorite: A new type of carbonaceous chondrite. *Science* **290**, 320-325.

Glavin, D. P., J. E. Elsila, A. S. Burton, M. P. Callahan, J. P. Dworkin, R. W. Hilts, and C. D. K. Herd (2012) Unusual nonterrestrial L-proteinogenic amino acid excesses in the Tagish Lake meteorite. *Meteoritics & Planetary Science* **47** (8), 1347-1364.

Herd, C. D. K, A. Blinova, D. N. Simkus, Y. Huang, R. Tarozo, C. M. O'D. Alexander, F. Gyngard, L. R. Nittler, G. D. Cody, M. L. Fogel, Y. Kebukawa, A. L. D. Kilcoyne, R. W. Hilts, G. F. Slater, D. P. Glavin, J. P. Dworkin, M. P. Callahan, J. E. Elsila, B. T. De Gregorio, and R. M. Stroud (2011) Origin and evolution of prebiotic organic matter as inferred from the Tagish Lake meteorite. *Science* **332**, 1304-1307.

Hilts, R. W, C. D. K. Herd, D. N. Simkus, and G. F. Slater (2014) Soluble organic compounds in the Tagish Lake meteorite. *Meteoritics & Planetary Science* **49** (4), 526-549.

Hiroi, T., M. E. Zolensky, and C. M. Pieters (2001) The Tagish Lake meteorite: A possible sample from a D-type asteroid. *Science* **293**, 2234-2236.

Izawa, M. R. M., R. L. Flemming, P. L. King, R. C. Peterson, and P. J. A. McCausland (2010) Mineralogical and spectroscopic investigation of the Tagish Lake carbonaceous chondrite by X-ray diffraction and infrared reflectance spectroscopy. *Meteoritics & Planetary Science* **45**, 675-698.

Jungclaus, G. A., G. U. Yuen, C. B. Moore (1976a) Evidence for the presence of low molecular weight alcohols and carbonyl compounds in the Murchison meteorite. *Meteoritics* **11**, 231-237.

Pizzarello, S. and W. Holmes (2009) Nitrogen-containing compounds in two CR2 meteorites: ^{15}N composition, molecular distribution and precursor molecules. *Geochimica et Cosmochimica Acta* **73**, 2150-2162.

Studier, M. H., R. Hayatsu, and E. Anders (1965) Organic compounds in carbonaceous chondrites. *Science* **149**, 1455-1459.

Vokrouhlicky, D., W. F. Bottke, and D. Nesvorny (2016) Capture of trans-Neptunian planetesimals in the main asteroid belt. *The Astronomical Journal* **152**(39), 1-20.

BIBLIOGRAPHY

Abdel-Magid A. F., K. G. Carson, B. D. Harris, C. A. Maryanoff, and R. D. Shah (1996) Reductive amination of aldehydes and ketones with sodium triacetoxyborohydride. Studies on direct and indirect reductive amination procedures. *Journal of Organic Chemistry* **61**, 3849-3862.

Allamandola, L. J., S. A. Sandford, and G. J. Valero (1988) Photochemical and thermal evolution of interstellar/precometary ice analogs. *Icarus* **76**, 225-252.

Aponte, J. C., J. P. Dworkin, and J. E. Elsila (2014) Assessing the origins of aliphatic amines in the Murchison meteorite from their compound-specific carbon isotopic ratios and enantiomeric composition. *Geochimica et Cosmochimica Acta* **141**, 331-345.

Aponte, J. C., J. E. Elsila, D. P. Glavin, S. N. Milam, S. B. Charnley, and J. P. Dworkin (2017) Pathways to meteoritic glycine and methylamine. *ACS Earth and Space Chemistry*, DOI: 10.1021/acsearthspacechem.6b00014

Awad, Z., T. Chigai, Y. Kimura, O. M. Shalabiea, and T. Yamamoto (2005) New rate constants of hydrogenation of CO on H_2O-CO ice surfaces. *The Astrophysical Journal* **626**, 262-271.

Baker, L., I. A. Franchi, I. P. Wright, and C. T. Pillinger (2002) The oxygen isotopic composition of water from Tagish Lake: Its relationship to low-temperature phases and to other carbonaceous chondrites. *Meteoritics & Planetary Science* **37**, 977-985.

Bisschop, S. E., G. W. Fuchs, E. F. van Dishoeck, and H. Linnartz (2007) H-atom bombardment of CO_2, HCOOH, and CH_3CHO containing ices. *Astronomy & Astrophysics* **474**, 1061-1071.

Bland, P. A., G. Cressey, and O. N. Menzies (2004) Modal mineralogy of carbonaceous chondrites by X-ray diffraction and Mossbauer spectroscopy. *Meteoritics & Planetary Science* **39** (1), 3-16.

Blinova, A. I., C. D. K. Herd, and M. J. M. Duke (2014a) Testing variations within the Tagish Lake meteorite - II: Whole-rock geochemistry of pristine samples. *Meteoritics & Planetary Science* **49** (6), 1100-1118.

Blinova, A. I., T. J. Zega, C. D. K. Herd and R. M. Stroud (2014b) Testing variations within the Tagish Lake meteorite - I: Mineralogy and petrology of pristine samples. *Meteoritics & Planetary Science* **49** (4), 473-502.

Bossa, J.-B. F. Duvernay, P. Theulé, F. Borget, L. d'Hendecourt, T. Chiavassa (2009) Methylammonium methylcarbamate thermal formation in interstellar ice analogs: a glycine salt precursor in protostellar environments. *Astronomy & Astrophysics* **506**, 601-608.

Botta, O., D. P. Glavin, G. Kminek, and J. L. Bada (2002) Relative amino acid concentrations as a signature for parent body processes of carbonaceous chondrites. *Origins of Life and Evolution of the Biosphere* **32**, 143-163.

Botta, O. and J. L. Bada (2002) Extraterrestrial organic compounds in meteorites. *Surveys in Geophysics* **23**, 411−467.

Brearley, A. J. (2014) Nebular versus parent body processing. *Treatise on Geochemistry 2nd Edition*, H. D. Holland and K. K. Turekian, Eds. (Elsevier, 2014), vol. 1, p. 309-334.

Briggs, D. and I. W. Fletcher (2013) Qualitative interpretation of spectra. *In TOF-SIMS: Materials Analysis by Mass Spectrometry, 2nd Edition*, J. C. Vickerman and D. Briggs, Eds. (IM Publications LLP and SurfaceSpectra Limited, 2013) p. 417-448.

Brown, P. G., A. R. Hildebrand, M. E. Zolensky, M. Grady, R. N. Clayton, T. K. Mayeda, E. Tagliaferri, R. Spalding, N. D. MacRae, E. L. Hoffman, D. W. Mittlefehldt, J. F. Wacker, J. A. Bird, M. D. Campbell, R. Carpenter, H. Gingerich, M. Glatiotis, E. Greiner, M. J. Mazur, P. J. A. McCausland, H. Plotkin, T. R. Mazur (2000) The fall, recovery, orbit, and composition of the Tagish Lake meteorite: A new type of carbonaceous chondrite. *Science* **290**, 320-325.

Browning, L. B., H. Y. McSween Jr., and M. Zolensky (1996) Correlated alteration effects in CM carbonaceous chondrites. *Geochimica et Cosmochimica Acta* **60** (14), 2621-2633.

Burk M. J., J. P. Martinez, J. E. Feaster, and N. Cosford (1994) Catalytic asymmetric reductive amination of ketones via highly enantioselective hydrogenation of the C=N double bond. *Tetrahedron* **50**, 4399-4428.

Callahan, M. P., K. E. Smith, J. Cleaves II, J. Ruzicka, J. C. Stern, D. P. Glavin, C. H. House, and J. P. Dworkin (2011) Carbonaceous meteorites contain a wide range of extraterrestrial nucleobases. *PNAS* **108** (34), 13995-13998.

Cancho, B., F. Ventura and M. T. Galceran (2001) Determination of aldehydes in drinking water using pentafluorobenzylhydroxylamine derivatization and solid-phase microextraction. *Journal of Chromatography* **943**, 1-13.

Charnley, S. B., P. Ehrenfreund, T. J. Millar, A. C. A. Boogert, A. J. Markwick, H. M. Butner, R. Ruiterkamp, and S. D. Rodgers (2004) Observational tests for grain chemistry: Posterior Isotopic labelling. *Monthly Notices of the Royal Astronomical Society* **347**, 157-162.

Chyba, C. F., P. J. Thomas, L. Brookshaw, and C. Sagan (1990) Cometary delivery of organic molecules to the early Earth. *Science* **249**, 366-373.

Clayton, R. N., and T. K. Mayeda (1999) Oxygen isotope studies in carbonaceous chondrites. *Geochimica et Cosmochimica Acta* **63**, 2089-2104.

Cleaves, H. J. (2008) The prebiotic geochemistry of formaldehyde. *Precambrian Research*, **164**, 111-118.

Cody, G. D., and C. M. O'D. Alexander (2005) NMR studies of chemical structural variation of insoluble organic matter from different carbonaceous chondrite groups. *Geochimica et Cosmochimica Acta* **69**, 1085-1097.

Cody, G. D., E. Heying, C. M. O'D. Alexander, L. R. Nittler, A. L. D. Kilcoyne, S. A. Sandford, and R. M. Stroud (2011) Establishing a molecular relationship between chondritic and cometary organic solids. *PNAS* **108**, 19171-19176.

Cooper, G., N., N. Kimmich, W. Belisle, J. Sarinana, K. Brabham, and L. Garrel (2001) Carbonaceous meteorites as a source of sugar-related organic compounds for the early Earth. *Nature* **414**, 879-883.

Cooper, G., A. Dugas, A. Byrd, P. M. Chang and N. Washington (2005) Keto-acids in carbonaceous meteorites. *36th Lunar and Planetary Science Conference*, #2381.

Cooper, G., C. Reed, D. Nguyen, M. Carter, and Y. Wang (2011) Detection and formation scenario of citric acid, pyruvic acid, and other possible metabolism precursors in carbonaceous meteorites. *PNAS* **108**, 14015-14020.

Corey, E. J., N. W. Gilman, and B. E. Ganem (1968) New methods for the oxidation of aldehydes to carboxylic acids and esters. *Journal of the American Chemical Society* **90**, 5616-5617.

Cronin, J. R. and S. Pizzarello (1983) Amino acids in meteorites. *Advances in Space Research* **3**, 5-18.

Cronin, J. R. and S. Chang (1993) Organic matter in meteorites: Molecular and isotopic analyses of the Murchison meteorite. *The Chemistry of Life's Origin.* J. M. Greenberg, C. X. Mendoza-Gomez, and V. Pirronello, Eds. (Kluwer Academic Publishers, 1993), p. 209-255.

Deamer, D., J. P. Dworkin, S. A Sandford, M. P. Bernstein, and L. J. Allamandola (2002) The first cell membranes. *Astrobiology* **2** (4), 371-381.

de Marcellus, P., C. Meinert, I. Myrgorodska, L. Nahon, T. Buhse, L. Le Sergeant D'Hendecourt, and U. J. Meierhenrich (2015) Aldehydes and sugars from evolved precometary ice analogs: Importance of ices in astrochemical and prebiotic evolution. *PNAS* **112**, 965-970.

Docherty, G., V. Jones, and R. P. Evershed (2001) Practical and theoretical considerations in the gas chromatography/combustion/isotope ratio mass spectrometry $\delta^{13}C$ analysis of small polyfunctional compounds. *Rapid Communications in Mass Spectrometry* **15**, 730-738.

Domagal-Goldman, S. and K. E. Wright (2016) The Astrobiology Primer V2.0. *Astrobiology* 16 (8), 561-653.

Dubey, M., J. Brison, D. W. Grainger, and D. G. Castner (2011) Comparison of Bi_1^+, Bi_3^+ and C_{60}^+ primary ion sources for TOF-SIMS imaging of patterned protein samples. *Surface and Interface Analysis* **43** (1-2), 261-264.

Ehrenfreund, P., D. P. Glavin, O. Botta, G. Cooper, and J. L. Bada (2001) Extraterrestrial amino acids in Orgueil and Ivuna: Tracing the parent body of CI type carbonaceous chondrites. *PNAS* **98** (5), 2138-2141.

Elsila, J. E., D. P. Glavin, and J. P. Dworkin (2009) Cometary glycine detected in samples returned by Starbust. *Meteoritics & Planetary Science* **44**, 1323-1330.

Elsila, J. E., S. B. Charnley, A. S. Burton, D. P. Glavin, and J. P. Dworkin (2012) Compound-specific carbon, nitrogen, and hydrogen isotopic ratios for amino acids in CM and CR chondrites and their use in evaluating potential formation pathways. *Meteoritics & Planetary Science* **47**, 1517-1536.

Elsila, J. E., J. C. Aponte, D. G. Blackmond, A. S. Burton, J. P. Dworkin, and D. P. Glavin (2016) Meteoritic amino acids: diversity in compositions reflects parent body histories. *ACS Central Science* **2** (6), 370-379.

Engel, M. H., S. A. Macko, and J. A. Silfer (1990) Carbon isotope composition of individual amino acids in the Murchison meteorite. *Nature* **348**, 47-49.

EPA Method 556: Determination of carbonyl compounds in drinking water by pentafluorobenzylhydroxylamine derivatization and capillary gas chromatography with electron capture detection (1998) National exposure research laboratory office of research and development. US Environmental Protection Agency, Cincinnati, Ohio, 45268.

Gilmore, I. (2013) Role of operating conditions in TOF-SIMS. *In TOF-SIMS: Materials Analysis by Mass Spectrometry, 2nd Edition*, J. C. Vickerman and D. Briggs, Eds. (IM Publications LLP and SurfaceSpectra Limited, 2013) p. 335-359.

Gilmour, I. (2003) Structural and isotopic analysis of organic matter in carbonaceous chondrites. *Treatise on Geochemistry 1st Edition*, H.D. Holland and K. K. Turekian, Eds. (Elsevier, 2004) vo1. 1, p. 269-290.

Gilmour, C. (2017) Economic significance of platinum group elements and water in asteroids: Insights from chondritic meteorites (Master's thesis), University of Alberta.

Glavin, D. P., J. P. Dworkin, A. Aubrey, O. Botta, J. H. Dotty III, Z. Martins, and J. L. Bada (2006) Amino acid analyses of Antarctic CM2 meteorites using liquid chromatography – time of flight – mass spectrometry. *Meteoritics & Planetary Science* **41** (6), 899-902.

Glavin, D. P. and J. P. Dworkin (2009) Enrichment of the amino acid L-isovaline by aqueous alteration on CI and CM meteorite parent bodies. *PNAS* **106** (14), 5487-5492.

Glavin, D. P., J. E. Elsila, A. S. Burton, M. P. Callahan, J. P. Dworkin, R. W. Hilts, and C. D. K. Herd (2012) Unusual nonterrestrial L-proteinogenic amino acid excesses in the Tagish Lake meteorite. *Meteoritics & Planetary Science* **47**, 1347-1364.

Glaze, W. H., M. Koga and D. Cancilla (1989) Ozonation byproducts. 2. Improvement of an aqueous-phase derivatization method for the detection of formaldehyde and other carbonyl compounds formed by the ozonation of drinking water. *Environmental Science & Technology* **23**, 838-847.

Grady, M. M., A. B. Verchovsky, I. A. Franchi, I. P. Wright, and C. T. Pillinger (2002) Light element geochemistry of the Tagish Lake CI1 chondrite: Comparison with CI1 and CM2 meteorites. *Meteoritics & Planetary Science* **37**, 713-735.

Grady, M. M., and I. P. Wright (2003) Elemental and isotopic abundances of carbon and nitrogen in meteorites. *Space Science Reviews* **106**, 231-248.

Guo, W., and J. M. Eiler (2007) Temperatures of aqueous alteration and evidence for methane generation on the parent bodies of the CM chondrites. *Geochimica et Cosmochimica Acta* **71**, 5565-5575.

Hagenhoff, B., D. Van Leyen, E. Niehuis, and A. Benninghoven (1989) Time-of-flight secondary ion mass spectrometry of insulators with pulsed charge compensation by low-energy electrons. *Journal of Vacuum Science and Technology A: Vacuum, Surfaces and Films* **7**, 3056-3064.

Henderson, A. (2013) Multivariate analysis of SIMS spectra. *In TOF-SIMS: Materials Analysis by Mass Spectrometry, 2nd Edition*, J. C. Vickerman and D. Briggs, Eds. (IM Publications LLP and SurfaceSpectra Limited, 2013) p. 449-483.

Henkel, C., T. L. Wilson, and J. Bieging (1982) Further ($^{12}C/^{13}C$) ratios from formaldehyde: A variation with distance from the galactic center. *Astronomy & Astrophysics* **109**, 344−351.

Henkel, T. and L. C. Lyon (2015) First in-situ analysis of amino acids in the Murchison meteorite with C_{60}-TOFSIMS. *78th Annual Meeting of the Meteoritical Society*, #5256.

Henkel, T. and L. C. Lyon (2016) Extended in-situ search of amino acids in the Murchison meteorite. *79th Annual Meeting of the Meteoritical Society*, #6437.

Herd, C. D. K, A. Blinova, D. N. Simkus, Y. Huang, R. Tarozo, C. M. O'D. Alexander, F. Gyngard, L. R. Nittler, G. D. Cody, M. L. Fogel, Y. Kebukawa, A. L. D. Kilcoyne, R. W. Hilts, G. F. Slater, D. P. Glavin, J. P. Dworkin, M. P. Callahan, J. E. Elsila, B. T. De Gregorio, and R. M. Stroud (2011) Origin and evolution of prebiotic organic matter as inferred from the Tagish Lake meteorite. *Science* **332**, 1304-1307.

Herd, C. D. K., R. W. Hilts, A. W. Skelhorne, and D. N. Simkus (2016) Cold curation of pristine astromaterials: Insights from the Tagish Lake meteorite. *Meteoritics & Planetary Science* **51**, 499-519.

Hildebrand, A. R., P. J. A. McCausland, P. G. Brown, F. J. Longstaff, S. D. J. Russell, E. Tagliaferri, J. F. Wacker, and M. J. Mazur (2006) The fall and recovery of the Tagish Lake meteorite. *Meteoritics & Planetary Science* **41** (3), 407-431.

Hilts, R. W, C. D. K. Herd, D. N. Simkus, and G. F. Slater (2014) Soluble organic compounds in the Tagish Lake meteorite. *Meteoritics & Planetary Science* **49** (4), 526-549.

Hiroi, T., M. E. Zolensky, and C. M. Pieters (2001) The Tagish Lake meteorite: A possible sample from a D-type asteroid. *Science* **293**, 2234-2236.

Holtom, P. D., C. J. Bennett, Y. Osamura, N. J. Mason, and R. I. Kaiser (2005). A combined experimental and theoretical study on the formation of the amino acid glycine (NH_2CH_2COOH) and its isomer ($CH_3NHCOOH$) in extraterrestrial ices. *The Astrophysical Journal* **626**, 940.

Huang, Y., Y. Wang, M. R. Alexandre, T. Lee, C. Rose-Petruck, M. Fuller, and S. Pizzarello (2005) Molecular and compound-specific isotopic characterization of monocarboxylic acids in carbonaceous meteorites. *Geochimica et Cosmochimica Acta* **69** (4), 1073-1084.

Huang, Y., J. C. Aponte, J. Zhao, R. Tarozo, and C. Hallmann (2015) Hydrogen and carbon isotopic ratios of polycyclic aromatic compounds in two CM2 carbonaceous chondrites and implications for prebiotic organic synthesis. *Earth and Planetary Science Letters* **426**, 101-108.

Huber, C., and G. Wächtershäuser (2003) Primordial reductive amination revisited. *Tetrahedron Letters* **44**, 1695-1697.

Hudson, E. D., K. Okuda, and P. A. Ariya (2007) Determination of acetone in seawater using derivatization solid-phase microextraction. *Analytical and Bioanalytical Chemistry* **388**, 1275-1282.

Hudson, R. L., Lewis, A. S., Moore, M. H., Dworkin, J. P., and M. P. Martin (2009) Enigmatic isovaline: investigating the stability, racemization and formation of a non-biological meteoritic amino acid. *ASP Conference Series* **420**, 157-162.

Irvine (1999) The composition of interstellar molecular clouds. *Space Science Reviews* **90**, 203-218.

Izawa, M. R. M., R. L. Flemming, P. L. King, R. C. Peterson, and P. J. A. McCausland (2010) Mineralogical and spectroscopic investigation of the Tagish Lake carbonaceous chondrite by X-ray diffraction and infrared reflectance spectroscopy. *Meteoritics & Planetary Science* **45**, 675-698.

Jungclaus, G. A., G. U. Yuen, C. B. Moore (1976a) Evidence for the presence of low molecular weight alcohols and carbonyl compounds in the Murchison meteorite. *Meteoritics* **11**, 231-237.

Jungclaus, G., J. R. Cronin, C. B. Moore, and G. U. Yuen (1976b) Aliphatic amines in the Murchison meteorite. *Nature* **261**, 126-128.

Kalia, J. and R. T. Raines (2008) Hydrolytic stability of hydrazones and oximes. *Angewandte Chemie* **47**, 7523-7526.

Kebukawa, Y., and G. D. Cody (2015) A kinetic study of the formation of organic solids from formaldehyde: Implications for the origin of extraterrestrial organic solids in primitive Solar System objects. *Icarus* **248**, 412-423.

Keenan, M. R. and P. G. Kotula (2004) Accounting for Poisson noise in the multivariate analysis of TOF-SIMS spectrum images. *Surface and Interface Analysis* **36**, 203-212.

Kminek, G., O. Botta, D. P. Glavin, and J. L. Bada (2002) Amino acids in the Tagish Lake meteorite. *Meteoritics & Planetary Science* **37**, 697-701.

Kobayashi, K., M. Tanaka, and S. Kawai (1980) Gas chromatographic determination of low-molecular-weight carbonyl compounds in aqueous solution as their O-(2,3,4,5,6-pentafluorobenzyl) oximes. *Journal of Chromatography* **187**, 413-417.

Kollmer, F. (2004) Cluster primary ion bombardment of organic materials. *Applied Surface Science* **231-232**, 153-158.

Krishnamurthy, R. V., S. Epstein, J. R. Cronin, S. Pizzarello, and G. U. Yuen (1992) Isotopic and molecular analyses of hydrocarbons and monocarboxylic acids of the Murchison meteorite. *Geochimica et Cosmochimica Acta* **56**, 4045-4058.

Krot, A. N., K. Keil, E. R. D. Scott, C. A. Goodrich, and M. K. Weisberg (2014) Classification of meteorites and their genetic relationships. *Treatise on Geochemistry 2nd Edition*, H. D. Holland and K. K. Turekian, Eds. (Elsevier, 2014) vol. 1, p. 1-63.

Krot, A. N., K. Nagashima, C. M. O'D Alexander, F. J. Ciesla, W. Fujiya, and L. Bonal (2015) Sources of water and aqueous activity on the chondrite parent asteroids. In *Asteroids IV*, P. Michel et al., Eds. University of Arizona Press, Tuscon, 635-660.

Kvenvolden, K., J. Lawless, K. Pering, E. Peterson, J. Flores, C. Ponnamperuma, I. R. Kaplan, C. Moore (1970) Evidence for extraterrestrial amino acids and hydrocarbons in the Murchison meteorite. *Nature* **228**, 923-926.

Lawless, J. G., and E. Peterson (1975) Amino acids in carbonaceous chondrites. *Origins of Life* **6**, 3-8.

Lee C.-W., J.-K. Kim, E.-S. Moon, Y. C. Minh, and H. Kang (2009) Formation of glycine on ultraviolet-irradiated interstellar ice-analog films and implications for interstellar amino acids. *The Astrophysical Journal* **697**, 428-435.

Le Lacheur, R. M., L. B. Sonnenberg, P. C. Singer, R. F. Christman, and M. J. Charles (1993) Identification of carbonyl compounds in environmental samples. *Environmental Science & Technology* **27**, 2745-2753.

Lien, Y. C. and W. W. Nawar (1974) Thermal degradation of some amino acids. *Journal of Food Science* **39**, 911-913.

Mantus, D. S., B. D. Ratner, B. A. Carlson, and J. F. Moulder (1993) Static secondary ion mass spectrometry of adsorbed proteins. *Analytical Chemistry* **65**, 1431-1438.

Martins, Z., O. Botta, M. L. Fogel, M. A. Sephton, D. P. Glavin, J. S. Watson, J. P. Dworkin, A. W. Schwartz, P. Ehrenfreund (2008) Extraterrestrial nucleobases in the Murchison meteorite. *Earth and Planetary Science Letters* **270**, 130-136.

McCollom, T. M. (2013) The influence of minerals on decomposition of the n-alkyl-α-amino acid norvaline under hydrothermal conditions. *Geochimica et Cosmochimica Acta* **104**, 330-357.

Meinert, C., I. Myrgorodska, P. de Marcellus, T. Buhse, L. Nahon, S. V. Hoffmann, L. Le Sergeant d'Hendecourt, U. J. Meierhenrich (2016) Ribose and related sugars from ultraviolet irradiation of interstellar ice analogs. *Science* **352**, 208-212.

Michel, R. and D. G. Castner (2006) Advances in time-of-flight secondary ion mass spectrometry analysis of protein films. *Surface and Interface Analysis* **38**, 1386-1392.

Miller, S. (1957) The mechanism of synthesis of amino acids by electric discharges. *Biochimica et Biophysica Acta* **23**, 480-489.

Monroe, A. A. and S. Pizzarello (2011) The soluble organic compounds of the Bells meteorite: Not a unique or unusual composition. *Geochimica et Cosmochimica Acta* **75**, 7585-7595.

Mumma, M. J., and S. B. Charnley (2011) The chemical composition of comets. *Annual Review of Astronomy and Astrophysics* **49**, 471-524.

Naraoka, H., A. Shimoyama, and K. Harada (1999) Molecular distribution of monocarboxylic acids in Asuka carbonaceous chondrites from Antarctica. *Origins of Life and Evolution of the Biosphere* **29**, 187-201.

Naraoka, H., D. Aoki, K. Fukushima, M. Uesugi, M. Ito, F. Kitajima, H. Mita, H. Yabuta, Y. Takano, T. Yada, Y. Ishibashi, Y. Karouji, T. Okada, and M. Abe (2015) TOF-SIMS analysis of carbonaceous particles in the sample catcher of the Hayabusa spacecraft. *Earth, Planets and Space* **67**, 1-9.

Oba, Y. and H. Naraoka (2006) Carbon isotopic composition of acetic acid generated by hydrous pyrolysis of macromolecular organic matter from the Murchison meteorite. *Meteoritics & Planetary Science* **41** (8), 1175-1181.

O'Brien, D. M., M. L. Fogel, and C. L. Boggs (2002) Renewable and nonrenewable resources: Amino acid turnover and allocation to reproduction in Lepidoptera. *PNAS* **99**, 4413-4418.

Oran, U., E. Ünveren, T. Wirth, and W. E. S. Unger (2004) Poly-dimethyl-siloxane (PDMS) contamination of polystyrene (PS) oligomer samples: a comparison of time-of-flight static secondary ion mass spectrometry (TOF-SSIMS) and X-ray photoelectron spectroscopy (XPS) results. *Applied Surface Science* **227**, 318-324.

Palme, H., K. Lodders, and A. Jones (2014) Solar system abundances of the elements. *Treatise on Geochemistry 2nd Edition*, H. D. Holland and K. K. Turekian, Eds. (Elsevier, 2014), vol. 2, p. 15-36.

Peltzer, E. T. and J. L. Bada (1978) A-Hydroxycarboxylic acids in the Murchison meteorite. *Nature* **272**, 443-444.

Peltzer E. T., J. L Bada, G. Schlesinger, and S. L. Miller (1984) The chemical conditions on the parent body of the Murchison meteorite: Some conclusions based on amino, hydroxy and dicarboxylic acids. *Advances in Space Research* **4**, 69-74.

Penzias, A. A. (1980) Nuclear processing and isotopes in the galaxy. *Science* **208**, 663-669.

Pizzarello, S. and J. R. Cronin (2000) Non-racemic amino acids in the Murray and Murchison meteorites. *Geochimica et Cosmochimica Acta* **64** (2), 329-338.

Pizzarello, S., M. Zolensky, and K. A. Turk (2003) Non racemic isovaline in the Murchison meteorite: chiral distribution and mineral association. *Geochimica et Cosmochimica Acta* **67**, 1589-1595.

Pizzarello, S., Y. S. Huang, and M. Fuller (2004) The carbon isotopic distribution of Murchison amino acids. *Geochimica et Cosmochimica Acta* **68**, 4963-4969.

Pizzarello, S., G. W. Cooper, G. J. Flynn (2006) The nature and distribution of the organic material in carbonaceous chondrites and interplanetary dust particles. *Meteorites and the Early Solar System II*, D. S. Lauretta and H. Y. McSween, Eds. (University of Arizona Press, 2006), p. 625-650.

Pizzarello, S. and W. Holmes (2009) Nitrogen-containing compounds in two CR2 meteorites: ^{15}N composition, molecular distribution and precursor molecules. *Geochimica et Cosmochimica Acta* **73**, 2150-2162.

Pizzarello, S., Y. Wang, and G. M. Chaban (2010) A comparative study of the hydroxy acids from the Murchison, GRA 95229 and LAP 02342 meteorites. *Geochimica et Cosmochimica Acta* **74**, 6206-6217.

Ralchenko, M., D. T. Britt, C. Samson, C. D. K. Herd, R. K. Herd, and P. J. A. McCausland (2014) Bulk physical properties of the Tagish Lake meteorite frozen pristine fragments. *LPSC XIV*, # 1021.

Reich, F. (2013) Sample handling for TOF-SIMS. *In TOF-SIMS: Materials Analysis by Mass Spectrometry, 2nd Edition*, J. C. Vickerman and D. Briggs, Eds. (IM Publications LLP and SurfaceSpectra Limited, 2013) p. 397-416.

Rodigast, M., A. Mutzel, Y. Iinuma, S. Haferkorn, and H. Herrmann (2015) Characterisation and optimization of a sample preparation method for the detection and quantification of atmospherically relevant carbonyl compounds in aqueous medium. *Atmospheric Measurement Technique* **8**, 2409-2416.

Rubin, A. E., J. M. Trigo-Rodriguez, H. Huber, and J. T. Wasson (2007) Progressive aqueous alteration of CM carbonaceous chondrites. *Geochimica et Cosmochimica Acta* **71**, 2361-2382.

Saison, D., D. P. De Schutter, F. DeIvaux, F. R. Delvaux (2009) Determination of carbonyl compounds in beer by derivatization and headspace solid-phase microextraction in combination with gas chromatography and mass spectrometry. *Journal of Chromatography A* **1216**, 5061-5068.Seaman, V. Y., M. J. Charles, and T. M. Cahill (2006) A sensitive method for the quantification of acrolein and other volatile carbonyls in ambient air. *Analytical Chemistry* **78**, 2405-2412.

Samuel, N. T, M. S. Wagner, K. D. Dornfeld, and D. G. Castner (2001) Analysis of poly(amino acids) by static time-of-flight secondary ion mass spectrometry (TOF-SIMS). *Surface Science Spectra* **8**, 163-184.

Schonberg, A. and R. Moubacher (1951) The Strecker degradation of α-amino acids. *Chemical Reviews* **50**, 261-277.

Schutte, W. A., P. A. Gerakines, T. R. Geballe, E. F. vanDishoeck, and J. M. Greenberg (1996) Discovery of solid formaldehyde toward the protostar GL 2136: Observations and laboratory simulation. *Astronomy & Astrophysics* **309**, 633-647.

Seaman, V. Y., M. J. Charles, and T. M. Cahill (2006) A sensitive method for the quantification of acrolein and other volatile carbonyls in ambient air. *Analytical Chemistry* **78**, 2405-2412.

Sears, D. W. G. and R. T. Dodd (1988) Overview and classification of meteorites. *Meteorites and the Earth Solar System*. J. F. Kerridge and M. S. Matthews, Eds. (University of Arizona Press) p. 3-31.

Sephton, M. A. (2002) Organic compounds in carbonaceous meteorites. *Natural Product Reports* **19**, 292-311.

Sephton, M. A. (2014) Organic geochemistry of meteorites. *Treatise on Geochemistry 2nd Edition*, H. D. Holland and K. K. Turekian, Eds. (Elsevier, 2014) vo1. 12, p. 1-31

Sephton, M. A., C. T. Pillinger, and I. Gilmour (1998) δ^{13}C of free and macromolecular aromatic structures in the Murchison meteorite. *Geochimica et Cosmochimica Acta* **62** (10), 1821-1828.

Sephton, M. A., and I. Gilmour (2000) Aromatic moieties in meteorites: Relics of interstellar grain processes. *The Astrophysical Journal* **540**, 588-591.

Sephton, M. A., and I. Gilmour (2001) Compound-specific isotope analysis of the organic constituents in carbonaceous chondrites. *Mass Spectrometry Reviews* **20**, 111-120.

Serrano, M., M. Silva, and M. Gallego (2013) Development of an environment-friendly microextraction method for the determination of aliphatic and aromatic aldehydes in water. *Analytica Chimica Acta* **784**, 77-84.

Shalabiea, O. M., and J. M. Greenberg (1994) Two key processes in dust/gas chemical modeling – photoprocessing of grain mantles and explosive desorption. *Astronomy & Astrophysics* **290**, 266-278.

Spaulding, R. S., and M. J. Charles (2002) Comparison of methods for extraction, storage, and silylation of pentafluorobenzyl derivatives of carbonyl compounds and multi-functional carbonyl compounds. *Analytical and Bioanalytical Chemistry* **372**, 808-816.

Stephan, T. (2001) TOF-SIMS in cosmochemistry. *Planetary and Space Science* **49**, 859-906.

Stephan, T., E. K. Jessberger, C. H. Heiss, and D. Rost (2003) TOF-SIMS analysis of polycyclic aromatic hydrocarbons in Allan Hills 84001. *Meteoritics & Planetary Science* **38** (1), 109-116.

Strassnig, S., T. Wenzl, and E. P. Lankmayr (2000) Microwave-assisted derivatization of volatile carbonyl compounds with *O*-(2,3,4,5,6-pentafluorobenzyl)hydroxylamine. *Journal of Chromatography* **891**, 267-273.

Studier, M. H., R. Hayatsu, and E. Anders (1965) Organic compounds in carbonaceous chondrites. *Science* **149**, 1455-1459.

Sugaya, N., K. Sakurai, T. Nakagawa, N. Onda, S. Onodera, M. Morita, and M. Tezuka (2004) Development of a headspace GC-MS analysis of carbonyl compounds (aldehydes and ketones) in household products after derivatization with *O*-(2,3,4,5,6-pentafluorobenzyl)-hydroxylamine. *Analytical Sciences* **20**, 865-870.

Takeuchi, A., T. Takigawa, M. Abe, T. Kawai, Y. Endo, T. Yasugi, G. Endo, and K. Ogino (2007) Determination of formaldehyde in urine by headspace gas chromatography. *Bulletin of Environmental Contamination and Toxicology* **79**, 1-4.

Taylor, R. (1987) The mechanism of thermal eliminations Part XXIII: [1] The thermal decomposition of pyruvic acid. *International Journal of Chemical Kinetics* **19**, 709-713.

Tielens, A. G. G. M. and D. C. B. Whittet (1997) Ice in star forming regions. *Molecules in Astrophysics: Probe and Processes*, E. F. van Dishoeck, Ed. (Springer Science & Business Media), 45-60.

Touboul, D., F. Kollmer, E. Niehuis, A. Brunelle, O. Laprevote (2005) Improvement of biological time-of-flight secondary ion mass spectrometry imaging with a bismuth cluster ion source. *Journal of the American Society for Mass Spectrometry* **16**, 1608-1618.

Tyler, B. J., C. Bruening, S. Rangaranjan, and H. F. Arlinghaus (2011) TOF-SIMS imaging of adsorbed proteins on topographically complex surfaces with Bi_3^+ primary ions.

Van Schmus, W. R. and J. A. Wood (1967) A chemical-petrologic classification for the chondritic meteorites. *Geochimica et Cosmochimica Acta* **31**, 747-765.

Vickerman, J. C. (2013) TOF-SIMS – An evolving mass spectrometry of materials. *In TOF-SIMS: Materials Analysis by Mass Spectrometry, 2nd Edition*, J. C. Vickerman and D. Briggs, Eds. (IM Publications LLP and SurfaceSpectra Limited, 2013) p. 1-37.

Vokrouhlicky, D., W. F. Bottke, and D. Nesvorny (2016) Capture of trans-Neptunian planetesimals in the main asteroid belt. *The Astronomical Journal* **152**(39), 1-20.

Watanabe, N. and A. Kouchi (2002) Efficient formation of formaldehyde and methanol by the addition of hydrogen atoms to CO in H_2O-CO ice at 10 K. *The Astrophysical Journal* **571**, 173-176.

Wing, M. R. and J. L. Bada (1992) The origin of the polycyclic aromatic hydrocarbons in meteorites. *Origins of Life and Evolution of the Biosphere* **21**, 375-383.

Wirström, E. S., S. B. Charnley, W. D. Geppert, and C. M. Persson (2012) Observations of carbon isotopic fractionation in interstellar formaldehyde. *43rd Lunar and Planetary Science Conference,* #1611.

Yamada, H., and I. Somiya (1989) The determination of carbonyl compounds in ozonated water by the PFBOA method. *Ozone Science & Engineering* **11**, 127-141.

Yanagawa, H., Y. Makino, K. Sato, M. Nishizawa, and F. Egami (1982) Novel formation of α-amino acids and their derivatives from oxo acids and ammonia in an aqueous medium. *The Journal of Biochemistry* **91**, 2087-2090.

Ye, Q., D. Zheng, L. Liu, and L. Hong (2011) Rapid analysis of aldehydes by simultaneous microextraction and derivatization followed by GC-MS. *Journal of Separation Science* **34**, 1607-1612.

Yesiltas, M. and Y. Kebukawa (2016) Associations of organic matter with minerals in Tagish Lake meteorite via high spatial resolution synchrotron-based FTIR microspectroscopy. *Meteoritics & Planetary Science* **51**, 584-595.

Yuen, G., N. Blair, D. J. Des Marais, and S. Chang (1984) Carbon isotope composition of low molecular weight hydrocarbons and monocarboxylic acids from Murchison meteorite. *Nature* **307**, 252-254.

Zolensky, M. E., K. Nakamura, M. Gounelle, T. Mikouchi, T. Kasama, O. Tachikawa, and E. Tonui (2002) Mineralogy of Tagish Lake: An ungrouped type 2 carbonaceous chondrite. *Meteoritics & Planetary Science* **37**, 737-761.

APPENDIX 1

Table A1.1. A summary, adapted from Rodigast et al. (2015), of the experimental conditions used for aqueous phase derivatization and extraction of aldehydes and/or ketones.

PFBHA (mg/mL)	Derivatization time	Derivatization temperature	Extraction solvent	Extraction time (min)	Reference
0.1	40 min aldehydes, 24 h ketones	Room temp.	Ethyl acetate	−	Kobayashi et al. (1980)
0.1	2 h (longer for ketones)	Room temp.	Hexane	0.5	Glaze et al. (1989)
1	1 h aldehydes, 1 day ketones	Room temp.	Hexane	−	Yamada and Somiya (1989)
>10-fold excess	24 h	Room temp.	Hexane, MTBE	1	Le Lacheur et al. (1993)
0.75	2 h	35°C	Hexane	3	EPA Method 556 (1998)
0.8	20 s	900 W	Toluene	−	Strassnig et al. (2000)
0.5	24 h	Room temp.	Dichloromethane	−	Spaulding and Charles (2002)
0.06	4 h	60°C	−	−	Sugaya et al. (2004)
0.2	24-96 h	Room temp.	Hexane	−	Seaman et al. (2006)
0.06	2 h	Room temp.	−	−	Hudson et al. (2007)
−	4 h	Room temp.	−	−	Takeuchi et al. (2007)
0.75	10 min	Room temp.	−	−	Saison et al. (2009)
Followed EPA Method 556					Pizzarello and Holmes (2009)
0.05	<10 min	Room temp.	Chlorobenzene	2	Ye et al. (2011)
0.5	1 min	60°C	Hexane	1	Serrano et al. (2013)
−	45 min	−	Dichloromethane	−	de Marcellus et al. (2015)
0.4	24 h	−	Dichloromethane	30	Rodigast et al. (2015)

Dash line − parameter not reported

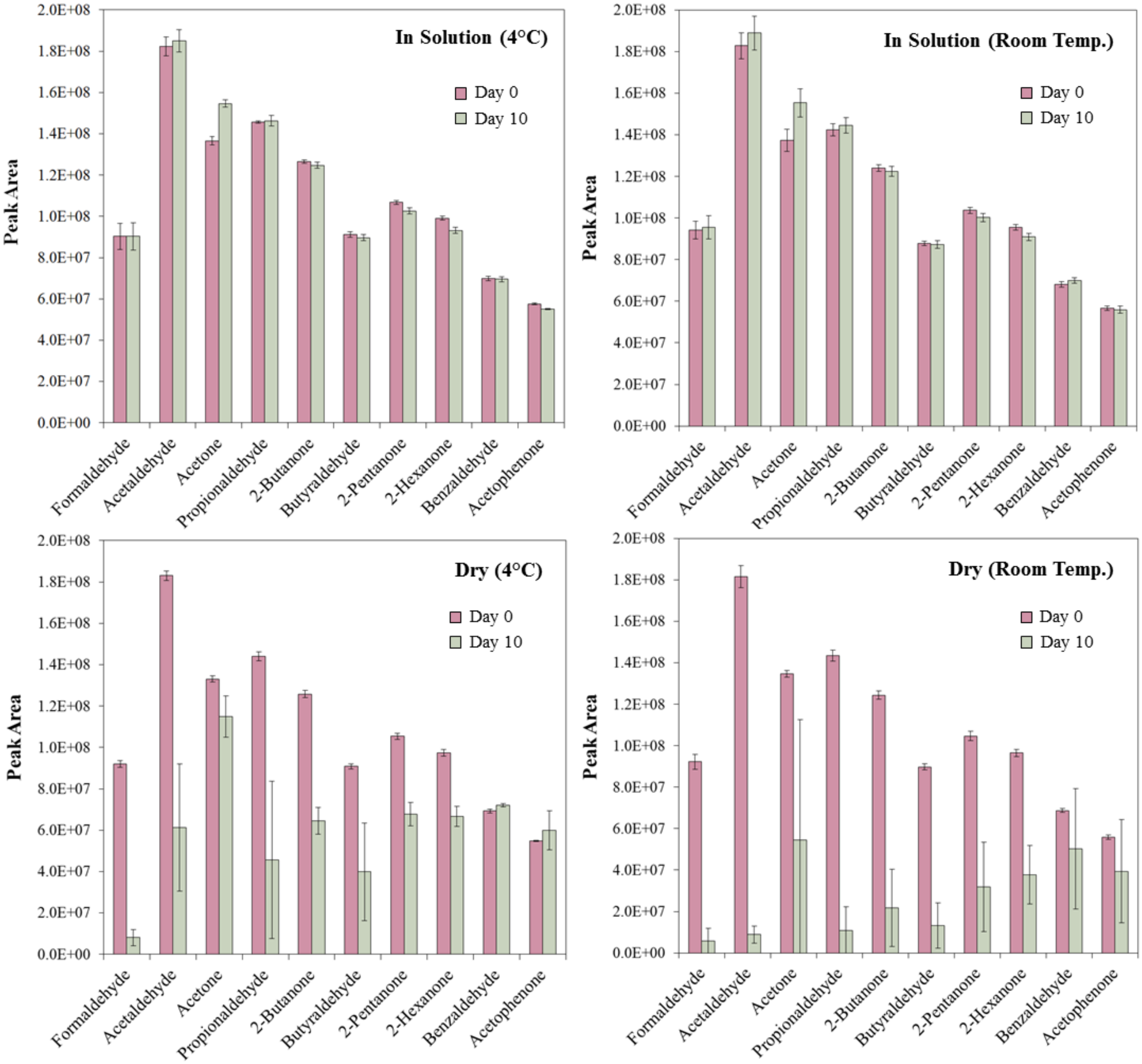

Figure A1.1. Abundances (GC-MS peak areas) of aldehyde and ketone derivatives (initial concentrations: 50 µg/mL) before and after storage at 4°C or room temperature. Dichloromethane was used as the extraction solvent for all samples. Solutions were evaporated to 1 mL volumes under a stream of nitrogen prior to the first GC-MS run (Day 0). Samples stored in solution were stored in their 1 mL volumes for 10 days. Samples stored dry were evaporated to dryness under a stream of nitrogen, immediately re-capped, stored dry for 10 days, and then re-constituted in 1 mL dichloromethane prior to the second GC-MS run (Day 10). All measurements were calibrated against an external standard (50 µg/mL underivatized acetophenone) to adjust for instrumental variations. Each bar represents an average of 3 replicate samples, and error bars represent one standard deviation from the mean.

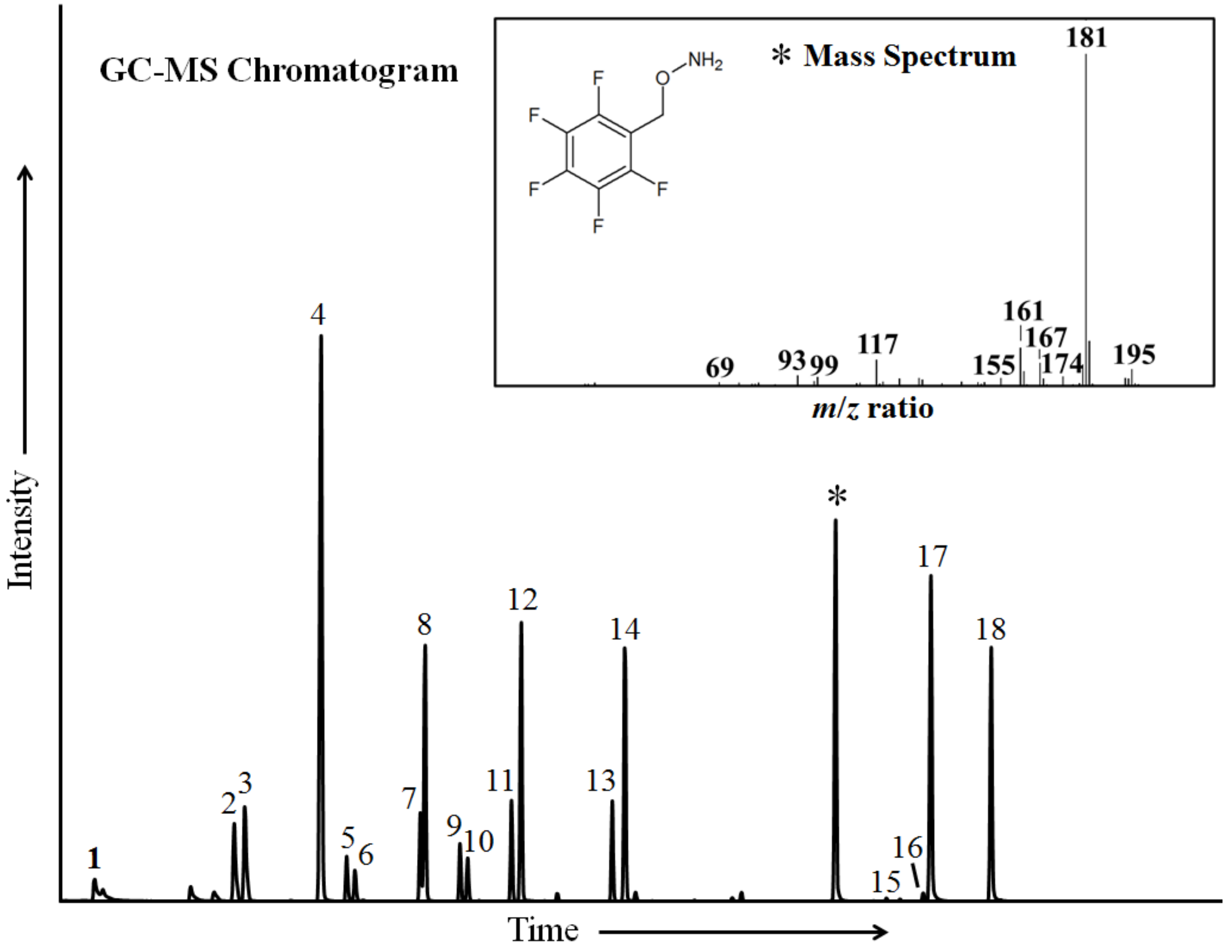

Figure A1.2. GC-MS chromatogram of aldehyde and ketone derivatives in dichloromethane after dry storage at 4°C for 10 days (initial concentrations: 50 µg/mL). The identities of the peaks are presented in Table 1. The GC-MS peak labeled with an asterisk is a decomposition product that was only observed in samples that had been stored dry. The mass spectrum displayed above the chromatogram represents the mass spectrum and compound identification provided by the NIST Mass Spectral Library for the decomposition product(*).

APPENDIX 1 REFERENCES

de Marcellus, P., C. Meinert, I. Myrgorodska, L. Nahon, T. Buhse, L. Le Sergeant D'Hendecourt, and U. J. Meierhenrich (2015) Aldehydes and sugars from evolved precometary ice analogs: Importance of ices in astrochemical and prebiotic evolution. *PNAS* **112**, 965-970.

EPA Method 556: Determination of carbonyl compounds in drinking water by pentafluorobenzylhydroxylamine derivatization and capillary gas chromatography with electron capture detection (1998) National exposure research laboratory office of research and development. US Environmental Protection Agency, Cincinnati, Ohio, 45268.

Glaze, W. H., M. Koga and D. Cancilla (1989) Ozonation byproducts. 2. Improvement of an aqueous-phase derivatization method for the detection of formaldehyde and other carbonyl compounds formed by the ozonation of drinking water. *Environmental Science & Technology* **23**, 838-847.

Hudson, E. D., K. Okuda, and P. A. Ariya (2007) Determination of acetone in seawater using derivatization solid-phase microextraction. *Analytical and Bioanalytical Chemistry* **388**, 1275-1282.

Kobayashi, K., M. Tanaka, and S. Kawai (1980) Gas chromatographic determination of low-molecular-weight carbonyl compounds in aqueous solution as their O-(2,3,4,5,6-pentafluorobenzyl) oximes. *Journal of Chromatography* **187**, 413-417.

Le Lacheur, R. M., L. B. Sonnenberg, P. C. Singer, R. F. Christman, and M. J. Charles (1993) Identification of carbonyl compounds in environmental samples. *Environmental Science & Technology* **27**, 2745-2753.

Pizzarello, S. and W. Holmes (2009) Nitrogen-containing compounds in two CR2 meteorites: ^{15}N composition, molecular distribution and precursor molecules. *Geochimica et Cosmochimica Acta* **73**, 2150-2162.

Rodigast, M., A. Mutzel, Y. Iinuma, S. Haferkorn, and H. Herrmann (2015) Characterisation and optimization of a sample preparation method for the detection and quantification of atmospherically relevant carbonyl compounds in aqueous medium. *Atmospheric Measurement Technique* **8**, 2409-2416.

Saison, D., D. P. De Schutter, F. DeIvaux, F. R. Delvaux (2009) Determination of carbonyl compounds in beer by derivatization and headspace solid-phase microextraction in combination with gas chromatography and mass spectrometry. *Journal of Chromatography A* **1216**, 5061-5068.Seaman, V. Y., M. J. Charles, and T. M. Cahill (2006) A sensitive method for the quantification of acrolein and other volatile carbonyls in ambient air. *Analytical Chemistry* **78**, 2405-2412.

Serrano, M., M. Silva, and M. Gallego (2013) Development of an environment-friendly microextraction method for the determination of aliphatic and aromatic aldehydes in water. *Analytica Chimica Acta* **784**, 77-84.

Spaulding, R. S., and M. J. Charles (2002) Comparison of methods for extraction, storage, and silylation of pentafluorobenzyl derivatives of carbonyl compounds and multi-functional carbonyl compounds. *Analytical and Bioanalytical Chemistry* **372**, 808-816.

Strassnig, S., T. Wenzl, and E. P. Lankmayr (2000) Microwave-assisted derivatization of volatile carbonyl compounds with *O*-(2,3,4,5,6-pentafluorobenzyl)hydroxylamine. *Journal of Chromatography* **891**, 267-273.

Sugaya, N., K. Sakurai, T. Nakagawa, N. Onda, S. Onodera, M. Morita, and M. Tezuka (2004) Development of a headspace GC-MS analysis of carbonyl compounds (aldehydes and ketones) in household products after derivatization with *O*-(2,3,4,5,6-pentafluorobenzyl)-hydroxylamine. *Analytical Sciences* **20**, 865-870.

Takeuchi, A., T. Takigawa, M. Abe, T. Kawai, Y. Endo, T. Yasugi, G. Endo, and K. Ogino (2007) Determination of formaldehyde in urine by headspace gas chromatography. *Bulletin of Environmental Contamination and Toxicology* **79**, 1-4.

Yamada, H., and I. Somiya (1989) The determination of carbonyl compounds in ozonated water by the PFBOA method. *Ozone Science & Engineering* **11**, 127-141.

Ye, Q., D. Zheng, L. Liu, and L. Hong (2011) Rapid analysis of aldehydes by simultaneous microextraction and derivatization followed by GC-MS. *Journal of Separation Science* **34**, 1607-1612.

APPENDIX 2

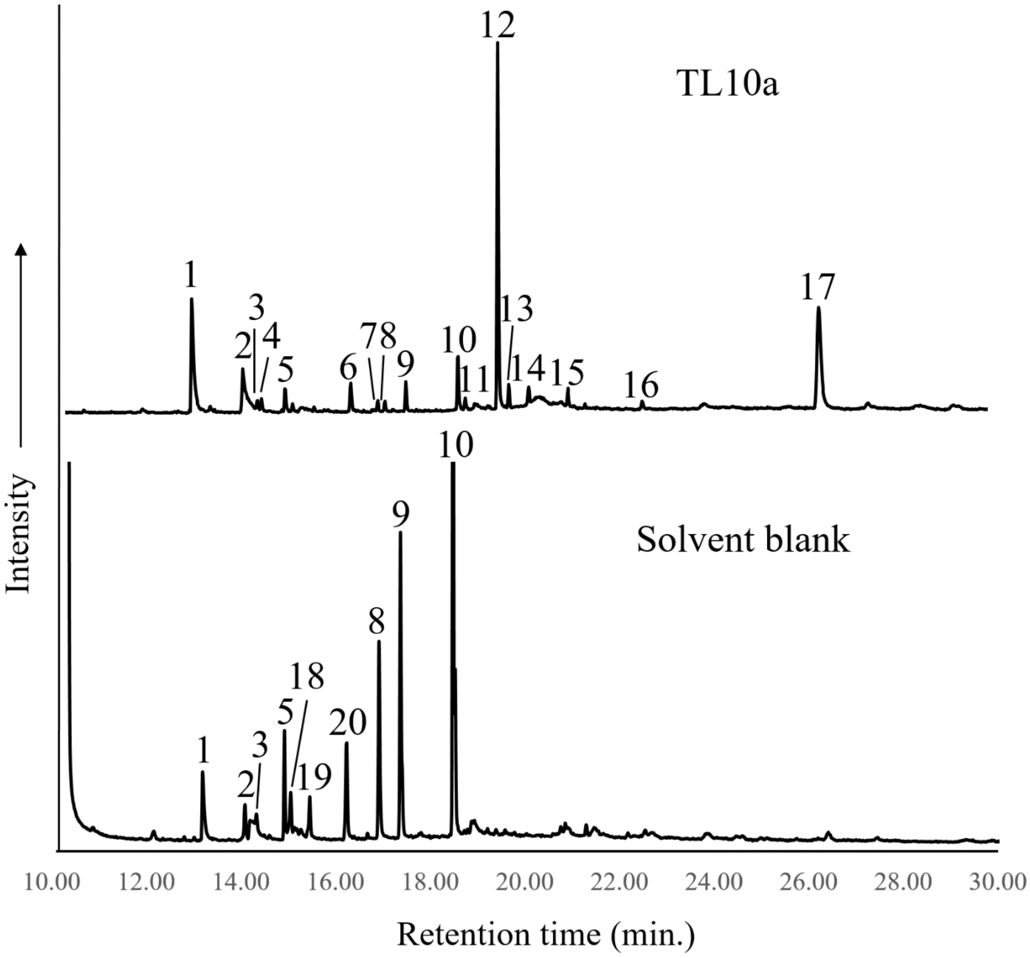

Figure A2.1. GC-MS chromatograms for the SPME analysis of a hot-water extract of TL10a and the corresponding procedural blank. The water extract was reacted with PFBHA to derivatize and isolate carbonyl compounds for the analysis of indigenous aldehydes and ketones. The derivatized carbonyl compounds were extracted from the solution using DCM and the remaining water extract was analyzed using SPME GC-MS technique. Peak identifications are listed in Table A2.1.

Table A2.1. Water-soluble organic compounds, including carboxylic acids, detected in a hot-water extract of TL10a and the corresponding procedural blank. The water extract was reacted with PFBHA to derivatize and isolate carbonyl compounds for the analysis of indigenous aldehydes and ketones. The derivatized carbonyl compounds were extracted from the solution using DCM and the remaining water extract was analyzed using SPME GC-MS technique. Probabilities (%) reported by the NIST Mass Spectral Library reflect the software's confidence for the individual peak identifications. The GC-MS spectra for TL10a and the blank are shown in Figure A2.2.

Compound	Compound number	Probability (%)
TL10a		
Acetic acid[a]	1	std.
Propanoic acid[a]	2	std.
2-methyl-propanoic acid[a]	3	31
2,2-dimethyl-propanoic acid	4	23
2-(2-ethoxyethoxy)-ethanol	5	79
2,3,4,5,6-pentafluorobenzyl alcohol[b]	6	96
Tetraoxacyclododecanone[b]	7	38
4-methyl-pentanoic acid	8	78
Hexanoic acid[a]	9	std.
Heptanoic acid[a]	10	67
Tetrafluorophenol[b]	11	97
Tetrafluorophenol[b]	12	93
Octanoic acid	13	std.
2-fluoro-3-(trifluoromethyl)phenol[b]	14	34
Nonanoic acid	15	std.
n-decanoic acid	16	29
Benzoic acid	17	std.
Solvent blank		
Acetic acid	1	std.
Propanoic acid	2	std.
2-methyl-propanoic acid	3	30
2-(2-ethoxyethoxy)-ethanol	5	91
Butanoic acid	18	std.
3-methyl-butanoic acid	19	86
Pentanoic acid	20	69
4-methyl-pentanoic acid	8	89
Hexanoic acid	9	std.
Heptanoic acid	10	62

[a] Terrestrial contaminant

[b] Reagent peaks derived from the PFBHA derivatization reaction of carbonyl compounds in the extract (see Figure A2.2)

std. – compound ID is based on matching retention time and spectrum with a carboxylic acid standard.

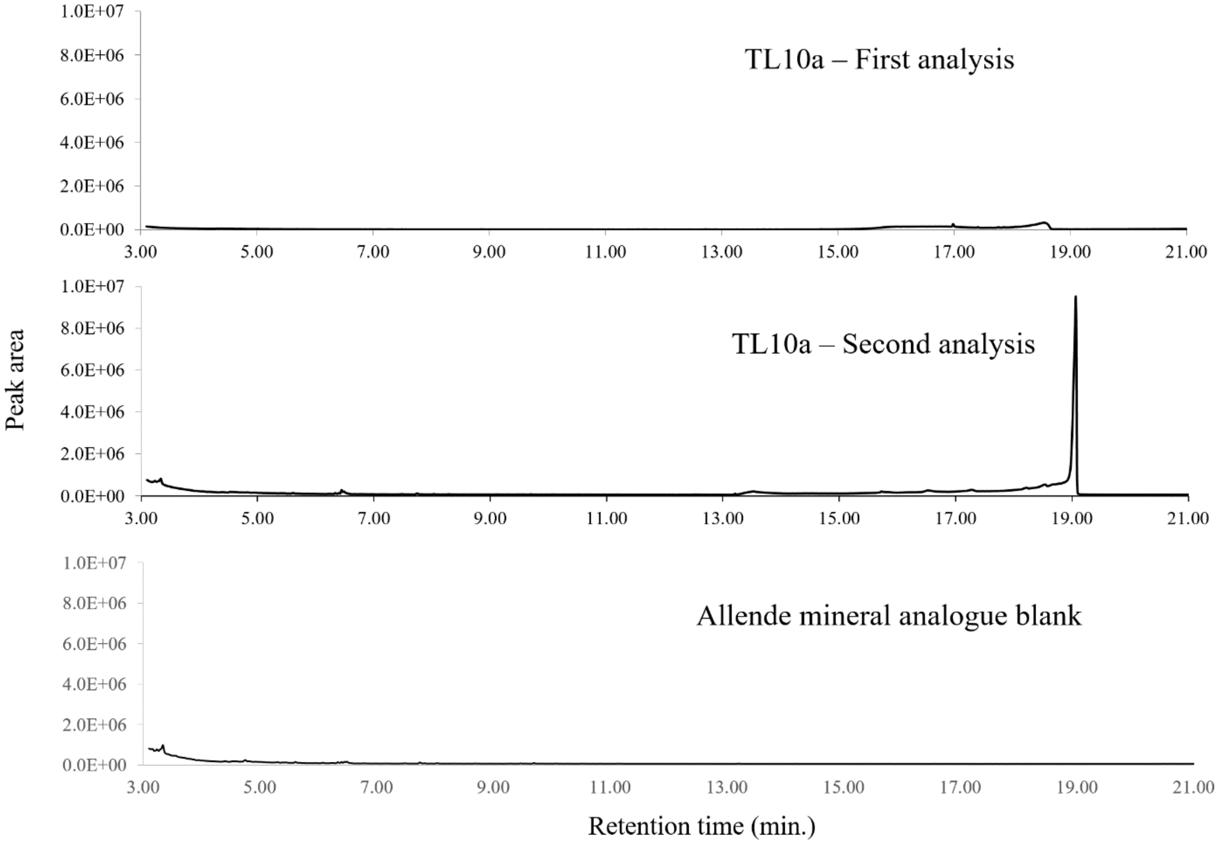

Figure A2.2. GC-MS chromatograms for two separate DCM extract analyses of TL10a, compared to the GC-MS chromatogram of the combusted Allende mineral analogue blank. The relatively large peak eluting at 19.00 minutes was identified by the NIST Mass Spectral Library as S_8.

Table A2.2. Probabilities (%) reported by the NIST Mass Spectral Library for the SPME GC-MS analyses of TL1, TL4 and TL10a (Table 3.5), reflecting the software's confidence for the individual peak identifications.

Compound	Probability (%)
Sample TL1	
Dodecamethyl-cyclohexasiloxane	96
2-chloroethanol	97
Acetic acid[a]	-
Formic acid[a]	-
Propanoic acid[a]	-
2-methyl-propanoic acid	85
2-(2-ethoxyethoxy)-ethanol	94
Butanoic acid[a]	-
2-methyl-butanoic acid	71
Pentanoic acid[a]	-
2-(2-chloroethoxy)-ethanol	97
3-methyl-pentanoic acid	20
Hexanoic acid[a]	-
2,2-oxybis-ethanol	85
2-[2-(2-ethoxyethoxy)ethoxy]-ethanol	49
1,4-dioxan-2-yl-hydroperoxide	37
Octanoic acid[a]	-
2-[2-(2-chloroethoxy)ethoxy]-ethanol	95
Nonanoic acid[a]	-
4-chloro-1-butanol	20
Tetraoxacyclododecanone	83
4-oxo-pentanoic acid	70
Triethylene glycol	38
Pentaoxadexadecanol	21
Benzoic acid[a]	-
Indole	55
2-methyl-benzoic acid	41
3-methyl-benzoic acid	27
Sample TL4	
Dodecamethyl-cyclohexasiloxane	98
2-chloroethanol	97
Acetic acid[a]	-
Formic acid[a]	-
2-(2-ethoxyethoxy)-ethanol	95
2-(2-chloroethoxy)-ethanol	97
2,2-oxybis-ethanol	77
2-[2-(2-ethoxyethoxy)ethoxy]-ethanol	43
1,4-dixoan-2-yl-hydroperoxide	44
Octanoic acid[a]	-
2-[2-(2-chloroethoxy)ethoxy]-ethanol	94
Nonanoic acid[a]	-

4-chloro-1-butanol	9
Tetraoxacyclododecanone	74
Triethylene glycol	53
Benzoic acid[a]	-
Indole	35
Sample TL10a	
Dodecamethyl-cyclohexasiloxane	96
2-chloroethanol	54
Acetic acid[a]	-
Phenyl-pentamethyl-disiloxane	16
2-(2-ethoxyethoxy)-ethanol[a]	95
Butyrolactone[a]	73
1-chloro-dodecane	7
Hexanoic acid[a]	-
Heptanoic acid[a]	-
Octanoic acid[a]	-
Nonanoic acid[a]	-
1,1-oxybis-octane[a]	14
n-decanoic acid	55
Benzoic acid[a]	-
Dodecanoic acid	87
Octadecanol	7

[a] Compound identification is based on a matching mass spectrum and retention time compared to a reference standard

Table A2.3. Probabilities (%) reported by the NIST Mass Spectral Library for the aliphatic and aromatic compounds detected in the DCM extracts of TL1, TL4 and TL10a (Table 3.6), reflecting the software's confidence for the individual peak identifications.

Compound	Probability (%)
Sample TL1	
3,5,5-trimethyl-2-hexene	42
3,5,5-trimethyl-2-hexene	16
Ethylbenzene	61
1,3-dimethyl-benzene	37
p-xylene	43
1,2,3,4,5-pentamethyl-cyclopentane	21
2,4,4-trimethyl-1-hexene	21
2,6-dimethyl-undecane	7
2,2,6-trimethyl-octane	21
2,2,6-trimethyl-octane	15
Mesistylene	23
2,2-dimethyl-decane	23
6-ethyl-2-methyl-octane	13
5-ethyl-2,2,3-trimethyl-heptane	12
2,6-dimethyl-octane	7
3-methyl-undecane	7
3,7-dimethyl-decane	6
Undecane	24
1,2,4,5-tetramethyl-benzene	16
Naphthalene	35
Dodecane	34
Pentamethyl-benzene	42
1,2-benzene-dicarboxylic acid, bis(2-methylpropyl) ester	21
Cyclic octaatomic sulfur	98
Fluoranthene	47
Pyrene	52
Sample TL4	
3,5,5-trimethyl-2-hexene	47
3,5,5-trimethyl-2-hexene	14
Ethylbenzene	50
1,3-dimethyl-benzene	31
p-xylene	31
1,2,3,4,5-pentamethyl-cyclopentane	31
2,4,4-trimethyl-1-hexene	27
2,2,6-trimethyl-octane	14
2,2,6-trimethyl-octane	19
2,2,6-trimethyl-octane	21
Mesistylene	24
2,2-dimethyl-decane	25
2,3,6,7-tetramethyl-octane	8
3-methyl-nonane	7

3,6-dimethyl-undecane	6
2,6,10-trimethyl-dodecane	7
4-methyl-dodecane	8
Undecane	10
Dodecane	20
1,2-benzene-dicarboxylic acid, bis(2-methylpropyl) ester	13
Cyclic octaatomic sulfur	98
Sample TL10a	
4-methyl-2-pentanol	48
2-ethyl-1-hexanol	58
Cyclic octaatomic sulfur	99

Table A2.4. Summary of the amino acid abundances (ppb) determined for non-hydrolyzed (“free”) and 6 M HCl-hydrolyzed (“total”) hot water extracts of Tagish Lake: TL5b, TL11h, TL11i (data from Glavin et al., 2012) and a non-pristine sample (data from Kminek et al., 2002).

	TL5b free	TL5b total	TL11h free	TL11h total	TL11i free	TL11i total	Non-pristine
D-Asp	1.7 ± 0.4	8.0 ± 1.8	13.6 ± 2.5	161 ± 14	< 0.3	< 1.0	11 ± 1
L-Asp	8.7 ± 0.6	20.1 ± 3.3	55.0 ± 5.6	430 ± 65	0.70 ± 0.2	2.6 ± 0.5	83 ± 8
D-Glu	1.6 ± 0.2	16.4 ± 0.5	41.2 ± 1.3	244 ± 23	< 0.2	< 0.2	16 ± 2
L-Glu	2.7 ± 0.6	50.6 ± 2.3	53.5 ± 13.8	844 ± 89	0.2 ± 0.1	5.8 ± 1.6	306 ± 48
D-Serine	1.3 ± 0.1	1.5 ± 0.1	23.6 ± 2.3	51.8 ± 7.3	< 0.2	< 0.2	n.d.
L-Serine	17.3 ± 1.5	13.9 ± 4.2	124 ± 23	181 ± 29	1.8 ± 0.1	2.1 ± 0.5	n.d.
D-Threonine	< 0.1	< 0.2	< 0.2	< 0.3	< 0.1	< 0.1	n.d.
L-Threonine	7.4 ± 1.8	3.5 ± 1.6	55.2 ± 5.3	97.3 ± 17.8	0.9 ± 0.3	1.3 ± 0.4	n.d.
Glycine	90.0 ± 6.4	129 ± 21	619 ± 184	987 ± 257	2.4 ± 0.4	9.7 ± 4.2	147 ± 17
β-Alanine	70.4 ± 14.1	82.3 ± 9.5	107± 19	150 ± 30	0.1 ± 0.1	13.5 ± 0.7	64 ± 10
D-Alanine	25.7 ± 0.7	54.1 ± 3.3	252 ± 32	387 ± 25	< 0.1	< 0.5	20 ± 5
L-Alanine	25.1 ± 0.7	49.7 ± 4.3	240 ± 33	363 ± 41	1.2 ± 1.0	1.6 ± 0.5	75 ± 18
γ-ABA	7.2 ± 1.0	216 ± 24	41.1 ± 2.8	374 ± 50	0.1 ± 0.1	< 1.0	77 ± 10
D-β-ABA	13.3 ± 2.0	11.5 ± 1.2	19.0 ± 3.8	36.0 ± 3.9	< 0.1	< 0.1	< 26[a]
L-β-ABA	12.5 ± 2.0	12.8 ± 1.4	17.4 ± 4.8	38.8 ± 3.0	< 0.1	< 0.1	
α-AIB	9.2 ± 0.8	20.7 ± 2.1	161 ± 29	179 ± 23	0.3 ± 0.1	1.3 ± 0.2	<27
D,L-α-ABA	10.2 ± 0.1	24.2 ± 3.9	62.1 ± 16.5	82.2 ± 15.2	< 0.1	< 0.2	84 ± 40
EACA	< 0.2	< 0.2	< 0.3	< 0.3	< 0.2	<0.2	n.d.
3-a-2,2-dmpa	1.5 ± 0.1	3.8 ± 0.1	9.2 ± 0.3	17.7 ± 0.6	< 0.1	< 0.1	n.d.
D,L-4-apa	1.3 ± 0.2	24.5 ± 0.8	5.3 ± 0.7	112.0 ± 6.0	< 0.1	< 0.1	n.d.
D,L-4-a-3-mba	1.0 ± 0.1	42.9 ± 1.3	4.3 ± 0.2	183.0 ± 5.0	< 0.2	< 0.3	n.d.
D,L-3-a-2-mba	2.1 ± 0.2	2.6 ± 0.2	4.3 ± 0.2	5.4 ± 0.7	< 0.1	< 0.2	n.d.
D,L-3-a-2-epa	2.7 ± 0.2	10.7 ± 1.6	6.1 ± 0.2	10.2 ± 0.4	< 0.5	< 1.0	n.d.
5-apa	1.2 ± 0.1	46.3 ± 1.2	2.7 ± 0.1	53.6 ± 1.1	< 0.1	< 0.2	n.d.
D,L-4-a-2-mba	1.7 ± 0.2	34.2 ± 0.7	4.5 ± 0.3	191.0 ± 7.0	< 0.3	< 0.5	n.d.
3-a-3-mba	< 0.5	< 1.5	< 2.6	< 12.0	< 0.1	< 0.1	n.d.
D-Isovaline	2.5 ± 0.2	6.6 ± 0.2	42.7 ± 1.6	43.7 ± 1.8	< 0.2	< 0.5	< 56[a]
D,L-3-apa	12.7 ± 0.5	10.6 ± 0.4	13.4 ± 0.4	12.7 ± 0.7	< 0.2	< 0.4	n.d.
L-Isovaline	3.1 ± 0.2	7.6 ± 0.2	41.9 ± 1.5	43.7 ± 1.7	< 0.2	< 0.5	
L-Valine	< 4.0	< 9.0	< 37.0	< 86.0	< 0.7	< 1.0	n.d.
D-Valine	1.9 ± 0.1	5.9 ± 0.1	7.1 ± 0.2	16.4 ± 0.5	< 0.2	< 0.4	n.d.
D-Norvaline	2.2 ± 0.2	2.6 ± 0.2	5.4 ± 0.2	6.8 ± 0.4	< 0.2	< 0.4	n.d.
L-Norvaline	1.9 ± 0.1	2.7 ± 0.1	5.6 ± 0.2	7.5 ± 0.4	< 0.2	< 0.3	n.d.

n.d. – not determined

[a] Enantiomeric identifications not determined

APPENDIX 3

A3.1. Two additional Tagish Lake TL1 chips were subsampled and analyzed via Bi_1^+-TOF-SIMS as follows. A small fragment of the TL1 specimen was split into two pieces by applying pressure to the outer surface of the chip with the sharp end of a clean scalpel. The meteorite chip split into two pieces along a natural fracture (Figure A3.1) and neither of the two newly exposed fracture surfaces came into contact with any external surfaces. The chips were mounted onto the TOF-SIMS sample holder with clean tweezers, and carbon tape as an adhesive on the outer surface of each chip. The holder was transferred to the nanoFAB laboratory inside a storage container filled with cleanroom air and the sample holder was quickly transferred into the TOF-SIMS instrument. The samples were exposed to laboratory air for less than one minute. The samples were analyzed using the same instrumental parameters that were used for both the Murchison samples and the other Tagish Lake sample: high current bunched mode, 256 x 256-pixel resolution, 10 shots/pixel, 500 x 500 μm^2 sample areas, 100 scans each. Only positive ion spectra were obtained. An electron flood gun was used for charge compensation. The surface of Chip 1 was scanned first to target sample areas that appeared to have sufficiently high and homogeneous total ion yields, reflecting relatively flat surface topographies, and the mirror image sample areas on Chip 2 were analyzed using the same parameters.

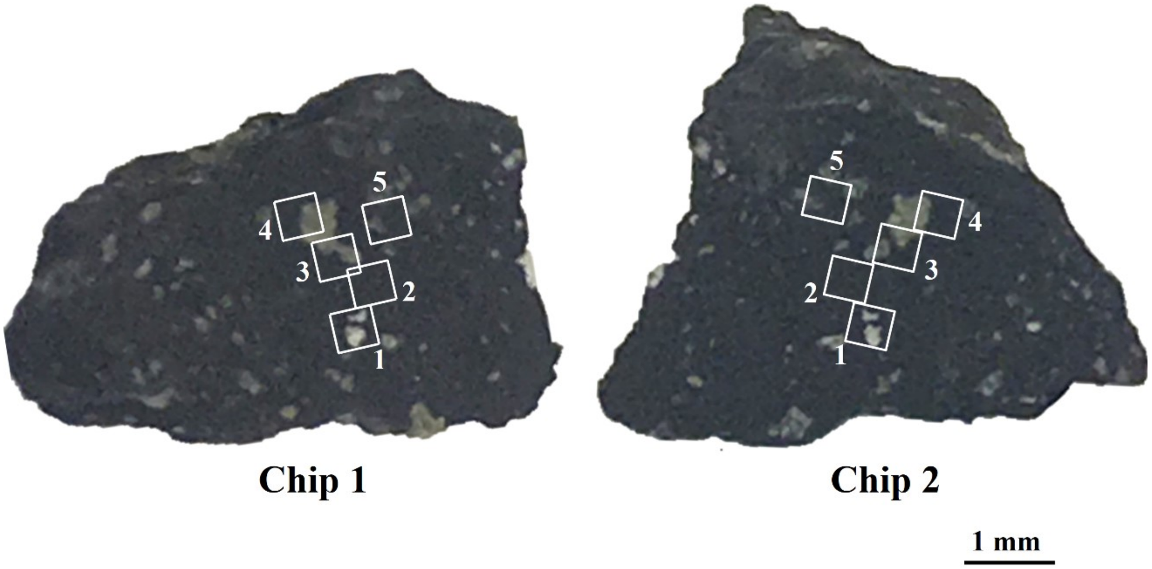

Figure A3.1. Mirror-image fresh fracture surfaces of two TL1 chips and the ten 500 x 500 μm^2 sample areas analyzed by Bi_1^+-TOF-SIMS.

Table A3.1. Amino acid-associated molecular ions and their detection (Y) or non-detection (N) within 500 x 500 μm^2 sample areas on mirror-image fresh fracture surfaces of the Tagish Lake meteorite (specimen TL1; 2 meteorite chips, 5 sample areas per chip; Figure A3.1).

Molecular ion	Amino acid(s)	TL1 Chip 1					TL1 Chip 2				
		Area 1	Area 2	Area 3	Area 4	Area 5	Area 1	Area 2	Area 3	Area 4	Area 5
NH_4^+	Ala, β-Ala, α-AIB, α-ABA, β-ABA, γ-ABA, Asp, Glu	Y	Y	*Insufficient total ion yield*	*Insufficient total ion yield*	*Insufficient total ion yield*	Y	*Insufficient total ion yield*	*Insufficient total ion yield*	Y	Y
$C_2H_3^+$	α-ABA, Asp	Y	Y				Y			Y	Y
CH_4N^+	Gly, β-Ala, γ-ABA	N	Y				Y			Y	Y
$C_3H_5^+$	α-AIB, γ-ABA, Asp	Y	Y				Y			Y	Y
$C_2H_6N^+$	Ala, β-ABA, Asp	N	Y				Y			Y	Y
$C_3H_6N^+$	Glu	N	N				N			N	N
$C_3H_8N^+$	α-AIB, α-ABA, β-ABA	N	Y				Y			Y	N
$C_4H_5O^+$	γ-ABA	N	N				N			N	N
$C_3H_4NO^+$	Asp	N	N				N			N	N
$C_2H_4NO_2^+$	Asp	N	N				N			N	N
[a]$C_2H_6NO_2^+$	Gly	Y	Y				Y			Y	Y
$C_4H_6NO^+$	Glu	N	N				N			N	N
$C_4H_8NO^+$	γ-ABA	N	N				N			N	N
$C_3H_6NO_2^+$	Asp	N	N				N			N	N
[a]$C_3H_8NO_2^+$	Ala, β-Ala	N	Y				Y			N	Y
$C_4H_8NO_2^+$	Glu	N	N				N			N	N
[a]$C_4H_{10}NO_2^+$	α-AIB, α-ABA, β-ABA, γ-ABA, Asp	N	N				N			N	N
[a]$C_4H_8NO_4^+$	Asp	N	N				N			N	N
[a]$C_5H_{10}NO_4^+$	Glu	N	N				N			N	N

[a] Intact amino acids – $[M+H]^+$ (where M is the molecular weight)